AD-A049 481 ARMY ENGINEER WATERWAYS EXPERIMENT STATION VICKSBURG MISS F/G 8/13
EFFECTS OF ANISOTROPIC VERSUS ISOTROPIC CONSOLIDATION IN CONSOL--ETC(U)
OCT 75 R T DONAGHE, F C TOWNSEND

UNCLASSIFIED WES-TR-S-75-13 NL

1 OF 2
AD
A049481

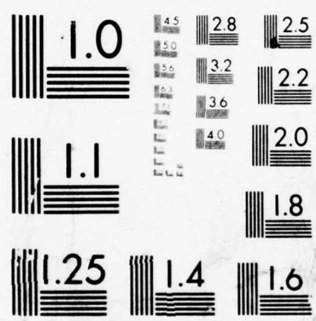

MICROCOPY RESOLUTION TEST CHART
NATIONAL BUREAU OF STANDARDS-1963-A

TECHNICAL REPORT S-75-13

EFFECTS OF ANISOTROPIC VERSUS ISOTROPIC CONSOLIDATION IN CONSOLIDATED-UNDRAINED TRIAXIAL COMPRESSION TESTS OF COHESIVE SOILS

by

Robert T. Donaghe and Frank C. Townsend

Soils and Pavements Laboratory
U. S. Army Engineer Waterways Experiment Station
P. O. Box 631, Vicksburg, Miss. 39180

October 1975

Final Report

Prepared for U. S. Army Engineer Division,
Lower Mississippi Valley
Vicksburg, Miss. 39180

Destroy this report when no longer needed. Do not return it to the originator.

Unclassified

SECURITY CLASSIFICATION OF THIS PAGE (When Data Entered)

REPORT DOCUMENTATION PAGE		READ INSTRUCTIONS BEFORE COMPLETING FORM
1. REPORT NUMBER (14) WES-TR-S-75-13 Technical Report S-75-13	2. GOVT ACCESSION NO.	3. RECIPIENT'S CATALOG NUMBER
4. TITLE (and Subtitle) (6) EFFECTS OF ANISOTROPIC VERSUS ISOTROPIC CONSOLIDATION IN CONSOLIDATED-UNDRAINED TRIAXIAL COMPRESSION TESTS OF COHESIVE SOILS.		5. TYPE OF REPORT & PERIOD COVERED (9) Final report. 6. PERFORMING ORG. REPORT NUMBER
7. AUTHOR(s) (10) Robert T. Donaghe, Frank C. Townsend		8. CONTRACT OR GRANT NUMBER(s)
9. PERFORMING ORGANIZATION NAME AND ADDRESS U. S. Army Engineer Waterways Experiment Station Soils and Pavements Laboratory P. O. Box 631, Vicksburg, Miss. 39180		10. PROGRAM ELEMENT, PROJECT, TASK AREA & WORK UNIT NUMBERS
11. CONTROLLING OFFICE NAME AND ADDRESS U. S. Army Engineer Division Lower Mississippi Valley P. O. Box 80, Vicksburg, Miss. 39180		12. REPORT DATE (11) Oct ~~ober 1~~975 13. NUMBER OF PAGES 111 (12) 122 P.
14. MONITORING AGENCY NAME & ADDRESS(if different from Controlling Office)		15. SECURITY CLASS. (of this report) Unclassified 15a. DECLASSIFICATION/DOWNGRADING SCHEDULE
16. DISTRIBUTION STATEMENT (of this Report) Approved for public release; distribution unlimited.		
17. DISTRIBUTION STATEMENT (of the abstract entered in Block 20, if different from Report)		
18. SUPPLEMENTARY NOTES		
19. KEY WORDS (Continue on reverse side if necessary and identify by block number) Cohesive soils Consolidation R tests (soils) Triaxial shear tests		
20. ABSTRACT (Continue on reverse side if necessary and identify by block number) The results of a series of consolidated-undrained (CU) triaxial compression tests performed on normally consolidated and overconsolidated specimens of two clays consolidated both isotropically (ICU tests) and anisotropically (ACU tests) are presented and analyzed in this report. The specimens were trimmed from samples of Vicksburg Buckshot clay (LL = 57) and a clay from the East Atchafalaya Basin Protection Levee (EABPL) project area (LL = 79), both of (Continued)		

DD FORM 1 JAN 73 1473 EDITION OF 1 NOV 65 IS OBSOLETE

Unclassified

SECURITY CLASSIFICATION OF THIS PAGE (When Data Entered)

038 100 JOB

Unclassified
SECURITY CLASSIFICATION OF THIS PAGE(When Data Entered)

20. ABSTRACT (Continued).

5g cm.

which had been consolidated from a slurry in large-diameter consolidometers under a maximum vertical consolidation pressure of 3.0 kg/cm^2. Effective major principal consolidation stresses $\bar{\sigma}_{1c}$ during reconsolidation prior to shear were 0.5, 1.5, 3.0, and 6.0 kg/cm^2. Effective principal stress ratios K_c, where $K_c = \bar{\sigma}_{3c}/\bar{\sigma}_{1c}$ and $\bar{\sigma}_{3c}$ is the lateral consolidation stress, used during reconsolidation were 1.0, 0.67, and 0.5. Data presented include stress-strain curves, pore pressure observations, final water content distributions within the specimens, and shear strength envelopes based on total and effective stresses. Test results indicate that the change in volume during consolidation and the water content at the end of consolidation are not a unique function of the vertical consolidation stresses $\bar{\sigma}_{1c}$ but are related to the mean effective consolidation stress $(\bar{\sigma}_{oct})_c$ where $(\bar{\sigma}_{oct})_c = (\bar{\sigma}_{1c} + \bar{\sigma}_{2c} + \bar{\sigma}_{3c})/3$ and $\bar{\sigma}_{2c}$ is the intermediate principal consolidation stress which, in the case of triaxial compression, is equal to $\bar{\sigma}_{3c}$, and to the deviator stress during consolidation. Anisotropic consolidation produced higher water contents (lower volume changes) than did isotropic consolidation for the same $\bar{\sigma}_{1c}$. The effect of K_c on volume change was more pronounced in the overconsolidated than in the normally consolidated ranges. The ratio of undrained strength s_u to $\bar{\sigma}_{1c}$ was greater for isotropically than for anisotropically consolidated specimens for a given $\bar{\sigma}_{1c}$ and was more dependent upon the K_c ratio in the overconsolidated than in the normally consolidated range, where it was only slightly affected by K_c ratios. Stress-strain characteristics were significantly affected by K_c ratios. The axial strain values at maximum deviator stresses $(\sigma_1 - \sigma_3)_{max}$ generally decreased with decreasing K_c ratio values. The reduction in axial strain values at $(\sigma_1 - \sigma_3)_{max}$ as K_c varied ranged from 33 to 98 percent for Buckshot clay and from 17 to 95 percent for EABPL clay, with the greatest reductions occurring in the normally consolidated range. Induced pore pressures at $(\sigma_1 - \sigma_3)_{max}$ decreased substantially with decreasing K_c ratios for a given $\bar{\sigma}_{1c}$ value. Likewise, the A pore pressure parameter values were considerably lower for anisotropically consolidated specimens. Strength envelopes based upon effective stresses taken at $(\sigma_1 - \sigma_3)_{max}$ show a decrease in angles of internal friction with decreasing K_c ratios. Strength envelopes based upon effective strength envelopes taken at maximum effective major principal stress ratios $(\bar{\sigma}_1/\bar{\sigma}_3)_{max}$ exhibit no effect due to K_c. Total stress envelopes based on Taylor's method of deriving strengths of anisotropically consolidated specimens from test results obtained from isotropically consolidated specimens slightly underestimate observed values. In this context, Taylor's method is an appropriate means of predicting strengths for various K sub c ratios from conventional ICU tests. ~~The~~ Use of hyperbolic stress-strain relationships derived from ICU tests in finite element codes for ACU conditions will lead to erroneous results. Further testing of anisotropically consolidated soils under stress systems that better simulate in situ conditions is needed. Stress systems applied by simple shear, plane strain, and triaxial extension devices are suggested. It is also recommended that a similar investigation be conducted on compacted specimens of Buckshot clay in order to study effects due to soil structure prior to anisotropic consolidation.

Unclassified
SECURITY CLASSIFICATION OF THIS PAGE(When Data Entered)

THE CONTENTS OF THIS REPORT ARE NOT TO BE USED FOR ADVERTISING, PUBLICATION, OR PROMOTIONAL PURPOSES. CITATION OF TRADE NAMES DOES NOT CONSTITUTE AN OFFICIAL ENDORSEMENT OR APPROVAL OF THE USE OF SUCH COMMERCIAL PRODUCTS.

PREFACE

The investigation reported herein was conducted for the U. S. Army Engineer Division, Lower Mississippi Valley (LMVD). The testing program was authorized by LMVD-G letter dated 31 August 1972, subject: Status of Soils and Pavements Laboratory projects for MRC and LMVD for FY 72 and proposed FY 73. The testing was performed at the U. S. Army Engineer Waterways Experiment Station (WES) during the period January-July 1973 by personnel of the Soils and Pavements Laboratory (S&PL).

The study was conducted by Mr. R. T. Donaghe, Laboratory Research Facility, Soil Mechanics Division, under the direct supervision of Dr. F. C. Townsend, Chief, Soils Research Facility, and the general supervision of Mr. C. L. McAnear, Chief, Soil Mechanics Division. Mr. S. J. Johnson, Special Assistant to the Chief, S&PL, provided technical advice. Messrs. J. P. Sale and R. G. Ahlvin were Chief and Assistant Chief, respectively, of the S&PL. This report was prepared by Mr. Donaghe and Dr. Townsend.

Directors of WES during the investigation were BG E. D. Peixotto, CE, and COL G. H. Hilt, CE. Mr. F. R. Brown was Technical Director.

CONTENTS

CONVERSION FACTORS, U. S. CUSTOMARY TO METRIC (SI)
UNITS OF MEASUREMENT

U. S. customary units of measurement used in this report can be converted to metric (SI) units as follows:

Multiply	By	To Obtain
inches	2.54	centimetres
pounds (mass)	0.4535924	kilograms
pounds (force) per square inch	6894.757	pascals
pounds (mass) per cubic foot	16.01846	kilograms per cubic metre
gallons	3.785412	cubic decimetres

EFFECTS OF ANISOTROPIC VERSUS ISOTROPIC CONSOLIDATION IN CONSOLIDATED-UNDRAINED TRIAXIAL COMPRESSION TESTS OF COHESIVE SOILS

PART I: INTRODUCTION

Background

1. Isotropic stress conditions are generally used in routine triaxial testing of naturally sedimented and compacted soils even though in situ stress conditions are usually anisotropic. The reason generally given for this testing inconsistency is that anisotropic consolidation requires complicated procedures and extra periods of time. Additionally, in the past it was thought that the angle of shearing resistance was not significantly affected by the method of consolidation; however, recent evidence indicates that this may not be the case for all soils. Also, it has been pointed out that the stress-deformation characteristics of anisotropically consolidated soils are very different from those determined on the same soil using isotropic consolidation. With the advent of numerical techniques which rely on the stress-deformation properties, it is becoming increasingly important that these properties be as representative as possible of field conditions.

Previous Investigations

2. Early investigations by Rendulic[1] indicated that the change in water content during consolidation and stress paths during shear are the same in consolidated-undrained (CU)* tests performed on both isotropically consolidated specimens (ICU tests) and anisotropically consolidated specimens (ACU tests), provided the vertical consolidation

---

* For convenience, symbols and unusual abbreviations are listed and defined in the Notation (Appendix C).

stress $\bar{\sigma}_{1c}$ is the same in both cases. This theory was emphasized by Taylor[2] and later confirmed experimentally by Henkel.[3] As a result of this theory, Skempton and Bishop[4] assumed that the pore pressure parameter at failure A_f and the effective angle of internal friction ϕ' are constant and are not influenced by the effective principal consolidation stress ratio K_c, where $K_c = \bar{\sigma}_{3c}/\bar{\sigma}_{1c}$ and $\bar{\sigma}_{3c}$ and $\bar{\sigma}_{1c}$ are the lateral consolidation stress and vertical consolidation stress, respectively. Later, Lowe and Karafaith[5] and Bjerrum and Lo[6] proposed semi-analytical expressions for predicting ACU test results from tests using ICU conditions during shear.

3. Studies by many investigators have both confirmed and denied the conclusions of the earlier researchers. Most of the disagreement appears to center around the hypothesis attributed to Rutledge,[7] which states that the water content after consolidation and the undrained strength are independent of K_c ratios. Among investigations that have tended to verify the Rutledge hypothesis are those conducted by Broms and Ratnam,[8] Henkel,[9] and Lee,[10] all of whom based their conclusions on tests of compacted soils having liquid limit (LL) values of less than 50 percent. Henkel, however, in a later study[11] stated that the assumption of the uniqueness of the water content versus $\bar{\sigma}_{1c}$ relationship may not hold for all clays. Among studies that have not verified the Rutledge hypothesis are those by Ladd,[12] Whitman, Ladd, and DaCruz,[13] and Khera and Krizek.[14] Ladd[12] performed ICU and ACU tests on six different clays (LL = 33-80), three of which were compacted and the remainder undisturbed. He showed that ϕ' based on maximum deviator stresses $(\sigma_1 - \sigma_3)_{max}$, where σ_1 is the major principal stress and σ_3 is the lateral stress, is as much as 4 deg lower for ACU tests. The differences averaged 4 deg for the undisturbed clays and less than 1 deg for the compacted soils, thereby indicating a possible effect due to initial structure. This possibility is strengthened by the observation that the difference in ϕ' at maximum obliquity $(\bar{\sigma}_1/\bar{\sigma}_3)_{max}$, where $\bar{\sigma}_1$ is the effective major principal stress and $\bar{\sigma}_3$ is the effective lateral stress, was less than 1 deg for all the soils tested. Whitman, Ladd, and DaCruz[13] tested a reconsolidated clay (LL = 63)

prepared by consolidating a slurry of the material in a large consolidometer. They observed that the ratio $s_u/\bar{\sigma}_{1c}$, where s_u is the undrained strength and $\bar{\sigma}_{1c}$ is the maximum vertical consolidation pressure may be independent of K_c when the specimen has been brought close to failure during consolidation. They also noted that for a given value of $\bar{\sigma}_{1c}$, water contents were lower in ACU than in ICU tests. Khera and Krizek[14] obtained similar results in tests performed on a clay (LL = 55) prepared for testing by passing premoistened soil through a sample extruder. Their tests showed that apart from its dependence on K_c , the $s_u/\bar{\sigma}_{1c}$ ratio for anisotropically consolidated specimens was also a function of the rate of strain during shear. Higher values of $s_u/\bar{\sigma}_{1c}$ were determined for lower K_c values when the rate of strain was increased.

4. Test data developed in all but one of the investigations (Khera and Krizek[14]) indicated that pore pressure parameters at failure A_f and axial strain values at failure were lower for ACU than for ICU test specimens. Khera and Krizek[14] found that the axial strain at failure was insensitive to the method of consolidation. Interestingly, they stated that the soil structure imparted by forcing soil through an extruder resulted in the clay particles aligning themselves with their long axes parallel to the direction of the $\bar{\sigma}_{1c}$ stress, a condition opposite that in naturally consolidated clays. This once again suggests a possible effect due to structure. Unfortunately, all of the investigators practically ignored the influence of K_c on stress-deformation characteristics during shear. Also, previous investigations have not shown effects of stress history and anisotropy due to in situ consolidation stresses on results of tests in which K_c was varied.

Purpose and Scope

5. The purpose of this investigation is to provide additional information concerning the adequacy of the Rutledge hypothesis[7] and also to provide stress-deformation data for use in determining the applicability of existing mathematical models used by various computer codes to predict stress-deformation characteristics. These objectives

were accomplished by performing CU triaxial compression tests with pore pressure measurements on specimens of two clays which were consolidated both isotropically and anisotropically prior to shear in such a manner that undrained shear strength and corresponding deformation characteristics could be developed in both the normally consolidated and overconsolidated ranges. In addition, tests were performed to determine effects due to strain rate and end restraint on strength and deformation characteristics of both ACU and ICU test specimens. In order to simulate the response of naturally sedimented and consolidated materials and to provide test specimens as nearly identical as possible, the soils used in the investigation were prepared in large consolidometers. Samples prepared in this manner have a known vertical stress-strain history from the slurry condition to the final consolidation pressure. The data developed in the investigation were analyzed, and significant differences concerning the effects of anisotropic consolidation were reported.

PART II: MATERIALS, TESTING PROGRAM, TESTING EQUIPMENT, SAMPLE PREPARATION, AND PROCEDURES

Description of Soil

6. The two soils tested in this investigation were Vicksburg Buckshot clay and a clay prepared from undisturbed samples taken from Test Section III of the East Atchafalaya Basin Protection Levee (EABPL) test area. The Vicksburg Buckshot clay was originally taken from a typical backswamp deposit in the lower Mississippi Valley and processed for use in a previous testing program. Prior to use in this investigation, it was air-dried, crushed, screened through a 1/4-in.* screen, and then ground in a coffee grinder. The EABPL clay consisted of a mixture of portions of undisturbed samples 22B, 22C, 23B, and 23C from boring 85-BUE, located at sta 1396+25 on the center line of the test section. This material was also taken from a backswamp deposit and was essentially an inorganic clay containing pieces of wood and sandy and silty seams. The wood and silty and sandy seams were discarded prior to the time the material was used in the investigation. Results of classification tests performed on reconsolidated samples of the two clays are as follows:

Characteristic	Vicksburg Buckshot Clay	EABPL Clay
Liquid limit	57	79
Plastic limit	21	26
Plasticity index	36	53
Specific gravity of solids	2.69	2.72

Testing Program

7. To determine the effect of the effective principal consolidation stress ratio K_c on the stress-deformation properties of clays,

* A table of factors for converting U. S. customary units of measurement to metric (SI) units is presented on page 4.

CU triaxial compression tests were to be performed on 1.4-in.-diam by 3-in.-high specimens of the two clays using standard end platens. Specimens of the clays were to be trimmed from samples consolidated from a slurry in 8-in.-diam consolidometers under a maximum vertical consolidation stress $\bar{\sigma}_{1c}$ of 3.0 kg/cm^2 and then reconsolidated both isotropically and anisotropically prior to shear under effective major principal stresses $\bar{\sigma}_{1c}$ of 0.5, 1.5, 3.0, and 6.0 kg/cm^2. Effective principal stress ratios K_c were to be 1, 0.67, and 0.5. Thus, for each soil, four tests were to be performed on isotropically consolidated specimens and eight tests were to be on anisotropically consolidated specimens.

8. In addition to the tests described in the preceding paragraph, several CU tests were to be performed on both isotropically and anisotropically consolidated specimens of the Buckshot clay to determine effects due to varying the rate of strain and the degree of end restraint. The effective major principal consolidation stresses $\bar{\sigma}_{1c}$ for these tests were to be 0.5 and 6.0 kg/cm^2, with specimens consolidated using K_c ratios of 1 and 0.5. Four tests using a tenfold increase in rate of strain and four tests using low-friction caps and bases were to be performed. Specimens tested using low-friction caps and bases were to be 1.5 in. high so that buckling during consolidation and shear could be avoided.

9. Finally, it was proposed that four specimens of the EABPL clay consolidated under K_o conditions (no lateral strain) be studied in CU triaxial tests, in which $\bar{\sigma}_{1c}$ stresses were to be the same as those used for the initial part of the testing program, i.e. 0.5, 1.5, 3.0, and 6.0 kg/cm^2. Results of these tests would be correlated with those obtained for specimens consolidated under a constant effective major principal stress ratio. The total proposed testing program is outlined in Table 1.* Testing was initiated on 17 January and completed in the first week of July 1973.

---

* Several changes (i.e., additional tests performed using slower rates of strain and several tests performed on 3.5-in.-high specimens) were made in the testing program as testing progressed. These changes and the reasons for them are noted in the discussion of test results.

Description of Equipment

10. A schematic diagram and a photograph of the testing apparatus used for anisotropically consolidating and shearing specimens are shown in Figures 1a and 1b, respectively. The testing apparatus for isotropically consolidating and shearing specimens (Figure 2) is the same as that shown in Figures 1a and 1b except for the lack of a pneumatic stress cell, which is not needed in isotropically consolidating and shearing specimens. The triaxial testing facility is shown in Figure 3. Triaxial chambers utilizing rolling diaphragms as piston seals were used to minimize piston friction. Chamber and back pressures were applied using compressed air controlled by pneumatic pressure regulators. The pneumatic cells used to apply $\bar{\sigma}_{1c}$ stresses during anisotropic consolidation were also pressurized with compressed air controlled by pneumatic pressure regulators. All pneumatic pressures were measured with Bourdon tube gages. Pore water pressures were measured with electronic pressure transducers. The force applied to the piston was measured using an electronic load cell. Transducers, load cells, and gages were calibrated so that all pressures and stresses were accurate to 0.02 kg/cm^2. Changes in height of the specimen were measured during consolidation with a dial indicator reading 0.01 mm per division and during shear with a displacement potentiometer calibrated to the nearest 0.001 in. During shear, the load cell, pore pressure transducer, and displacement potentiometer readings were automatically plotted by an x-y-y recorder. De-aired distilled water was used to saturate the specimen and also for the chamber fluid. The volume of water entering and leaving the specimen during saturation and consolidation was measured using glass burettes reading 0.1 cc per division. The enlarged caps and bases utilized for the tests performed with low end restraint had completely plane, highly polished bearing surfaces.* Low friction was provided by a thin layer of high-vacuum silicone

---

* Caps and bases normally used in CU triaxial tests in the Soils Research Facility are separated from the specimen by a 1.4-in.-diam by 1/8-in.-thick disk of sintered stainless steel.

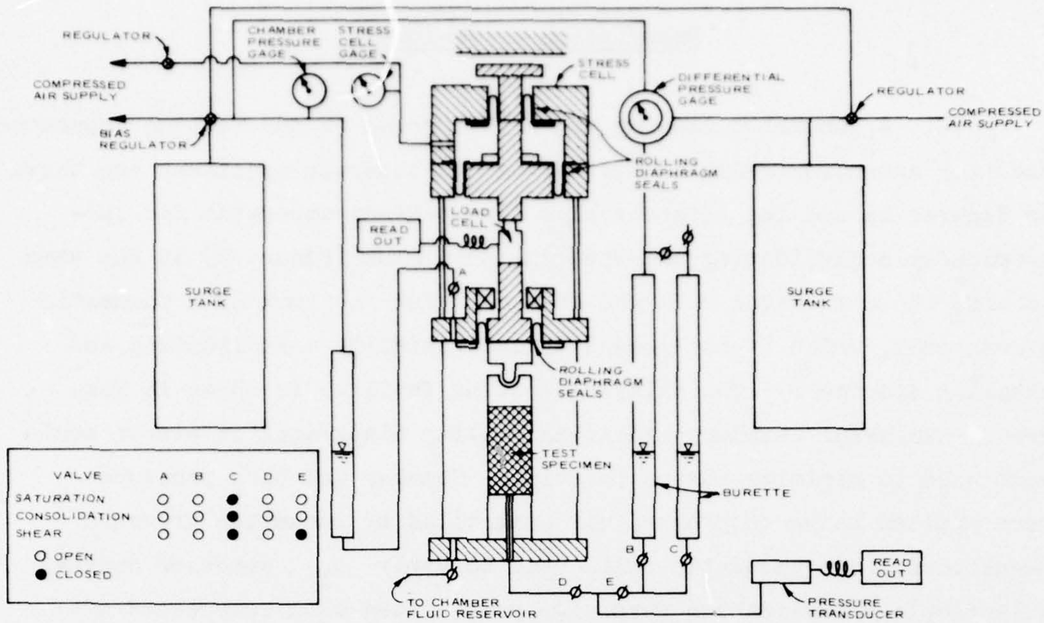

a. Schematic drawing

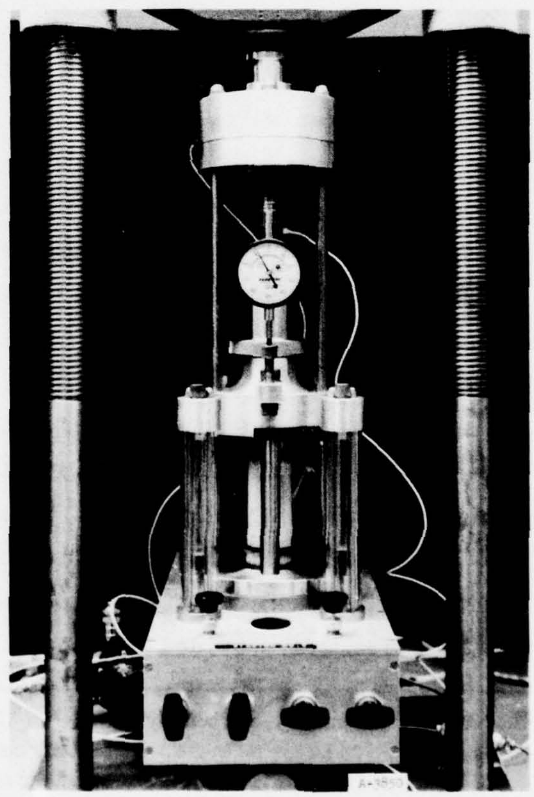

b. Photograph

Figure 1. Testing apparatus used for anisotropically consolidating and shearing specimens

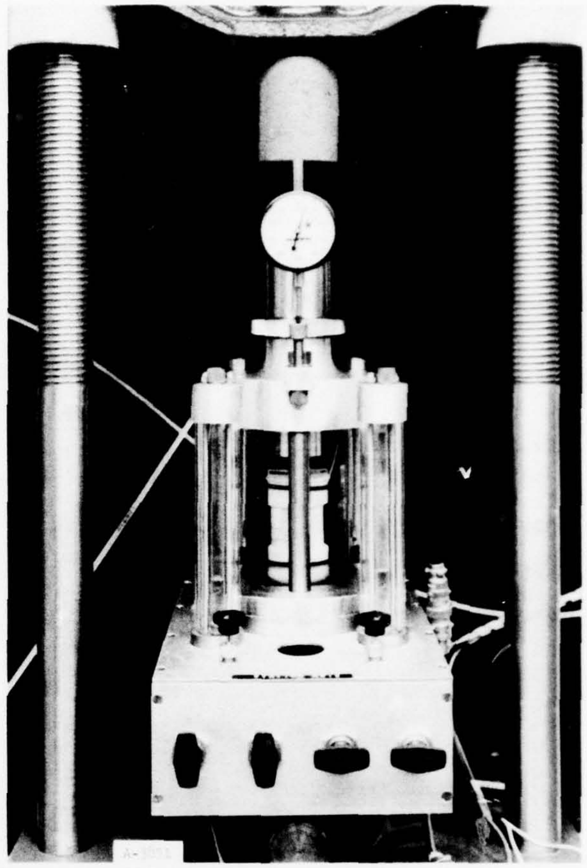

Figure 2. Testing apparatus for isotropically consolidating and shearing specimens. Specimen 1.5 in. high being tested using low-friction cap and base

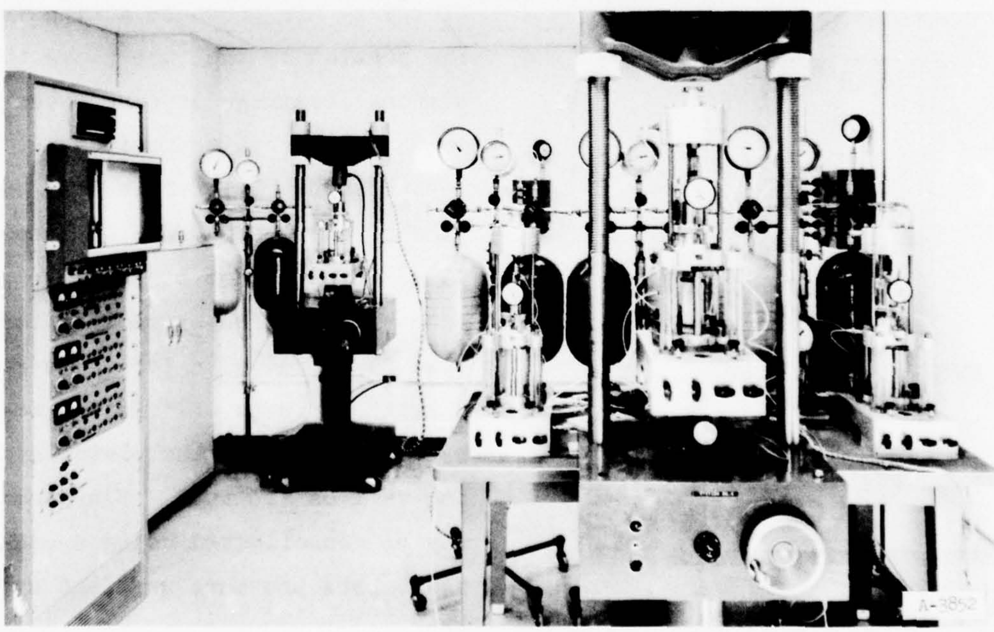

Figure 3. Triaxial testing facility

grease and a thin Teflon disk which separated the ends of the specimen from the bearing surfaces. The bases had drainage ports in their sides, over which filter strips made from Whatman No. 1 chromotography paper and extending from the perimeter of the specimen were placed. In each test, filter strips were evenly spaced around the perimeter and extended over the total height of the specimen. Fifty percent of the specimen circumference was covered by the strips.

Sample Preparation

Slurry consolidometers

11. The test specimens were trimmed from samples consolidated from a slurry in 8-in.-diam consolidometers under a maximum vertical consolidation stress of 3.0 kg/cm^2. The consolidometers were designed and fabricated at Northwestern University, Evanston, Illinois. As shown in Figure 4, the consolidometer is essentially a large vertical steel tube sealed at both ends. A piston having a cross-sectional area the same as that of the inside of the tube is forced against the slurry by air pressure acting in the portion of the tube above the piston. Drainage of pore water from the slurry is provided by porous stones located in the lower face of the piston and the upper face of the bottom seal of the tube. The inside surface of the tube is coated with Teflon to reduce the effects of friction between the side of the piston and the wall of the tube. Slurries may be consolidated using a constant pore pressure gradient by

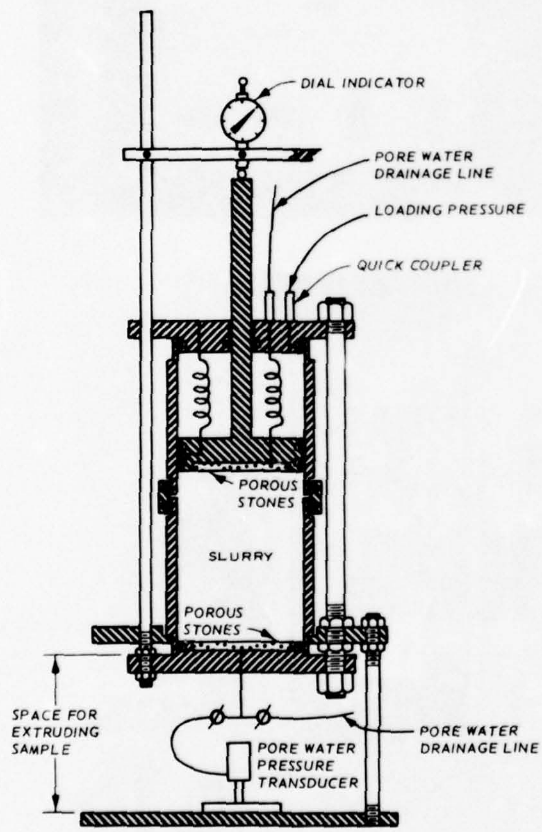

Figure 4. Slurry consolidometer

closing the valve on the bottom pore water drainage line and using a servovalve, which automatically opens to increase the pressure acting on the piston when the pore pressure at the bottom of the slurry falls below a preset value and which closes automatically when the pore pressure is increased beyond a preset value. Drainage in this case is from the top of the sample only. Suggested operational procedures for the consolidometers are given in Reference 15.

Slurry preparation and placement

12. The three Buckshot slurries were prepared by sifting predetermined amounts of air-dried soil through a No. 60 sieve into containers containing preweighed amounts of boiling, de-aired, demineralized water. Boiling, de-aired water was used to keep the amount of air in the slurry at a minimum during the preparation procedure. Amounts of air-dried soil were computed by assuming a final consolidated sample height of 5 in. and estimating the sample density after consolidation. The weight of water was determined by assuming a final slurry water content of 1.5 times the LL. The mixture of soil and water was continually stirred during the process of adding soil. The amounts of time spent preparing the slurries ranged from 3 to 5 hr.

13. The EABPL slurry was prepared by blending batches of undisturbed soil with de-aired, demineralized water in a 1-gal-capacity, heavy-duty blender. The blender was filled to approximately one-third of its capacity with soil at its natural water content, and water was added until the water content of the resulting soil-water mixture was 1.5 times the LL of the soil. Each mixture of soil and water was blended for a period of 3 min and then emptied into a large container. This procedure was repeated until a quantity of slurry sufficient for two consolidated samples was prepared. As in the preparation of the Buckshot slurries, computations for the proper amount of soil were based on a final consolidated sample height of 5 in. and an estimate of the sample density after consolidation. The total slurry was thoroughly mixed prior to being placed in the consolidometers.

14. The slurries of both materials were placed in the consolidometers by drawing them under vacuum from their containers through

a 1/2-in.-ID nylon tube passing from the container to the evacuated consolidometer. The tubing was forced through a hole in a rubber stopper placed in the piston opening located in the upper end plate of the consolidometer. The vacuum in the consolidometer also allowed placement of the slurries under almost completely de-aired conditions, and as can be seen from the initial specimen conditions given in Table 2, it assured high saturation values for the consolidated samples.

15. After placement of the slurry was completed, the upper end plate was removed, and the piston was placed in the consolidometer. Then the upper end plate was replaced, and loading was initiated. The first slurry of each material was consolidated using the controlled pore pressure gradient method mentioned in paragraph 11. Based on the rate of loading of these samples, a procedure for manually loading the remaining samples was developed so that the total time of consolidation could be decreased. (During manual loading the sample may be drained from both top and bottom as opposed to drainage from the top only when the controlled pore pressure gradient procedure is used.) Using manual loading, the total time of consolidation averaged 2-1/2 months for both materials. All samples were rebounded in at least three stages and allowed to come to equilibrium under a no-load condition prior to being removed from the consolidometer. After being removed from the consolidometers, the samples were covered with several layers of paraffin and then stored in a humid room. Examples of water content distributions and of void ratio and pressure versus elapsed time relationships are given in Figures 5 and 6, respectively. Additional information on methods of slurry preparation and characteristics of samples consolidated in the consolidometer are discussed in Reference 17.

Triaxial specimen preparation

16. Individual test specimens were trimmed from the samples so that the vertical axes of the specimens were parallel to that of the sample. To avoid effects due to friction between the side of the piston and the wall of the tube, specimens were trimmed to no closer than 1/2 in. from the edge of the sample. Each specimen was weighed immediately after trimming and then placed on a saturated porous stone

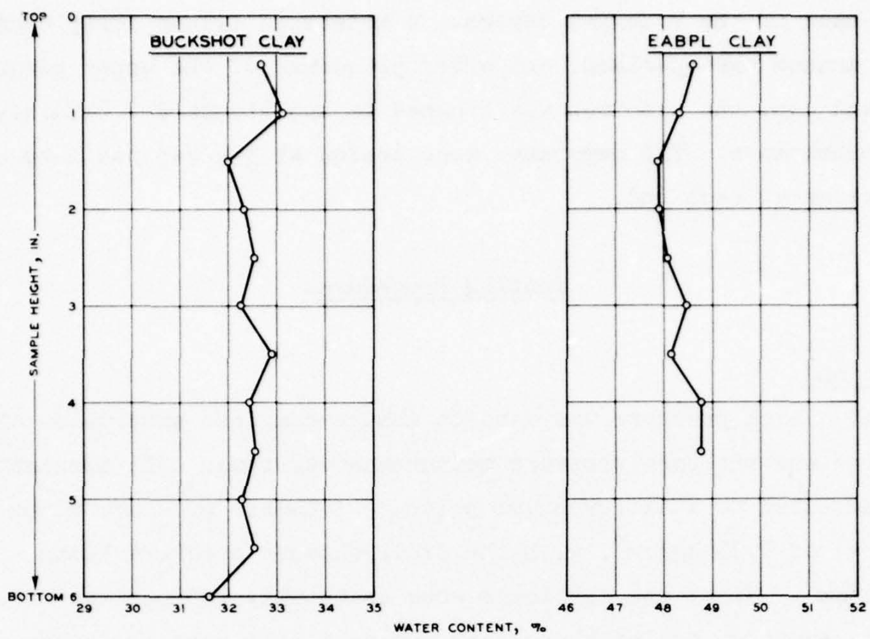

Figure 5. Examples of vertical water content profiles for reconsolidated samples of Buckshot and EABPL clays

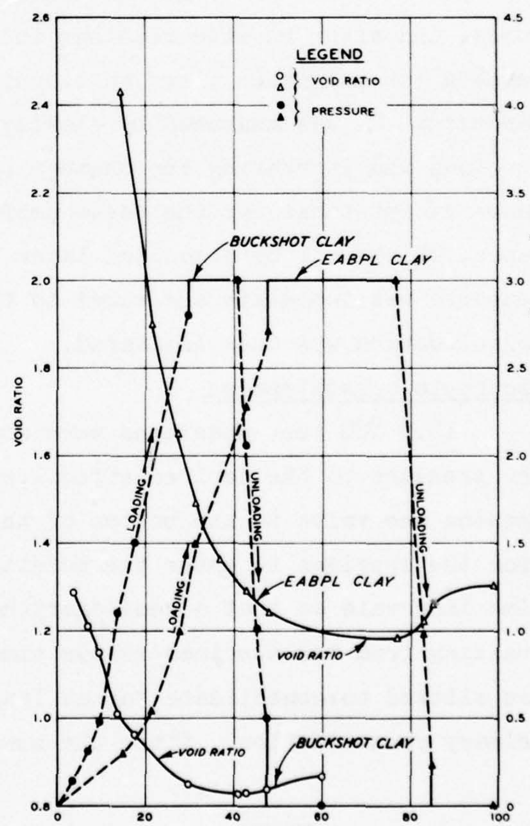

Figure 6. Examples of void ratio and pressure versus elapsed time relationships for samples of Buckshot and EABPL clays consolidated from a slurry

on the base of the triaxial device. A moistened filter strip cage was placed around the specimen, and after placement of the upper porous stone and cap, the specimen was encased in two standard 0.012-in.-thick rubber membranes. The membranes were sealed at the cap and base using two O-rings at each end.

Testing Procedures

Saturation

17. Back pressure was used to ensure complete saturation of the specimens and the pore pressure measurement systems. All specimens were subjected to a differential pressure (chamber pressure minus back pressure) of 0.25 kg/cm^2, with the final chamber pressure being 4.50 kg/cm^2. Since the specimens were essentally 100 percent saturated prior to testing, the back pressure was primarily used to saturate the pore pressure measurement systems. Access to water at the bottom of the specimens was provided immediately upon application of these pressures, and after burette readings indicated that equilibrium had been reached (in all cases after an overnight period), the pore pressure parameter B was measured by closing the valve to the bottom of the specimen and increasing the chamber pressure by 0.25 kg/cm^2. In all cases except those for the tests performed using low-friction caps and bases, which will be discussed later in this report, the pore pressure response was immediate and equal to the increase in chamber pressure. Consolidation was then initiated.

Isotropic consolidation

18. ICU test specimens were consolidated by increasing the chamber pressure to the desired effective consolidation stress and then opening the valve to the bottom of the specimen, thus allowing water from the specimen to enter the burette. Burette readings were taken at time intervals so that a semilogarithmic plot of the volume of water draining from the specimen versus time could be made. Each specimen was allowed to consolidate for at least 24 hr after completion of primary consolidation. After the burette readings indicated that an

equilibrium condition had been achieved, the valve to the bottom of the specimem was closed and the vertical height indicator was read. Shear was then initiated.

Anisotropic consolidation

19. ACU test specimens were consolidated by almost simultaneously increasing the major and minor principal stresses in small increments using the desired K_c ratio. The major principal stress (applied using the pneumatic stress cell) was increased in 0.50-kg/cm^2 increments, while the lateral stress (chamber pressure) was increased in increments dictated by the desired effective consolidation stress ratio. Sufficient time (usually 8 hr) was allowed between increments to complete primary consolidation. Immediately after each increase in stress, the valve to the bottom of the specimen was opened to allow water to enter the burette. The burette and vertical dial readings were plotted versus the logarithm of time so that the time for completion of consolidation could be determined. The longest time required to consolidate an ACU test specimen was 14 days for the Buckshot clay consolidated under $K_c = 0.5$ to $\bar{\sigma}_{1c} = 6.0$ kg/cm^2, while 4 days was required to consolidate the ICU specimen of the same material to $\bar{\sigma}_{1c} = 6.0$ kg/cm^2. After each specimen was consolidated for a sufficient time (at least 48 hr) under the desired total stress level, the valve to the bottom of the specimen was closed and shear was initiated.

K_o consolidation

20. Specimens of the EABPL clay were consolidated under K_o conditions (no lateral strain) by increasing the major and minor principal stresses almost simultaneously. This was accomplished by using an estimated K_c ratio and then adjusting the $\bar{\sigma}_{3c}$ value so that the change in volume as indicated by burette readings was equal to the product of the change in height indicated by the dial indicator and the original specimen cross-sectional area. The major principal consolidation stress $\bar{\sigma}_{1c}$ was increased in 0.50-kg/cm^2 increments. Sufficient time was allowed between increments to complete primary consolidation. Upon completion of consolidation under the total desired $\bar{\sigma}_{1c}$ value, undrained shear was initiated.

Shear

21. Upon completion of consolidation, specimens were axially loaded at a constant rate of strain. When the specimen had been deformed to 20 percent axial strain or when the limit of the piston travel had been reached, the test was stopped and the chamber pressure was removed, with the valve to the bottom of the specimen remaining closed. The chamber was then quickly moved to the humid room where the drainage line to the bottom of the specimen was removed. The membranes covering the specimen were removed, and the specimen was cut into five horizontal slices. Water contents of the slices were then determined. The zero readings of the load cell and transducer were checked at the end of the test.

PART III: TEST RESULTS AND ANALYSIS

22. Results of the 41 CU triaxial tests performed on the two soils are summarized in Tables 2 and 3 and presented graphically in Figures 7-78. The tests are grouped in the tables and figures according to major principal consolidation stress $\bar{\sigma}_{1c}$. Tests 1-22 were performed on specimens of Vicksburg Buckshot clay, and tests 22-41 were performed on specimens of the EABPL clay. The results are discussed under the following headings:

- a. Specimen properties.
- b. Deviator stresses.
- c. Induced pore pressures.
- d. Effective stresses.
- e. Strength envelopes.
- f. Hyperbolic stress-strain behavior.

Specimen Properties

Initially

23. The homogeneity of the consolidated slurries is reflected by the data indicating initial specimen conditions (Tables 2 and 3). Water contents of the Buckshot specimens ranged from 31.8 to 33.5 and averaged 32.5 percent. Water contents of the EABPL clay varied from 46.1 to 48.2 and averaged 47.3 percent. Dry unit weights of the Buckshot specimens ranged from 88.4 to 90.7 and averaged 90.1 pcf. Those of the EABPL specimens varied from 72.9 to 75.1 and averaged 73.8 pcf.

Volume changes during consolidation

24. Consolidation data given in Tables 2 and 3* indicate that the K_c ratios significantly affected the volume change characteristics of both soils. As can be seen in Figures 7-10, the change in volume during consolidation, i.e., the reduction in volume, of ACU test

---

* Tests 30, 32, and 34 were performed on 3.5-in.-high specimens after previous tests on standard 3.0-in.-high specimens indicated height-diameter ratios after consolidation of considerably less than 2:1.

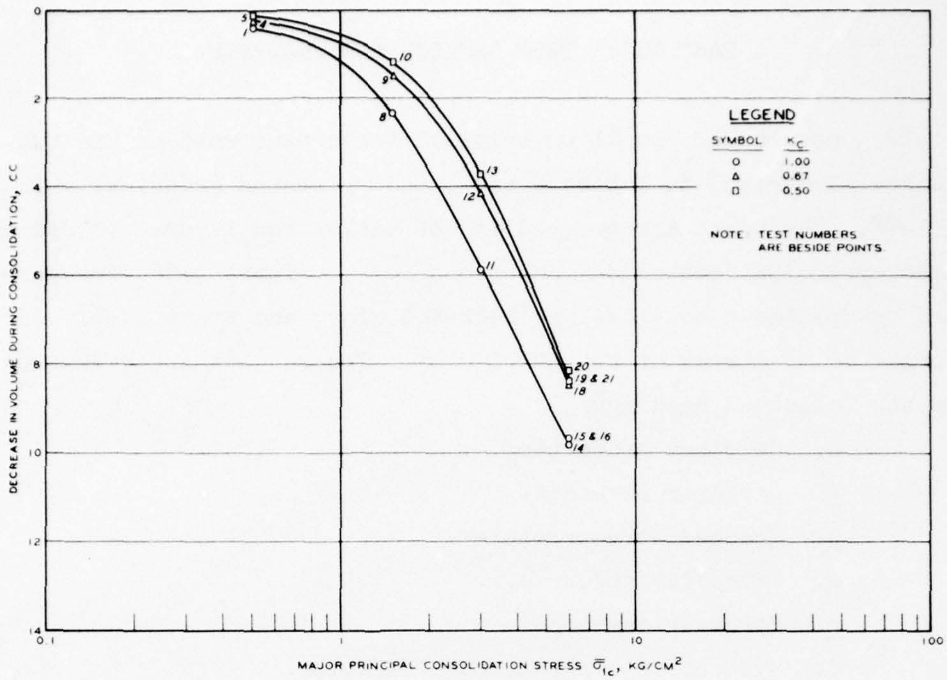

Figure 7. Change in volume during consolidation versus the logarithm of the vertical effective consolidation stress for anisotropically and isotropically consolidated specimens of Buckshot clay

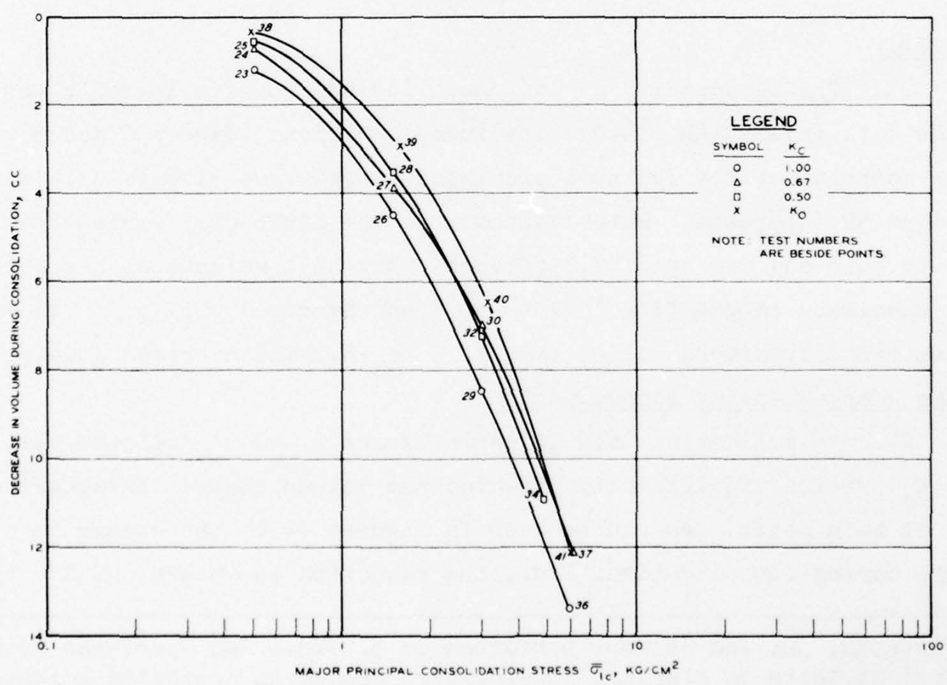

Figure 8. Change in volume during consolidation versus the logarithm of the vertical effective consolidation stress for anisotropically and isotropically consolidated specimens of EABPL clay

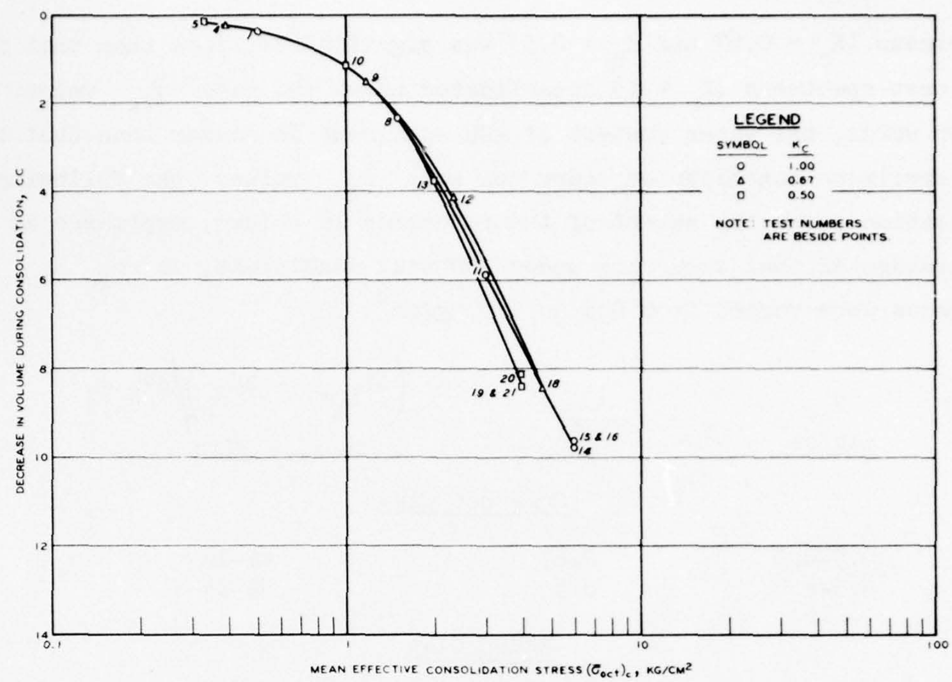

Figure 9. Change in volume during consolidation versus the logarithm of the mean effective consolidation stress for anisotropically and isotropically consolidated specimens of Buckshot clay

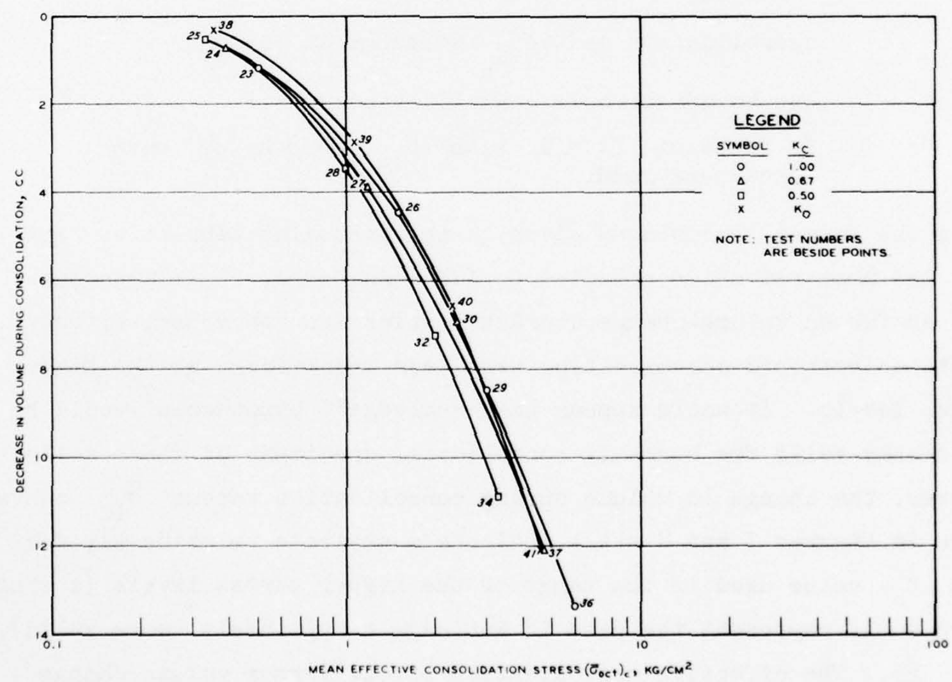

Figure 10. Change in volume during consolidation versus the logarithm of the mean effective consolidation stress for anisotropically and isotropically consolidated specimens of EABPL clay

specimens (K_c = 0.67 and K_c = 0.5) was significantly less than that for ICU test specimens (K_c = 1) consolidated under the same $\bar{\sigma}_{1c}$ value. In other words, the water content of ACU specimens is higher than that for ICU specimens consolidated under the same $\bar{\sigma}_{1c}$ value. The following tabulation shows the extent of the reduction in volume, expressed as a percentage of that occurring under ICU test conditions, as $\bar{\sigma}_{1c}$ stresses were varied from 0.5 to 6.0 kg/cm^2.

$\bar{\sigma}_{1c}$ kg/cm^2	K_c	$\left(\Delta V_{K_c=1} - \Delta V_{K_c}\right) / \Delta V_{K_c=1}$ %
	Buckshot Clay	
0.5-6.0	0.67	44-13
0.5-6.0	0.5	80-14
	EABPL Clay	
0.5-6.0	0.67	40-10
0.5-6.0	0.5	60--*

Note: $\Delta V_{K_c=1}$ = change in volume due to isotropic consolidation and ΔV_{K_c} = change in volume due to anisotropic consolidation.

* Tests at K_c = 1 with $\bar{\sigma}_{1c}$ = 4.8 kg/cm^2 were not performed.

Since the larger percentages given in the preceding tabulation represent the most reduction relative to ICU conditions, it is apparent that as far as volume-change characteristics are concerned, effects due to anisotropic consolidation were less significant at the higher stress levels. It would appear that Rutledge's hypothesis[7] would be reasonably valid for normally consolidated specimens of these soils; however, the change in volume during consolidation versus $\bar{\sigma}_{1c}$ curves shown in Figures 7 and 8 still indicate a separate relationship for each K_c value used in the range of the higher stress levels (a single curve would represent the data if Rutledge's hypothesis[7] were valid).

25. The effective consolidation stress versus volume change

relationship appears to be better represented by the relationship between the mean effective consolidation stress $(\bar{\sigma}_{oct})_c$ (i.e. $(\bar{\sigma}_{1c} + \bar{\sigma}_{2c} + \bar{\sigma}_{3c})/3$, where $\bar{\sigma}_2'$ is the intermediate principal consolidation stress) and volume change during consolidation depicted in Figures 9 and 10. Whitman, Ladd, and DaCruz[13] have demonstrated that plots of $(\bar{\sigma}_{oct})_c$ versus water content provide a better relationship than do plots of $\bar{\sigma}_{1c}$ versus water content, and this is consistent with elastic theory in which volumetric strain in the general case is expressed as a function of $\bar{\sigma}_1 + \bar{\sigma}_2 + \bar{\sigma}_3$, where $\bar{\sigma}_1$ is the major principal stress and $\bar{\sigma}_2$ and $\bar{\sigma}_3$ are the intermediate and minor principal stresses, respectively. Nevertheless, these curves (Figures 9 and 10) do diverge slightly at the higher stress levels, probably due to additional volume changes occurring as a result of the higher deviator stresses acting during anisotropic consolidation at these stress levels.

26. While these data suggest that Rutledge's empirical observations[7] are valid for practical purposes as far as normally consolidated specimens are concerned, it should nevertheless be recognized that an identical water content or change in volume for ICU and ACU specimens can occur only under special conditions. In this context, volumetric strain during anisotropic consolidation can be expressed as a function of the mean effective consolidation stress and deviator stress (due to K_c ratio) during consolidation (References 18 and 19) or as:

$$\frac{\Delta V}{V} = \alpha\left(\bar{\sigma}_{oct}\right)_c + \beta\left(\bar{\tau}_{oct}\right)_c \tag{1}$$

where

ΔV = change in volume

V = volume

α = parameter of volumetric strain due to $(\bar{\sigma}_{oct})_c$

$(\bar{\sigma}_{oct})_c$ = mean effective consolidation stress

β = parameter of volumetric strain due to $(\bar{\tau}_{oct})_c$

$(\bar{\tau}_{oct})_c$ = mean shear stress during consolidation

In the case of isotropic consolidation, no deviatoric, i.e. shear, stresses are acting and $\left(\bar{\tau}_{oct}\right)_c$ equals zero; hence,

$$\frac{\Delta V}{V} = \alpha\left(\bar{\sigma}_{oct}\right)_c \tag{2}$$

Therefore, the divergence of the relationships presented in Figures 9 and 10 at the higher stress levels may be attributed to the additional volume changes occurring as a result of the higher deviator stresses acting during anisotropic consolidation.

K_o characteristics

27. Plots of $\bar{\sigma}_{1c}$ versus specimen cross-sectional areas after consolidation are given in Figures 11 and 12. The areas were computed by dividing the change in volume during consolidation by the change in height. Figure 11 shows that the K_c ratios used in tests performed on the Buckshot clay using standard end platens were not sufficient to encompass K_o conditions (no change in specimen cross-sectional area). The K_o value for this soil based on results determined using standard end platens is apparently less than 0.5. The same relationship for the EABPL clay given in Figure 12 shows that the K_o values for this soil are between 0.5 and 0.67. Figure 13 gives the relationships between K_c and specimen cross-sectional areas after consolidation for the EABPL clay. By plotting K_c values at points where the curves cross the line representing the specimen cross-sectional area prior to consolidation A_o versus the corresponding $\bar{\sigma}_{1c}$ values, a relationship between K_o and $\bar{\sigma}_{1c}$ may be obtained. This relationship is given in Figure 14. Included in the same figure are K_o values determined by the tests performed on specimens consolidated to the same $\bar{\sigma}_{1c}$ value but with K_c being varied throughout the consolidation phase to maintain the initial specimen cross-sectional area. As can be seen in this figure, these relationships are practically identical, thus suggesting that K_o values may be determined from tests in which K_c ratios are maintained constant and $\bar{\sigma}_{1c}$ values are varied.

28. As a matter of interest, K_o values computed from effective

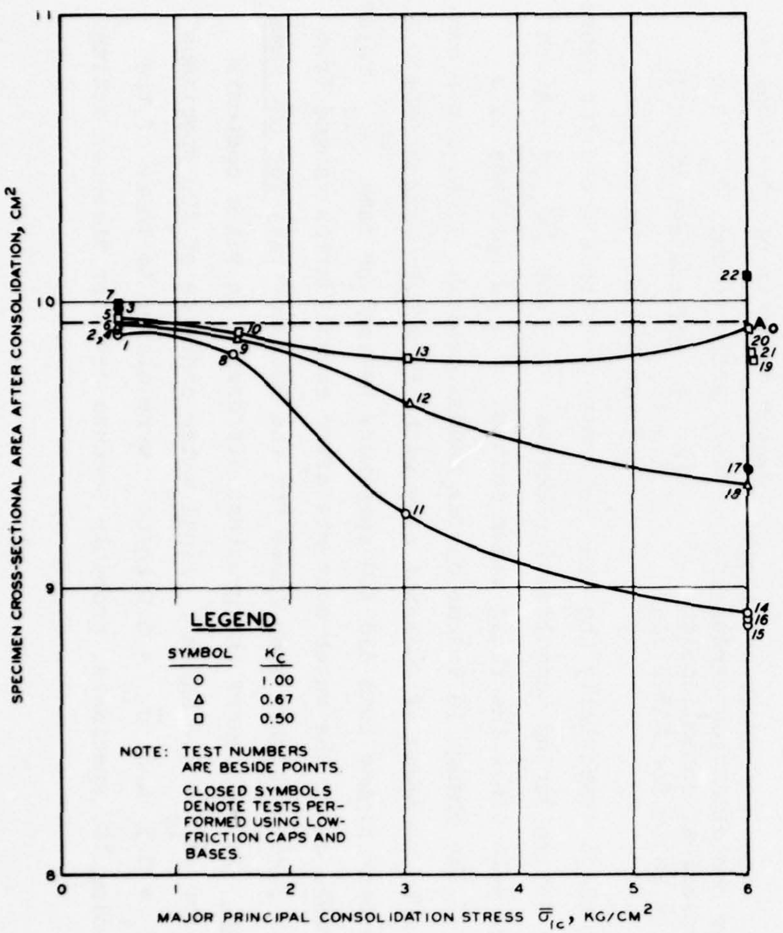

Figure 11. Specimen cross-sectional area after consolidation versus major principal consolidation stress for Buckshot clay

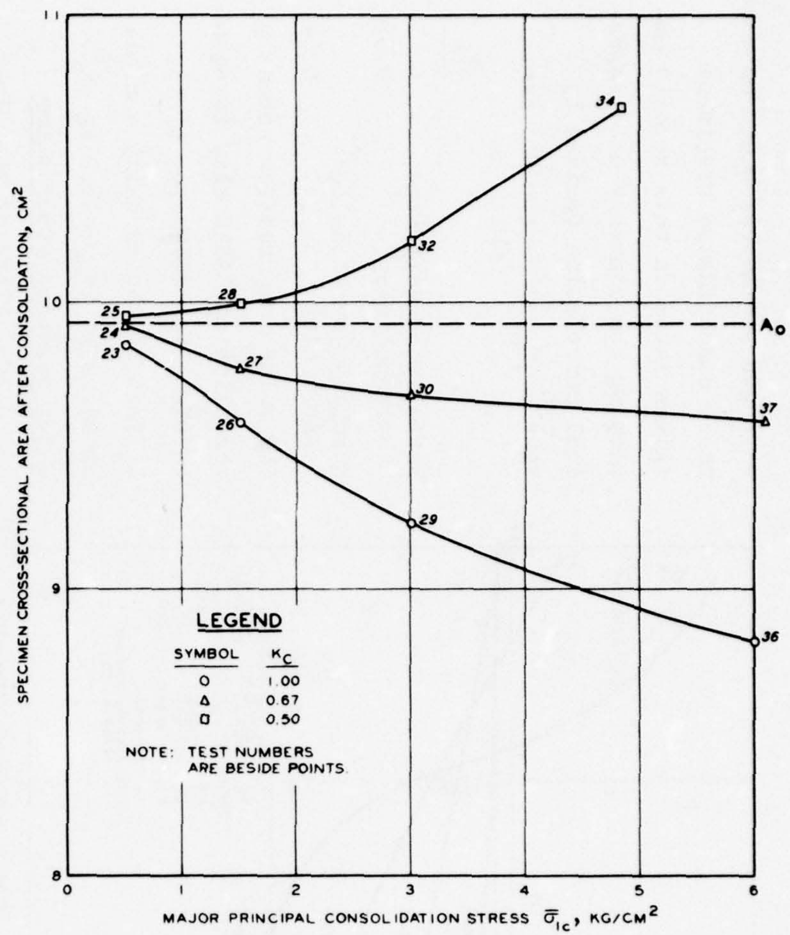

Figure 12. Specimen cross-sectional area after consolidation versus major principal consolidation stress for EABPL clay

strength parameters based on normally consolidated specimens (given later in this report) employing the commonly used empirical correlation derived by Jaky[20] ($K_o = 1 - \sin \phi'$) are:

	K_o
Normally consolidated Buckshot clay	0.55
Normally consolidated EABPL clay	0.64

The value computed for normally consolidated EABPL clay is equal to the value developed by the K_o test in the normally consolidated range ($\bar{\sigma}_{1c} = 6.0$ kg/cm^2).

<u>Water contents after shear</u>

29. Plots of the final water contents of specimens of both soils versus $\bar{\sigma}_{1c}$ and $\left(\bar{\sigma}_{oct}\right)_c$ values are given in Figures 15-18. These plots, of course, reflect essentially the same information as that noted for plots of volume change during consolidation versus $\bar{\sigma}_{1c}$ and $\left(\bar{\sigma}_{oct}\right)_c$ given in Figures 7-10 since the final water content of a CU specimen is a function of the change in volume during consolidation. Final water contents of ACU specimens of Buckshot clay with $K_c = 0.5$ ranged from 0.1 to 1.9 percent higher than did ICU specimens having the same $\bar{\sigma}_{1c}$ values. For the EABPL clay, the water contents after consolidation ranged from 0.6 to 1.7 percent higher than those for the Buckshot clay <u>for the same conditions.</u> In both cases the greatest difference in water contents occurred for $\bar{\sigma}_{1c} = 3.0$ kg/cm^2. Final water contents of ACU specimens having $K_c = 0.5$ and $\bar{\sigma}_{1c} = 6.0$ kg/cm^2 were closer to those of the corresponding ICU specimens, probably because deviator stresses acting

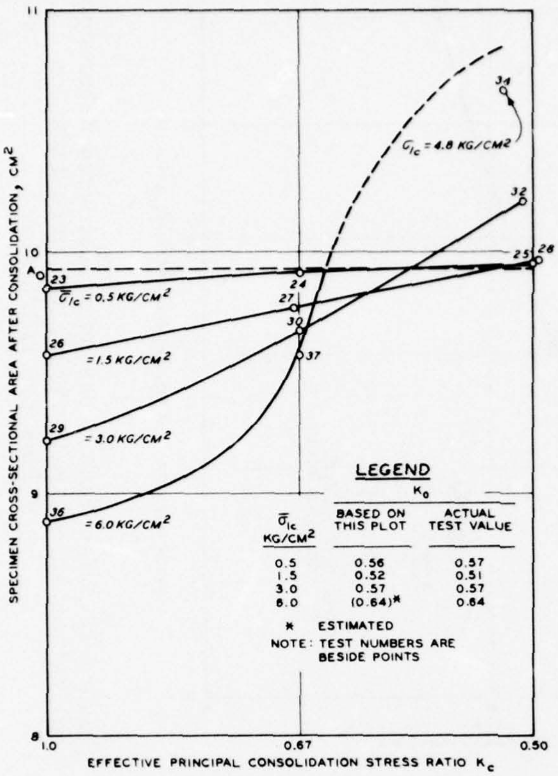

Figure 13. Specimen cross-sectional area after consolidation versus effective principal consolidation stress ratio for EABPL clay

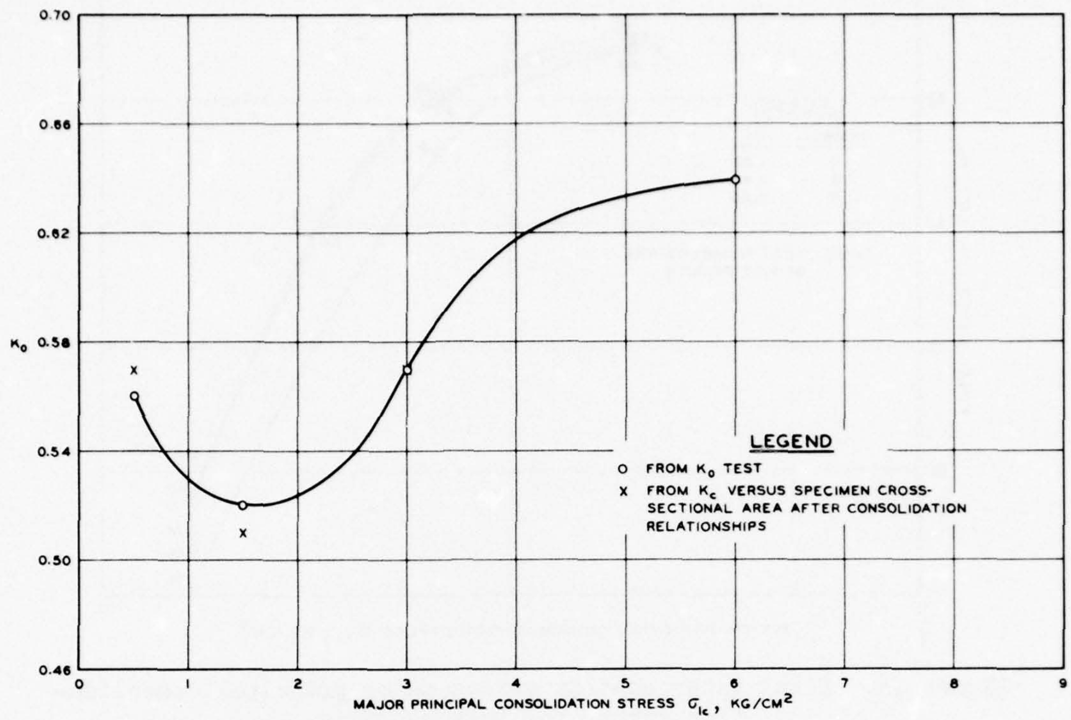

Figure 14. K_o versus major principal consolidation stress for EABPL clay

during consolidation produced significant volume changes.

30. The distributions of final water content within the specimens are given in Tables 4 and 5, and the difference between the water content of the center slice and the water content of the three middle slices as related to K_c values is given in Figures 19 and 20. It was anticipated that if K_c ratios had a significant effect on soil structure (and thus the shear strength), the effect would be apparent by consistent differences in water content distributions within the specimens after testing. However, as can be seen in the tables and figures, there is no discernable pattern of variation. This should have been expected since there were significant differences in the specimen conditions (water content, mean effective stress, etc.) after consolidation for each $\bar{\sigma}_{1c}$ value.

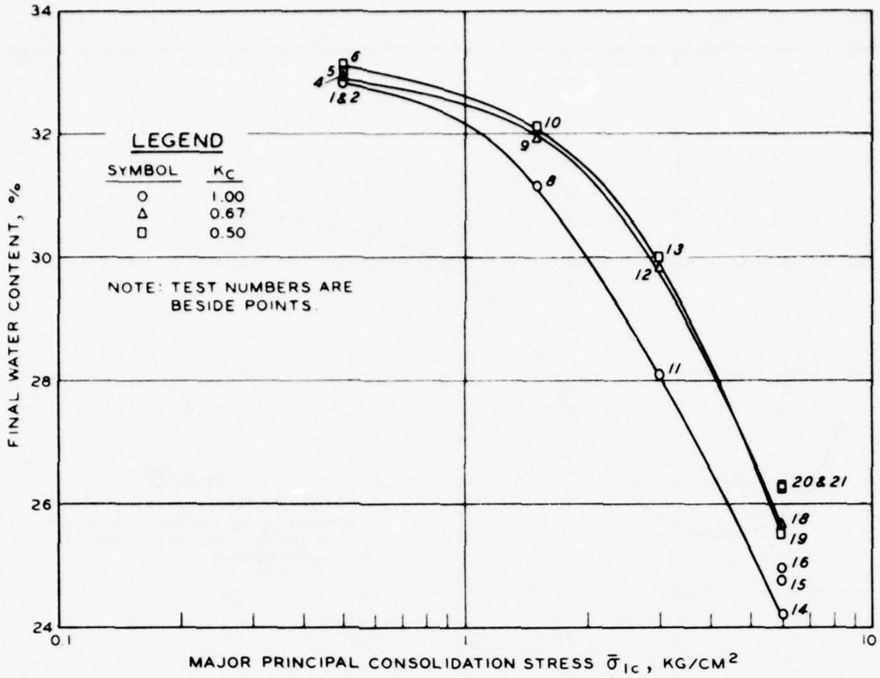

Figure 15. Final water content versus major principal consolidation stress for Buckshot clay

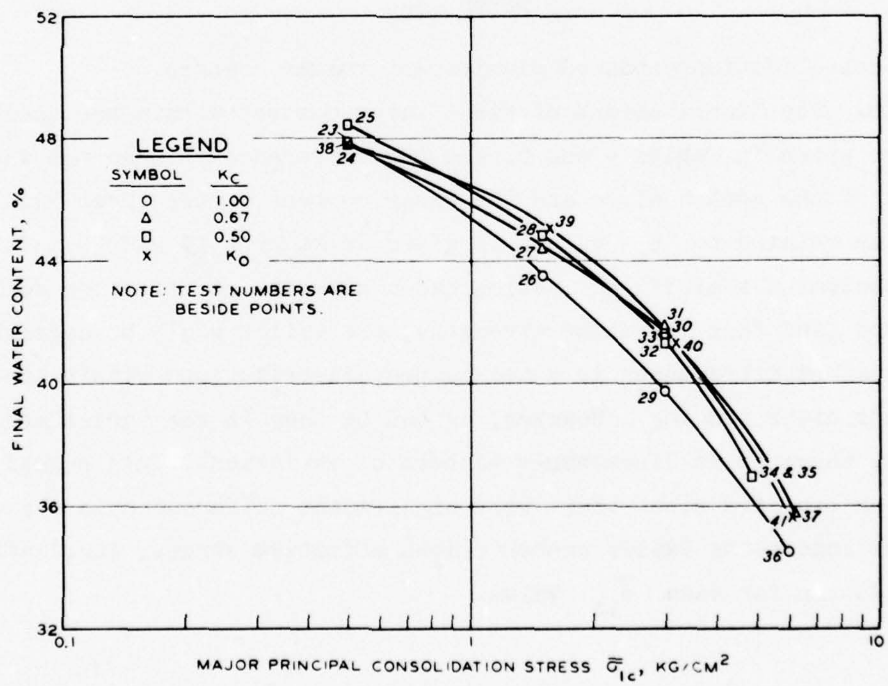

Figure 16. Final water content versus major principal consolidation stress for EABPL clay

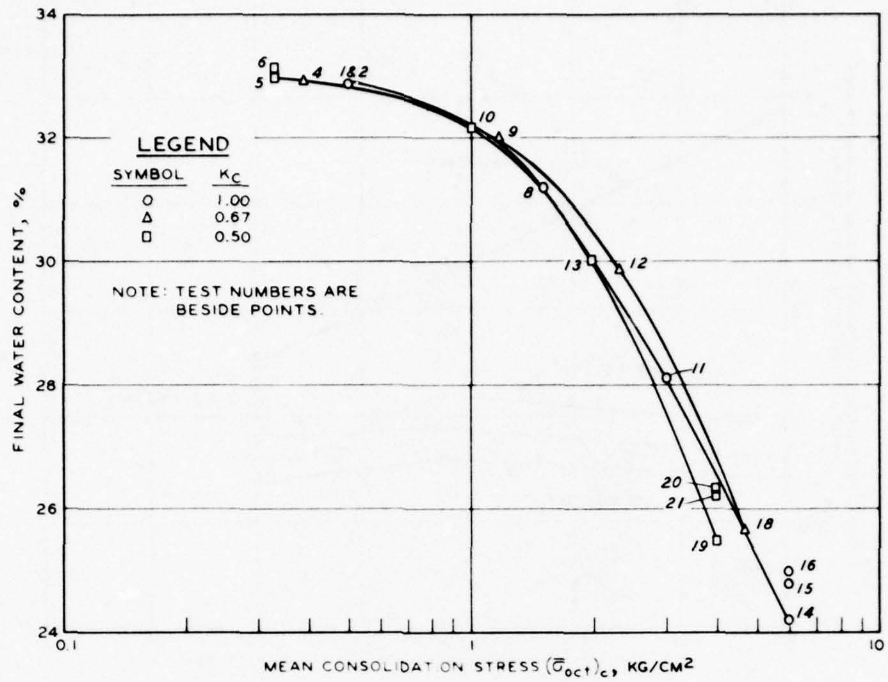

Figure 17. Final water content versus mean consolidation stress for Buckshot clay

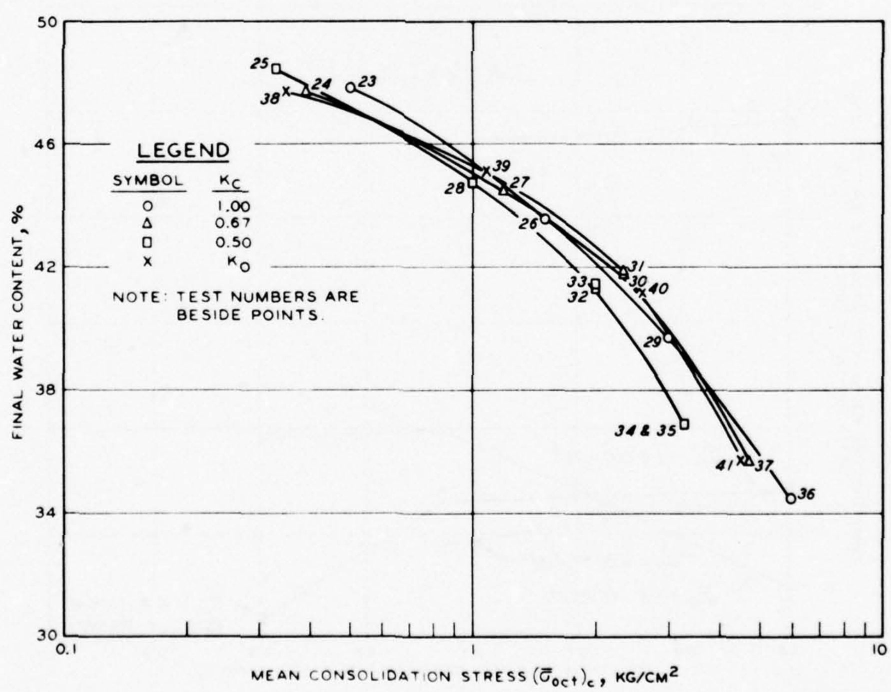

Figure 18. Final water content versus mean consolidation stress for EABPL clay

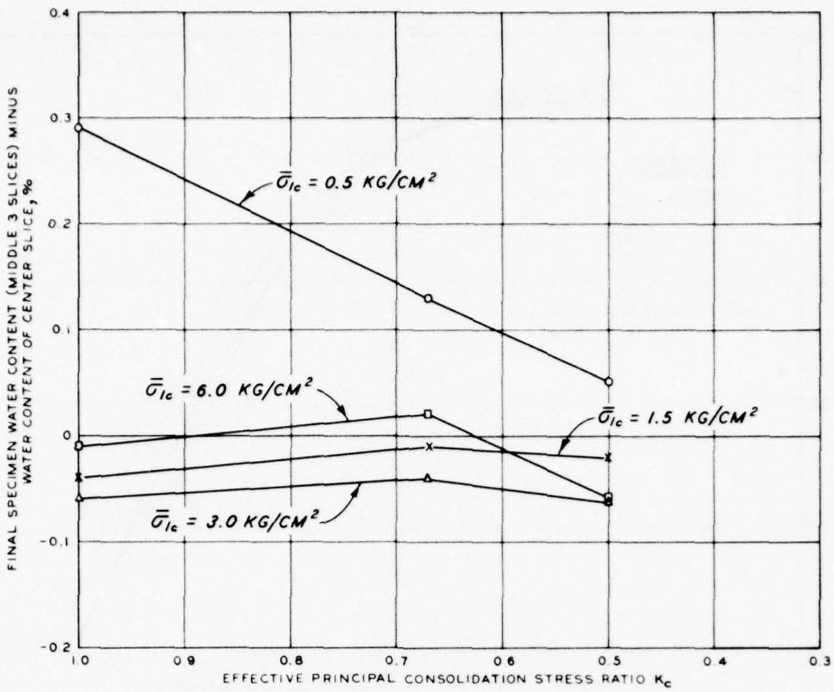

Figure 19. Final specimen water content (middle 3 slices) minus water content of center slice versus effective principal consolidation stress ratio for Buckshot clay

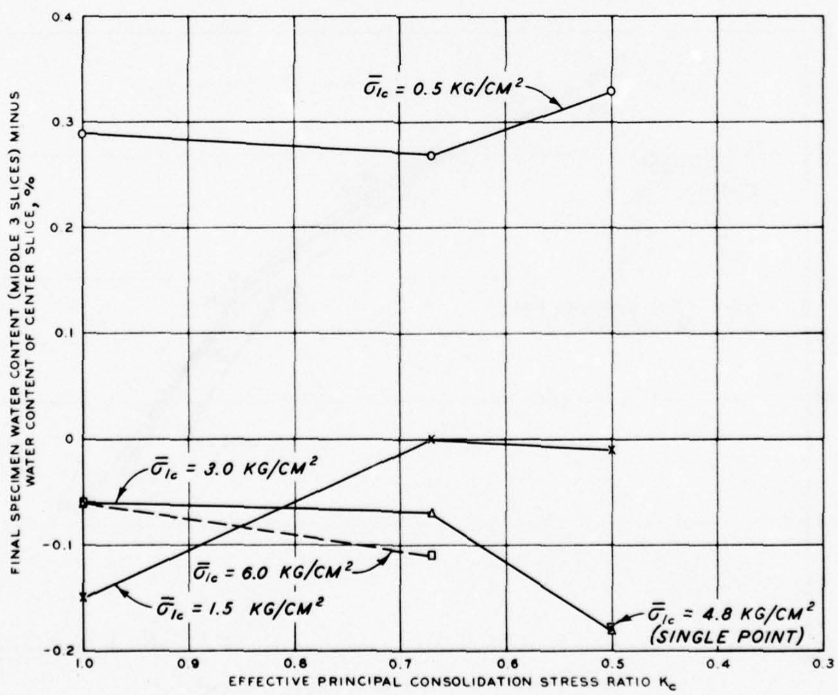

Figure 20. Final specimen water content (middle 3 slices) minus water content of center slice versus effective principal consolidation stress ratio for EABPL clay

Effects of strain rate on
final water content distribution

31. In order to determine strain rate effects during shear, tests were performed on specimens of Buckshot clay consolidated using K_c ratios of 1.0 and 0.5 with $\bar{\sigma}_{1c}$ values of 0.5 and 6.0 kg/cm^2. Rates of strain were 0.6 and 0.06 percent per minute for tests at $\bar{\sigma}_{1c}$ = 0.5 kg/cm^2 and 0.6, 0.06, and 0.012 percent per minute for tests at $\bar{\sigma}_{1c}$ = 6.0 kg/cm^2. Tests performed using the 0.012 percent per minute strain rate were added to the original testing program after it was determined that times to failure using the standard 0.06 percent per minute rate were too short. Final water content distributions and failure sketches of the specimens with $\bar{\sigma}_{1c}$ = 6.0 kg/cm^2 are given in Figure 21. The final water content distributions indicate that at least during the latter stages of shear, pore water generally migrated toward the center of the specimen for both ICU and ACU test specimens. The effect of strain rate on pore water migration can be seen in Figure 22, which shows a plot of the difference between the water content of the center slice and the water content of the middle three slices versus the elapsed time of undrained shear. These curves show that the water content of the center portion of both ICU and ACU specimens increased as the time of shear increased. A possible explanation for this behavior can be seen in the failure sketches in Figure 21. All of these specimens failed by bulging; however, the bulging became more localized toward the center and bottom as the time of shear was increased. This is seen mainly as an effect of end restraint, since as the time of shear is increased, pore pressure gradients within the specimens dissipate and shear strains become more concentrated in the middle portion of the specimens. The increased shear deformation in this part of the specimens probably altered the soil structure sufficiently to cause an increase in void ratio at large strains. It is of interest to note that strain rate effects were not as significant for the ACU as for the ICU specimens in that the water content distributions for the ACU specimens (shown in Figure 21) generally indicate less variation in final water content. Also, the difference between the water content of the center slice and that of the three

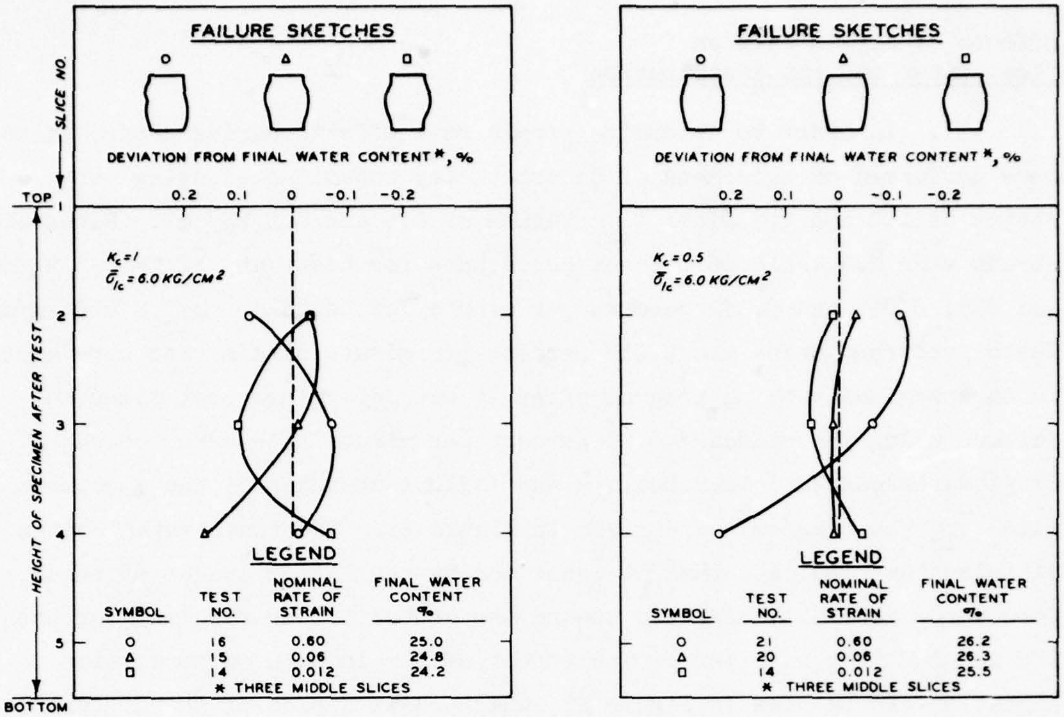

Figure 21. Final water content distributions of isotropically and anisotropically consolidated specimens of Buckshot clay sheared at three different rates of strain

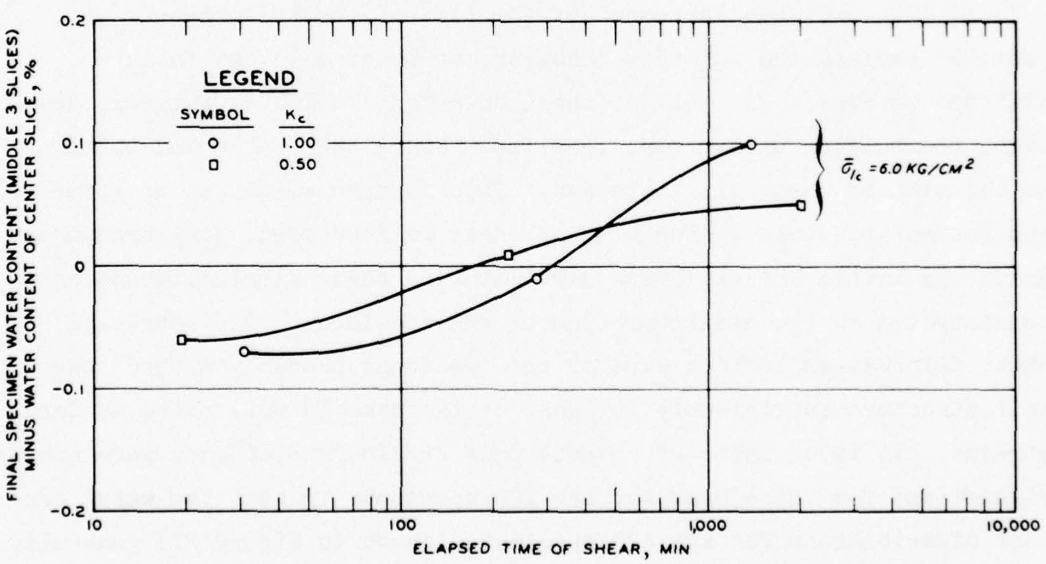

Figure 22. Final specimen water content (middle 3 slices) minus water content of center slice versus elapsed time of shear for Buckshot clay

middle slices as related to the elapsed times of shear given for ACU specimens shows that the change in volume occurring in the zone of maximum shear deformation was less for ACU than for ICU specimens. This is further evidence which suggests effects due to the structure imparted by stress conditions during consolidation.

Modes of failure

32. All of the specimens, with the exception of those tested using low-friction caps and bases, failed by bulging; however, in many cases the bulging was localized in either the center or top or bottom portions. Localized bulging occurred most often for specimens consolidated under low stress levels (overconsolidated specimens). At low stress levels, i.e. $\left(\bar{\sigma}_{oct}\right)_c < 1.0$ kg/cm^2, both ICU and ACU specimens of the Buckshot clay bulged excessively in either the top or bottom portions. At the same low stress levels, ACU specimens of the EABPL clay bulged excessively in their center portions, and ICU specimens bulged uniformly. Localized bulging of specimens of both clays consolidated at higher stress levels occurred only in tests having $K_c = 0.67$, and in tests performed at slow rates of strain. The localized bulging occurred in only the central portions of these specimens. It is thought that the localized bulging is a function of the boundary conditions at the tops and bottoms of the specimens. In the case of specimens of the Buckshot clay tested at low stress levels, it could be possible that the coefficient of friction of soil on the rather smooth surface of the porous sintered steel disk was less than the tangent of the angle of internal friction ϕ' of the overconsolidated soil, in which case movement of the soil relative to either the top or bottom disk might have caused localized bulging and failure in the portion of the specimen closest to the movement. As for the excessive bulging in the middle portions of the anisotropically consolidated EABPL specimens tested at low stress levels, pore pressure gradients within these relatively weak specimens would probably not be too high during consolidation, and significant shear strains due to the anisotropic stress conditions could have been concentrated in the center portion of the specimens in somewhat the same manner as that described

for tests performed at slow rates of strain. Shear deformation during undrained shear would then tend to be confined to the middle portion of the specimens since this portion, having already undergone significant shear strains, would be somewhat weaker. Localized bulging during undrained shear at the higher stress levels with $K_c = 0.67$ was also probably due to excessive shear deformation in the middle portions of the specimens during consolidation. A possible explanation for non-localized bulging of specimens of both soils consolidated at higher stress levels with $K_c = 0.5$ may be that this value was close to the K_o value for the Buckshot clay (see Figure 11), and nonuniform shear strains should not occur under these conditions since there is no lateral strain. In the case of the EABPL clay, consolidation using $K_c = 0.5$ resulted in near-failure conditions, and pore pressure gradients probably were not dissipated quickly enough to concentrate shear strains in the central portions of the specimens as they deformed.

33. Specimens of both clays tested using low-friction caps and bases deformed cylindrically or expanded at one end more than at the other during undrained shear.

34. When the water content distributions and failure conditions described in the above paragraphs are examined, it should be noted that these are final specimen conditions and may not be indicative of conditions during the initial stages of shear. Also, it should be noted that the possibility of nonuniform conditions in samples from which the specimens were trimmed would affect the final water content distribution. Finally, it is possible that removing the failed specimen from the chamber and slicing it into sections altered the results of the comparison between the water content distributions and the end-of-shear condition.

Deviator Stresses

Effect of K_c

35. Stress-strain curves. Stress-strain curves for both clays showing the effects of varying K_c ratios while maintaining $\bar{\sigma}_{1c}$

stresses are given in Figures 23 and 24. Also included in Figure 24 are stress-strain curves for the K_o tests performed on the EABPL clay. These relationships were developed from results of tests performed using the slowest rates of strain so that effects due to strain rate could be minimized.* Cross-sectional areas used to compute the stresses were corrected for localized bulging according to the procedure outlined in Appendix A. As can be seen in Figures 23 and 24, maximum deviator stresses and the axial strain values at which they developed generally decreased with decreasing values of K_c for $\bar{\sigma}_{1c}$ stresses less than 3.0 kg/cm^2. For $\bar{\sigma}_{1c}$ stresses equal to and greater than 3.0 kg/cm^2,** axial strain values at which maximum deviator stresses developed were also less for ACU ($K_c < 1$) than for ICU specimens; however, the maximum deviator stresses for $K_c = 0.5$ were slightly higher than those developed for $K_c = 0.67$.

36. Reductions in maximum deviator stresses. Reductions in maximum deviator stress occurring as K_c was varied for each $\bar{\sigma}_{1c}$ value are given in the following tabulation:

$\bar{\sigma}_{1c}$, kg/cm^2	Value of $(\sigma_1 - \sigma_3)_{max}$ at $K_c = 1$, kg/cm^2	Percent Reduction in $(\sigma_1 - \sigma_3)_{max}$ at Indicated Values of K_c: Between $K_c = 1$ and $K_c = 0.67$	Between $K_c = 1$ and $K_c = 0.5$
	Buckshot Clay		
0.5	1.25	3.2	4.8
1.5	1.68	5.4	6.6
3.0	2.41	12.9	12.0
6.0	4.02	9.0	4.2

(Continued)

* A discussion of methods for comparing ACU and ICU test results is given later in the report (paragraph 54). It should be pointed out at this time, however, that the conclusions may have been somewhat altered if results had been compared on the basis of equivalent strain rates.

** A test of the EABPL clay at $\bar{\sigma}_{1c} = 6.0$ kg/cm^2 with $K_c = 0.5$ was not performed since the axial strain during consolidation would have exceeded the available piston travel of the testing apparatus.

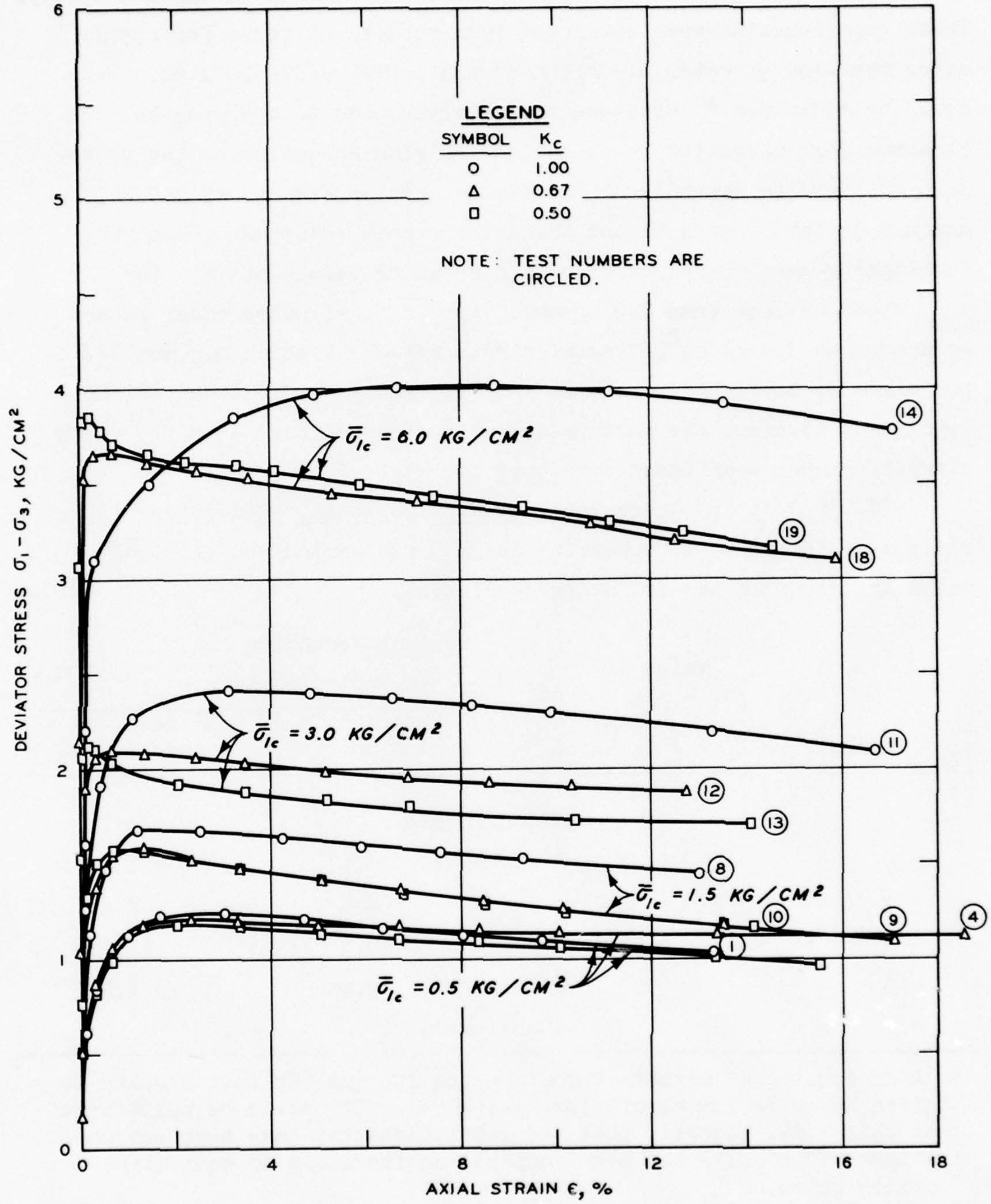

Figure 23. Deviator stress versus axial strain for Buckshot clay

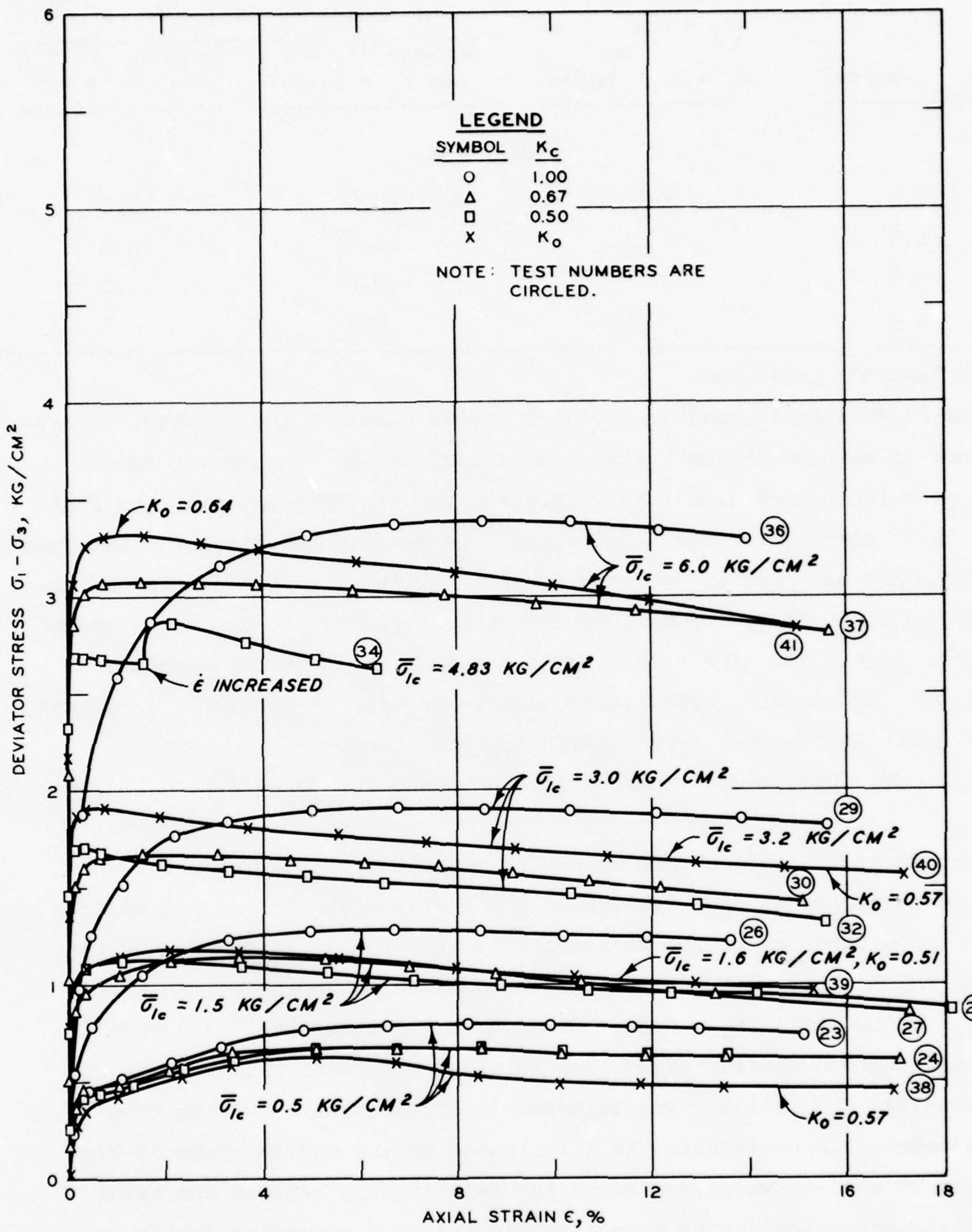

Figure 24. Deviator stress versus axial strain for EABPL clay

$\bar{\sigma}_{1c}$, kg/cm^2	Value of $(\sigma_1 - \sigma_3)_{max}$ at $K_c = 1$, kg/cm^2	Percent Reduction in $(\sigma_1 - \sigma_3)_{max}$ at Indicated Values of K_c: Between $K_c = 1$ and $K_c = 0.67$	Between $K_c = 1$ and $K_c = 0.5$
		EABPL Clay	
0.5	0.80	15.0	15.0
1.5	1.29	11.6	12.4
3.0	1.91	12.6	11.0
6.0	3.38	8.6	--*

* Test not performed.

The reductions in maximum deviator stress based on the greatest difference in maximum deviator stress occurring as K_c was varied for each $\bar{\sigma}_{1c}$ value ranged from 3 to 13 percent for the Buckshot clay and from 9 to 15 percent for the EABPL clay. The maximum reduction for the Buckshot clay occurred at $\bar{\sigma}_{1c} = 3.0$ kg/cm^2 with $K_c = 0.67$. In the case of the EABPL clay, the maximum reduction occurred at $\bar{\sigma}_{1c} = 0.5$ kg/cm^2 with $K_c = 0.5$. For both clays the reduction in maximum deviator stress for normally consolidated specimens $\left(\bar{\sigma}_{1c} = 6.0 \text{ kg/cm}^2\right)$ was not as great as that for overconsolidated specimens.

37. Reductions in axial strain values at $(\sigma_1 - \sigma_3)_{max}$. The reductions in axial strain values at which maximum deviator stresses were developed as K_c was varied for a given $\bar{\sigma}_{1c}$ value ranged from 33 to 98 percent for the Buckshot clay and from 17 to 95 percent for the EABPL clay, with the greatest reductions occurring at the higher $\bar{\sigma}_{1c}$ values with $K_c = 0.5$. Other investigators (Lee[10] and Ladd[12]) have observed similar reductions in axial strain to failure with decreasing K_c ratios. The increase in brittleness resulting from anisotropic consolidation is illustrated by the curves shown in Figures 25 and 26, which represent the relationship between the axial strain occurring during consolidation and that occurring during undrained shear for ICU and ACU specimens of both clays. The introduction of a deviator stress acting during consolidation produced an

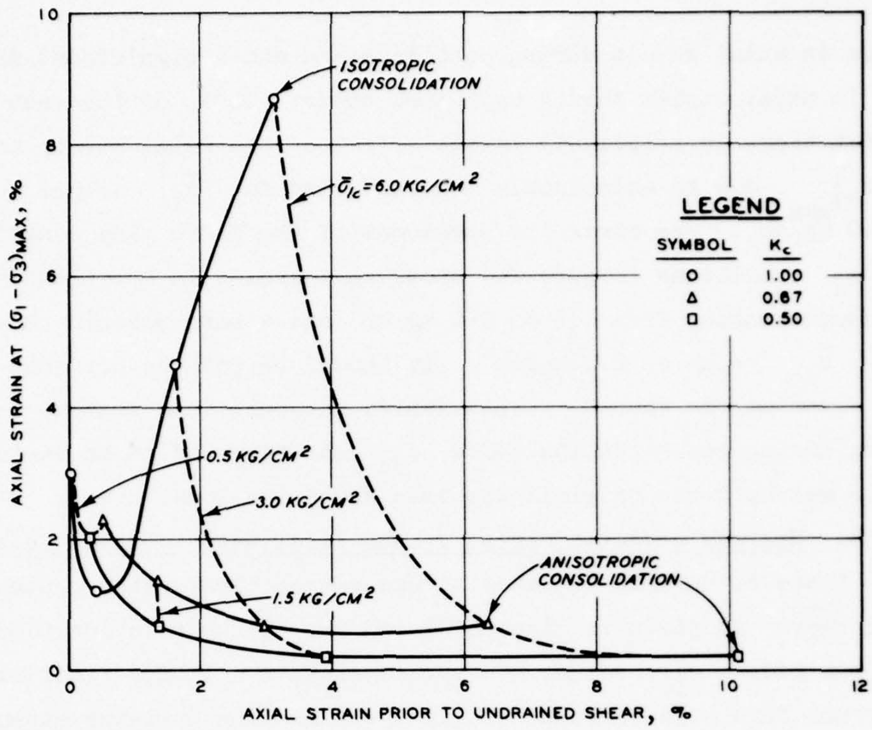

Figure 25. Axial strain at $\left(\sigma_1 - \sigma_3\right)_{max}$ versus axial strain prior to undrained shear for Buckshot clay

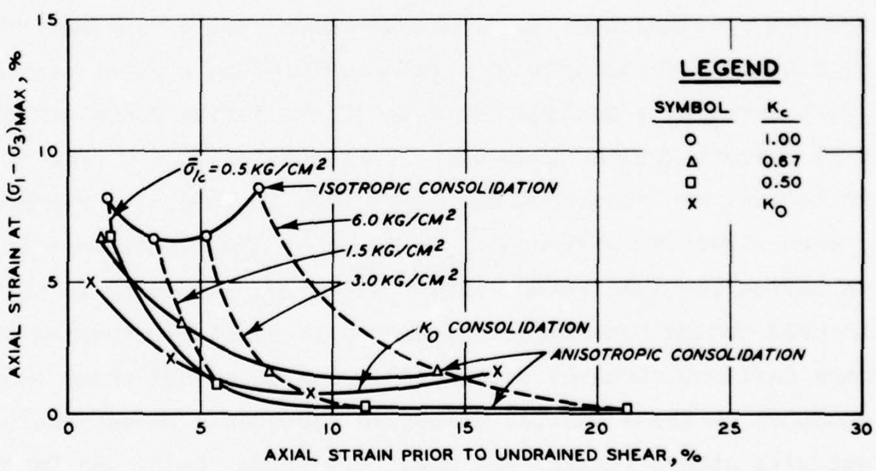

Figure 26. Axial strain at $\left(\sigma_1 - \sigma_3\right)_{max}$ versus axial strain prior to undrained shear for EABPL clay

increase in axial strain during consolidation and a significant decrease in axial strain during undrained shear. It is of interest to note that there is relatively little effect on the axial strain at $(\sigma_1 - \sigma_3)_{max}$ due to anisotropic consolidation for $\bar{\sigma}_{1c}$ values greater than 3.0 kg/cm^2. The curve for specimens of the EABPL clay consolidated under K_o conditions (Figure 26) shows an increase in brittleness for $\bar{\sigma}_{1c}$ values ranging from 0.5 to 3.0 kg/cm^2 and a more plastic behavior for the $\bar{\sigma}_{1c}$ value of 6.0 kg/cm^2. It should be pointed out that the $\bar{\sigma}_{3c}/\bar{\sigma}_{1c}$ ratios for the K_o tests varied not only from test to test but also during consolidation since $\bar{\sigma}_{3c}$ stresses had to be varied in order to maintain the original specimen cross-sectional area.

38. Maximum deviator stress versus final water content relationships. Plots of maximum deviator stress versus final water content for the two clays are given in Figures 27 and 28. These relationships show that for a given $\bar{\sigma}_{1c}$ value, ACU specimens have a larger final water content and fail at a correspondingly lower maximum deviator stress than do ICU specimens. The plots also show that at any given final water content resulting from $\bar{\sigma}_{1c}$ values in excess of 1.5 kg/cm^2, the maximum deviator stress for an ACU specimen is greater than that for an ICU specimen. For example, the plot in Figure 27 shows that a specimen of Buckshot clay consolidated using a K_c value of 0.67 to a water content of 26.0 percent develops a maximum deviator stress during undrained shear which is 11 percent greater than that developed for an ICU specimen consolidated to the same water content ($K_c = 1$). It should be remembered that the mean effective stress $(\bar{\sigma}_{1c} + \bar{\sigma}_{2c} + \bar{\sigma}_{3c})/3$ conditions in specimens having the same water content will vary according to the K_c ratio used during consolidation; hence, it would be expected that the maximum deviator stresses developed during undrained shear would depend somewhat on these initial effective stresses. These results are consistent with others (Henkel and Sowa,[11] Whitman, Ladd, and DaCruz,[13] and Ladd[12]) in that anisotropic consolidation produces two compensating effects on undrained strength, which are as follows:

a. For any given $\bar{\sigma}_{1c}$, anisotropic consolidation produces

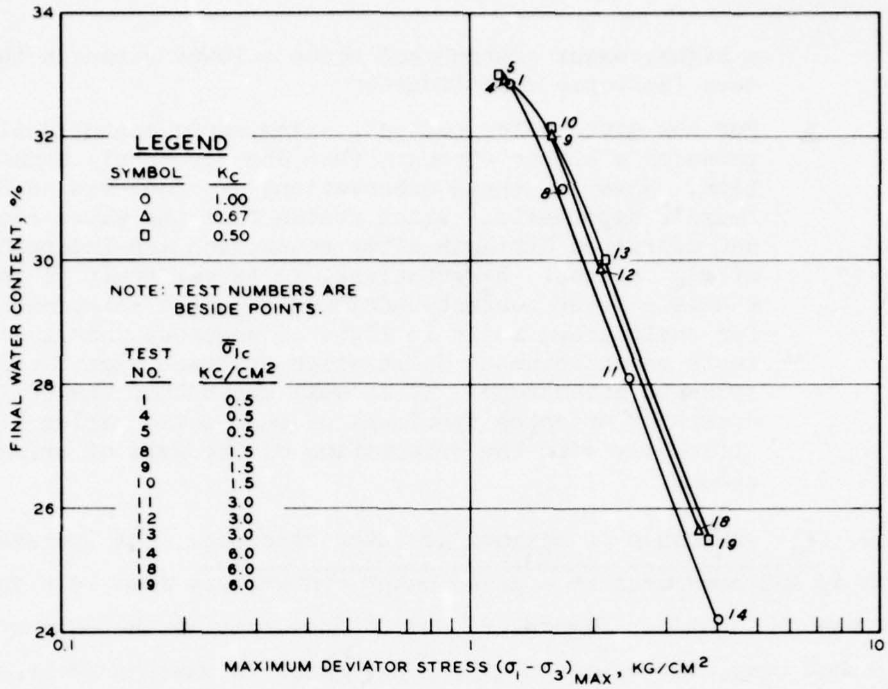

Figure 27. Final water content versus maximum deviator stress for Buckshot clay

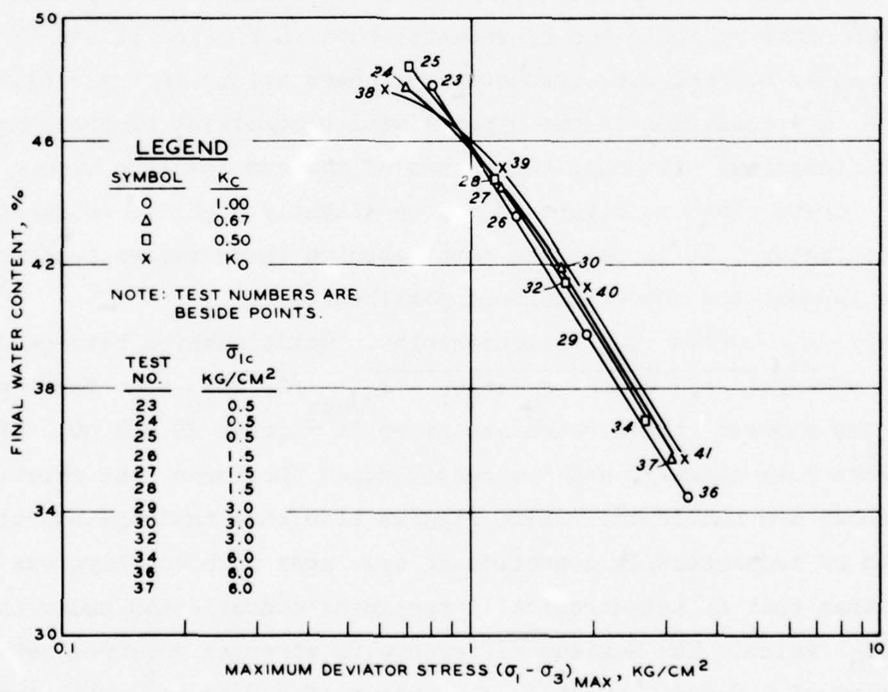

Figure 28. Final water content versus maximum deviator stress for EABPL clay

a higher water content and hence a lower strength than does isotropic consolidation.

b. For any given water content, anisotropic consolidation produces a higher strength than does isotropic consolidation. However, these observations are converse to Rutledge's hypothesis,[7] which states that the water content and undrained strength after saturation are independent of K_c ratios. Nevertheless, it is difficult to imagine a unique water content-undrained strength relationship for undisturbed soils in light of numerous undrained tests on undisturbed soils which evidence significant strength anisotropy. It is well known that the failure stress of oriented specimens of such soils varies significantly with the orientation of the axis of principal stress.

39. K_o influence on maximum deviator stresses. The increased strength of ACU specimens at a given water content may also be a function of the K_c ratio. Figures 27 and 28 show that in the case of the Buckshot clay, the greatest difference noted in maximum deviator stresses for a given water content was between K_c values of 1.0 and 0.5, whereas the greatest difference noted for the EABPL clay was between K_c values of 1.0 and 0.67. Since K_o values for the Buckshot and EABPL clays as indicated by results shown in Figures 11 and 12 are approximately 0.5 and 0.6, respectively, there exists the possibility that the K_o condition is the upper limiting condition controlling these differences. Although the values of maximum deviator stress for the K_o tests shown in Figure 28 may be slightly high due to short times to failure, it is felt the plot based on these values tends to further suggest the above-mentioned possibility.

40. s_u versus $\bar{\sigma}_{1c}$ relationships. Relationships between undrained strength s_u where $s_u = (\sigma_1 - \sigma_3)_{max}/2$, and $\bar{\sigma}_{1c}$ for tests having the slowest strain rates are given in Figures 29 and 30. Since there were both normally and overconsolidated specimens, the relationships shown are nonlinear. These figures also show that the undrained strength of isotropically consolidated specimens of both clays was higher than that of anisotropically specimens consolidated under the same $\bar{\sigma}_{1c}$ value. The maximum difference in strength occurred between K_c ratios of 1.0 and 0.67 at a $\bar{\sigma}_{1c}$ value of 6.0 kg/cm^2, with the

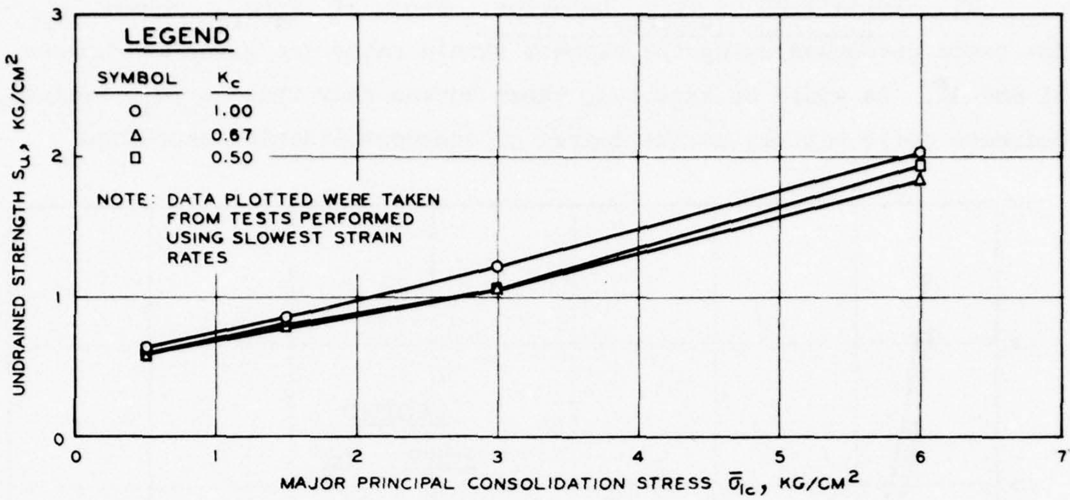

Figure 29. Undrained strength versus major principal consolidation stress for Buckshot clay

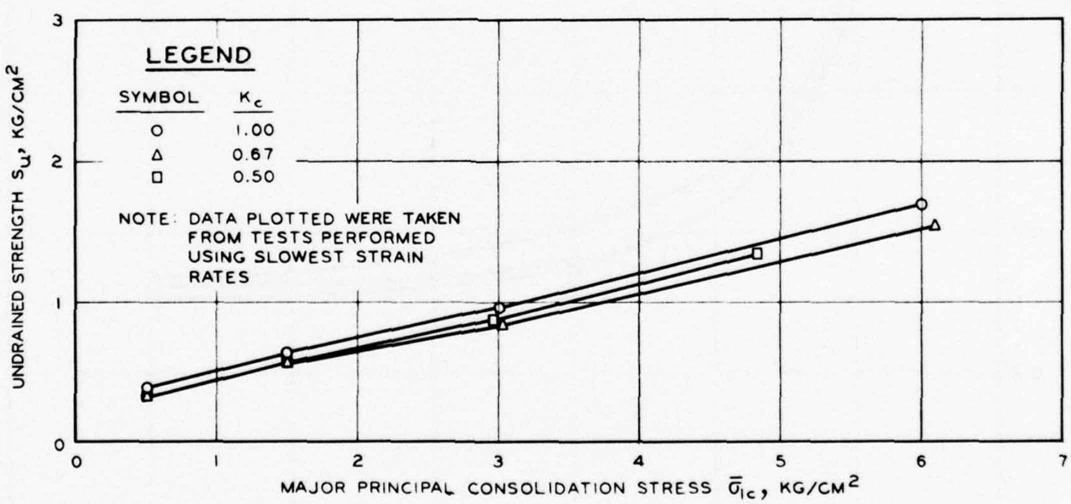

Figure 30. Undrained strength versus major principal consolidation stress for the EABPL clay

differences being 0.19 and 0.26 kg/cm^2 for the Buckshot and EABPL clays, respectively. The reductions in strength amounted to 9 and 15 percent for the respective clays.

41. Normalized $s_u/\bar{\sigma}_{1c}$ behavior. Plots of $s_u/\bar{\sigma}_{1c}$ versus $\bar{\sigma}_{1c}$ for tests performed using the slowest strain rates are given in Figures 31 and 32. As would be expected, these curves show that $s_u/\bar{\sigma}_{1c}$ values decrease quite rapidly as the degree of overconsolidation decreases

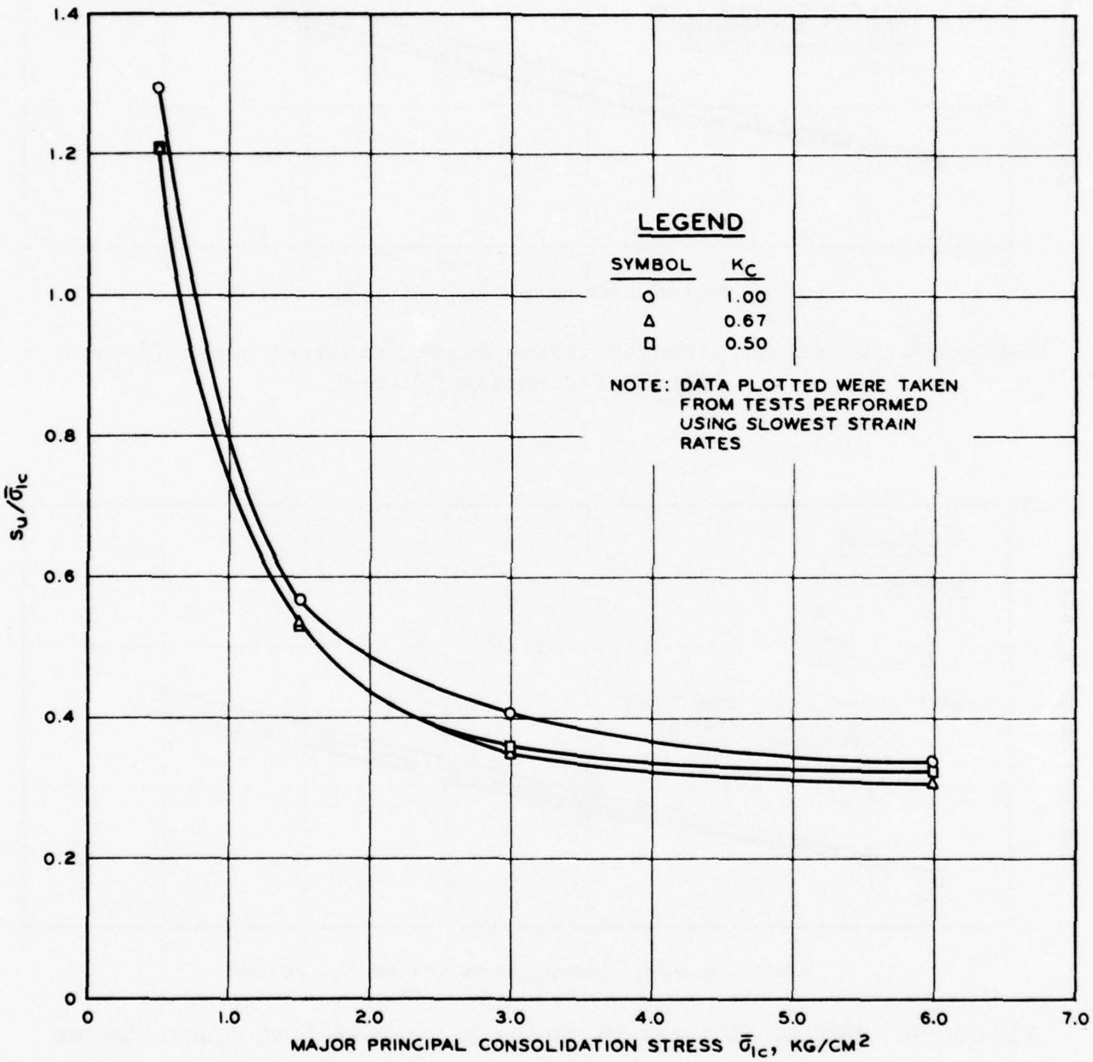

Figure 31. $s_u/\bar{\sigma}_{1c}$ versus major principal consolidation stress for Buckshot clay

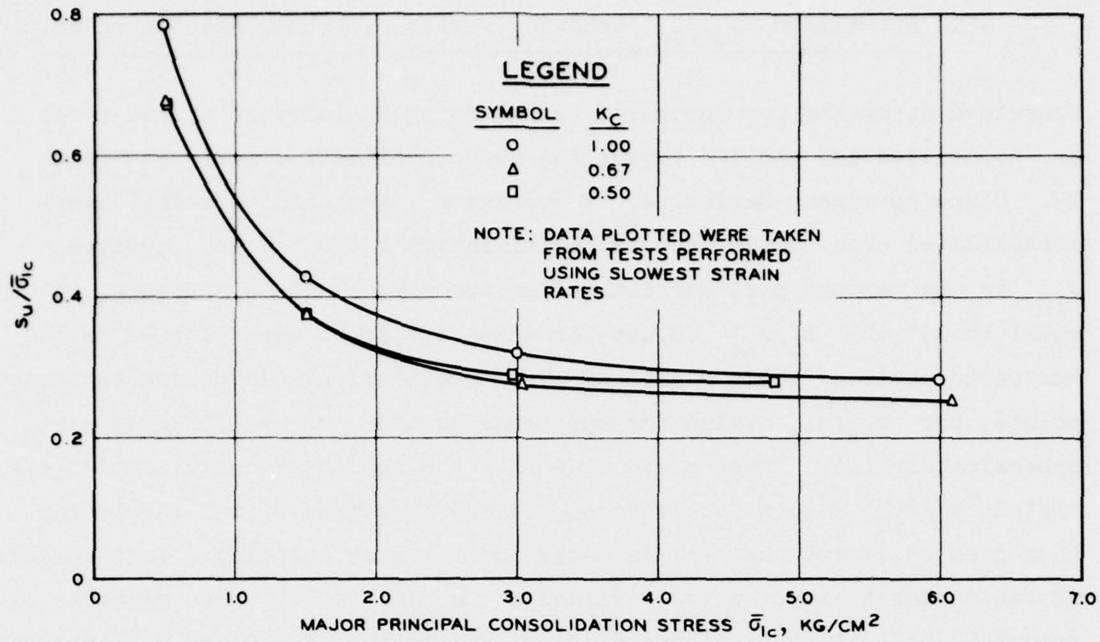

Figure 32. $s_u/\bar{\sigma}_{1c}$ versus major principal consolidation stress for EABPL clay

(i.e., $\bar{\sigma}_{1c}$ values ranging from 0.5 to 3.0 kg/cm^2), and they become horizontal in the range of $\bar{\sigma}_{1c}$ values for normally consolidated specimens (i.e., $\bar{\sigma}_{1c}$ values greater than 3.0 kg/cm^2). There is a significant effect on the $s_u/\bar{\sigma}_{1c}$ versus $\bar{\sigma}_{1c}$ relationships due to the method of consolidation. The $s_u/\bar{\sigma}_{1c}$ values for normally consolidated specimens of Buckshot clay taken at $\bar{\sigma}_{1c} = 6.0$ kg/cm^2 range from 0.35 for $K_c = 1.0$ to 0.31 for $K_c = 0.67$, while $s_u/\bar{\sigma}_{1c}$ values for the EABPL clay at the same condition vary from 0.28 for $K_c = 1.0$ to 0.25 for $K_c = 0.67$. The curves indicate approximately the same differences in $s_u/\bar{\sigma}_{1c}$ values for K_c ratios of 1.0 and 0.67 in the overconsolidated region. The curves for $K_c = 0.5$ for both clays are almost identical to those for $K_c = 0.67$ in the overconsolidated range and are located between the curves for K_c ratios of 1.0 and 0.67 in the normally consolidated region. Values of $s_u/\bar{\sigma}_{1c}$ in the normally consolidated region for the $K_c = 0.5$ ratio are 0.32 for the Buckshot clay and 0.28 for the EABPL clay.

42. <u>Normalized $s_u/\bar{\sigma}_{1c}$ behavior versus overconsolidation ratio.</u> Undrained strengths for specimens tested using the slowest strain rates are normalized and plotted versus the overconsolidation ratio in Figure 33. Since specimens having $\bar{\sigma}_{1c} = 3.0\ kg/cm^2$ are still somewhat overconsolidated even though the overconsolidation ratio $\bar{\sigma}_{1p}/\bar{\sigma}_{1c}$, where $\bar{\sigma}_{1p}$ is the maximum past vertical effective consolidation pressure, is equal to 1,* the $s_u/\bar{\sigma}_{1c}$ values for these specimens were plotted on the curves to estimate their degree of overconsolidation. According to these points, the $\bar{\sigma}_{1p}/\bar{\sigma}_{1c}$ value for specimens having $\bar{\sigma}_{1c} = 3.0\ kg/cm^2$ is approximately 1.5. These plots show that the method of consolidation affected $s_u/\bar{\sigma}_{1c}$ values for overconsolidated specimens of the EABPL clay to a greater degree than it did those for the Buckshot clay. In the case of the Buckshot clay, $s_u/\bar{\sigma}_{1c}$ values at $\bar{\sigma}_{1p}/\bar{\sigma}_{1c} = 6.0$ were reduced from 1.25 to 1.19 (i.e. 5 percent) for K_c ratios of 1.0 and 0.5, whereas in the case of the EABPL clay, $s_u/\bar{\sigma}_{1c}$ values were reduced from 0.79 to 0.68 (i.e. 14 percent) for the same conditions. K_o consolidation of the EABPL clay at $\bar{\sigma}_{1p}/\bar{\sigma}_{1c} = 6.0$ reduced the $s_u/\bar{\sigma}_{1c}$ value based on $K_c = 1.0$ by 19 percent. Values of $s_u/\bar{\sigma}_{1c}$ for normally consolidated specimens of both soils (tests having $\bar{\sigma}_{1p}/\bar{\sigma}_{1c} = 1.0$) were affected similarly by K_c ratios. In both cases the greatest differences in $s_u/\bar{\sigma}_{1c}$ occurred between $K_c = 1.0$ and 0.67, with $s_u/\bar{\sigma}_{1c}$ values being reduced by approximately 10 percent for the $K_c = 0.67$ condition. Ladd[12] and Khera and Krizek[14] have shown that s_u/σ_{1c} ratios for normally consolidated clays are practically unchanged ($\pm$15 percent) by K_c. The results presented in Figure 33 confirm these previous conclusions but demonstrate that for overconsolidated clays, $s_u/\bar{\sigma}_{1c}$ may be more dependent on K_c ratios. It should be pointed out, however, that the relationships shown in Figure 33 were not developed in the same manner as were those by Ladd[12] and most other investigators. The usual method for developing $s_u/\bar{\sigma}_{1c}$

---

* Specimens were reconsolidated in the triaxial apparatus from the no-load condition at which samples were removed from the slurry consolidometers. Normally consolidated specimens would not be obtained at $\bar{\sigma}_{1c} = 3.0\ kg/cm^2$ since virgin compression characteristics are not developed in a reloading cycle until after the $\bar{\sigma}_{1p}$ value is reached.

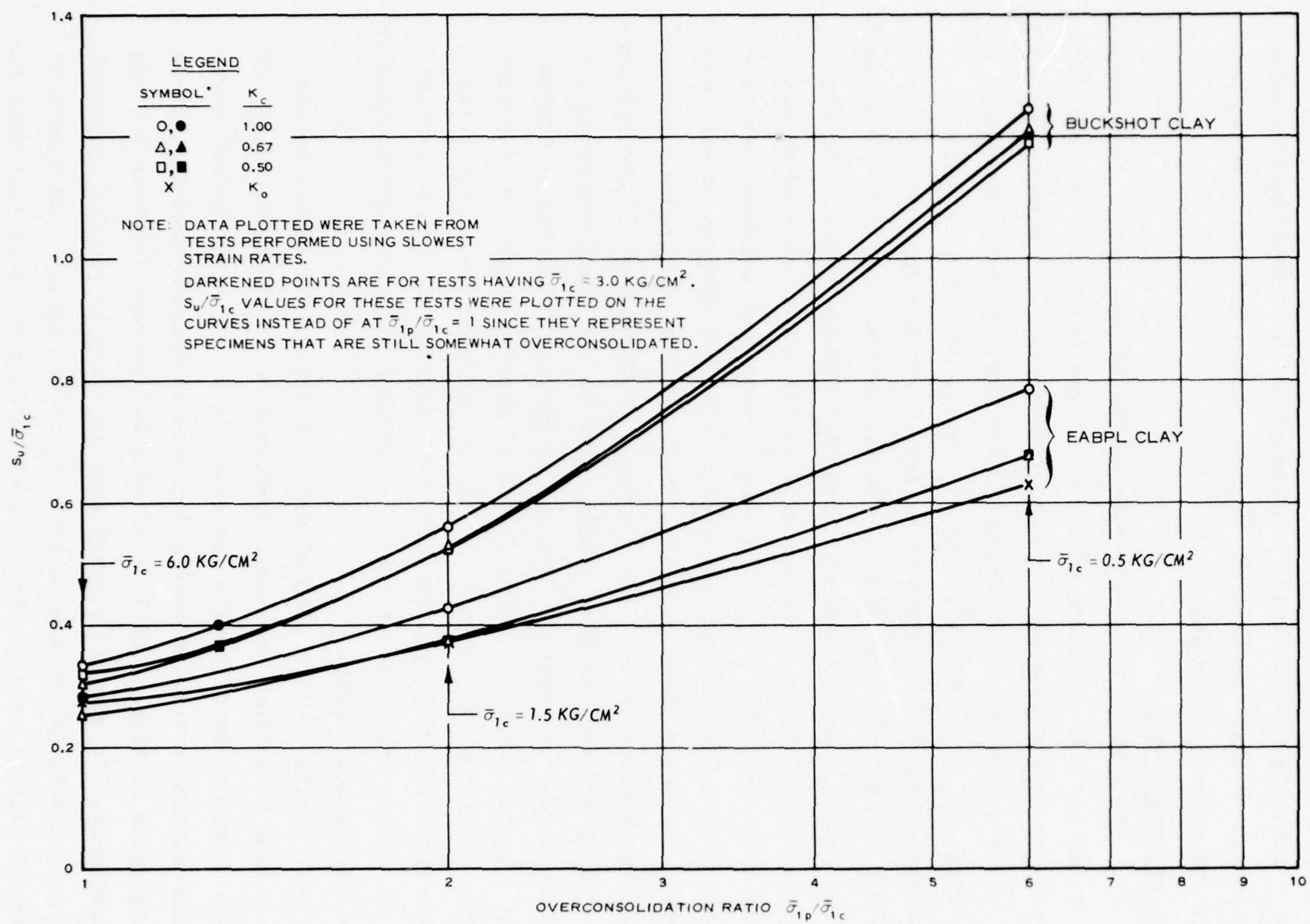

Figure 33. $s_u/\bar{\sigma}_{1c}$ versus overconsolidation ratio

versus $\bar{\sigma}_{1p}/\bar{\sigma}_{1c}$ relationships is to consolidate specimens using a $\bar{\sigma}_{1c}$ value greater than $\bar{\sigma}_{1p}$ and then rebounding them to obtain the desired $\bar{\sigma}_{1p}/\bar{\sigma}_{1c}$ ratios prior to shear. Specimens in this investigation were consolidated so that the desired $\bar{\sigma}_{1p}/\bar{\sigma}_{1c}$ ratio was developed at the end of the consolidation phase.

Effect of strain rate

43. The effects of strain rate on the stress-strain characteristics of ICU and ACU specimens of Buckshot clay are shown in Figure 34. The rates of strain used were 0.6 and 0.06 percent per minute for tests with $\bar{\sigma}_{1c}$ = 0.5 kg/cm^2 and 0.6, 0.06, and 0.012 percent per minute for tests with $\bar{\sigma}_{1c}$ = 6.0 kg/cm^2. The K_c ratio used for anisotropic consolidation was 0.5. Points of maximum curvature for specimens with $\bar{\sigma}_{1c}$ = 0.5 kg/cm^2 occurred from 0.9 to 1.2 percent strain for ICU specimens and from 1.1 to 1.3 percent strain for ACU specimens. In both cases the larger strain value occurred at the slower rate of strain. For ICU specimens with $\bar{\sigma}_{1c}$ = 6.0 kg/cm^2, points of maximum curvature occurred from 1.4 to 2.8 percent strain, with the largest strain value occurring for the slowest rate of strain. Points of maximum curvature for ACU specimens with $\bar{\sigma}_{1c}$ = 6.0 kg/cm^2 occurred from 0.2 to 0.3 percent strain, with the smaller strain value in this case occurring for the slowest rate of strain. With the exception of the ACU specimens having $\bar{\sigma}_{1c}$ = 6.0 kg/cm^2 where points of maximum curvature coincided with the strain values at failure, the deviator stress at the point of maximum curvature was approximately 90-95 percent of that at failure. Deviator stress values at the point of maximum curvature decreased with increased times of shear.

44. Figure 35 is a plot of deviator stress at failure versus elapsed time to failure for tests performed on the Buckshot clay. If the two slower rates of strain for tests with $\bar{\sigma}_{1c}$ = 6.0 kg/cm^2 are considered, the curves indicate a decrease in maximum deviator stress per log cycle of time to failure of only 2-3 percent for both ICU and ACU specimens. It should be noted that in order to provide comparable times to failure, ACU specimens with $\bar{\sigma}_{1c}$ = 6.0 kg/cm^2 would have to be sheared using a rate of strain equal to 20 percent of that used for ICU specimens.

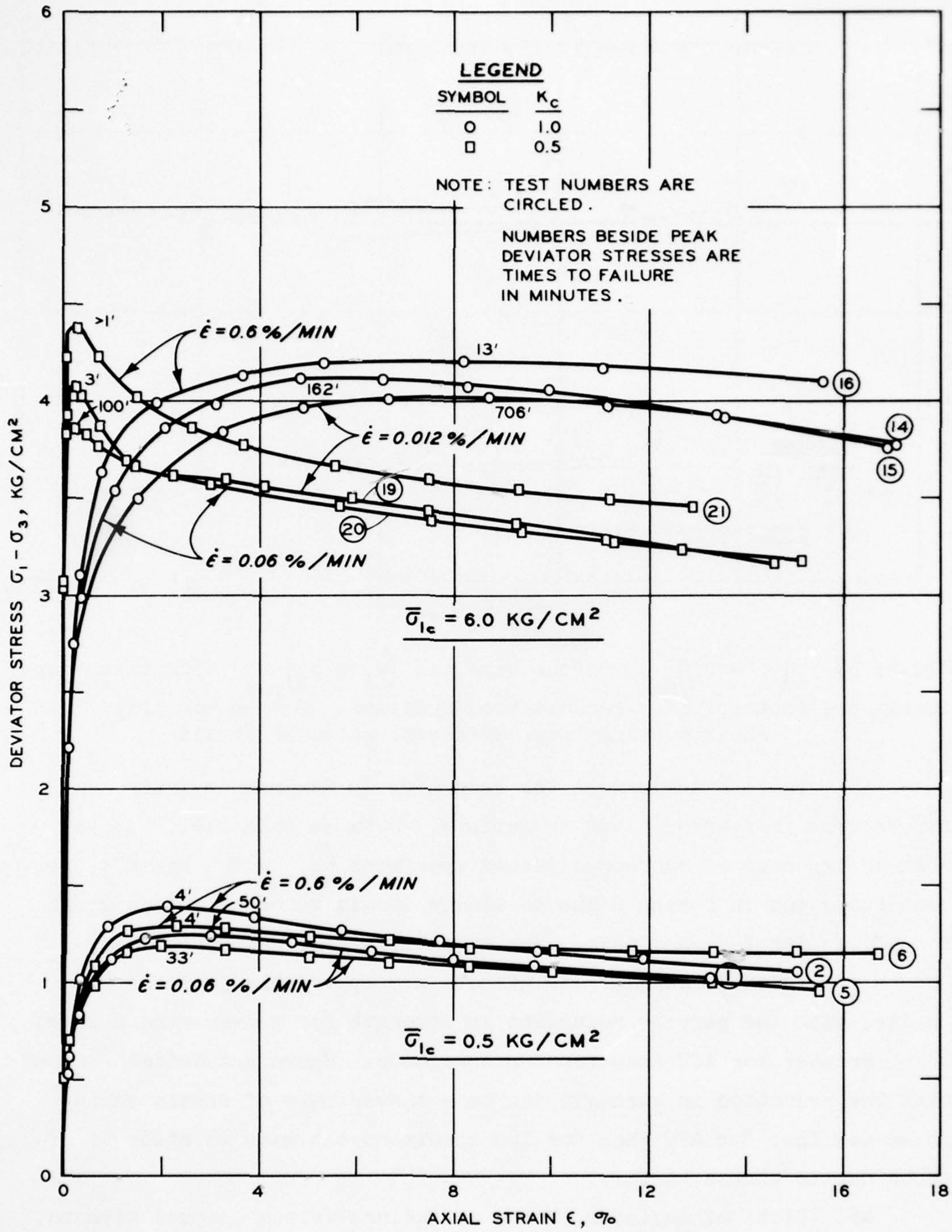

Figure 34. Deviator stress versus axial strain for isotropically and anisotropically consolidated specimens of Buckshot clay sheared using different rates of strain

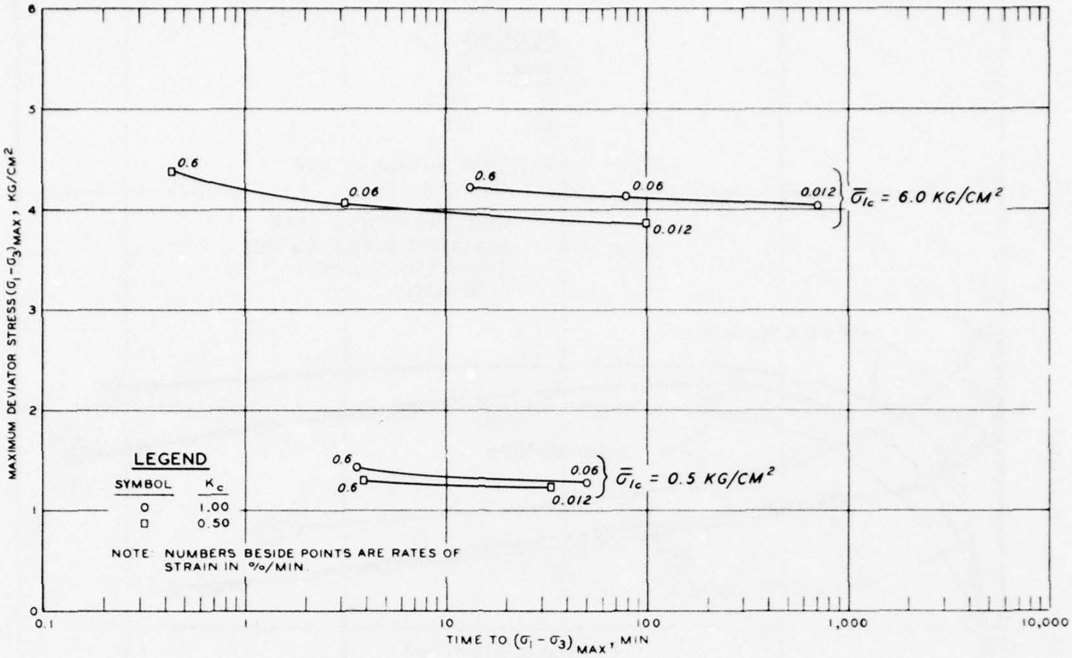

Figure 35. $\left(\sigma_1 - \sigma_3\right)_{max}$ versus time to $\left(\sigma_1 - \sigma_3\right)_{max}$ for anisotropically and isotropically consolidated specimens of Buckshot clay sheared using three different rates of strain

45. Table 6 summarizes the reduction in maximum deviator stress with increasing times to failure. Data in this table suggest that in the case of overconsolidated specimens $\left(\bar{\sigma}_{1c} = 0.5 \text{ kg/cm}^2\right)$, percent reduction in strength due to slower strain rates is not as great for ACU as for ICU specimens. For normally consolidated specimens $\left(\bar{\sigma}_{1c} = 6.0 \text{ kg/cm}^2\right)$, strain rate effects are apparently just the opposite, with the percent reduction in strength for slower strain rates being greater for ACU than for ICU specimens. Khera and Krizek[14] found that the reduction in strength due to a slower rate of strain during shear was less for ACU than for ICU specimens but made no study of effects due to stress history.

46. Plots of deviator stress at failure versus elapsed time to failure for tests performed on specimens of EABPL clay having $\bar{\sigma}_{1c}$ values of 3.0 and 4.8 kg/cm² and K_c ratios of 1.0 and 0.5 are given

in Figure 36.* The tests having the slower strain rates were performed after it was determined that times to failure using the standard 0.06 percent per minute rate of strain were too short (4-6 min). These plots indicate that maximum deviator stresses for the EABPL clay may be more sensitive to rates of strain than are those for the Buckshot clay. For rates of strain of 0.06 and 0.010 percent per minute, maximum deviator stresses of specimens with $\overline{\sigma}_{1c} = 4.8$ kg/cm^2 and $K_c = 0.5$ were 2.96 and 2.70, respectively, which was a reduction of 9 percent. In the case of specimens of the Buckshot clay with $\overline{\sigma}_{1c} = 6.0$ kg/cm^2 and $K_c = 0.5$, the reduction in maximum deviator stress resulting from varying strain rates over a comparable range (0.06-0.012 percent per minute) was only 5 percent.

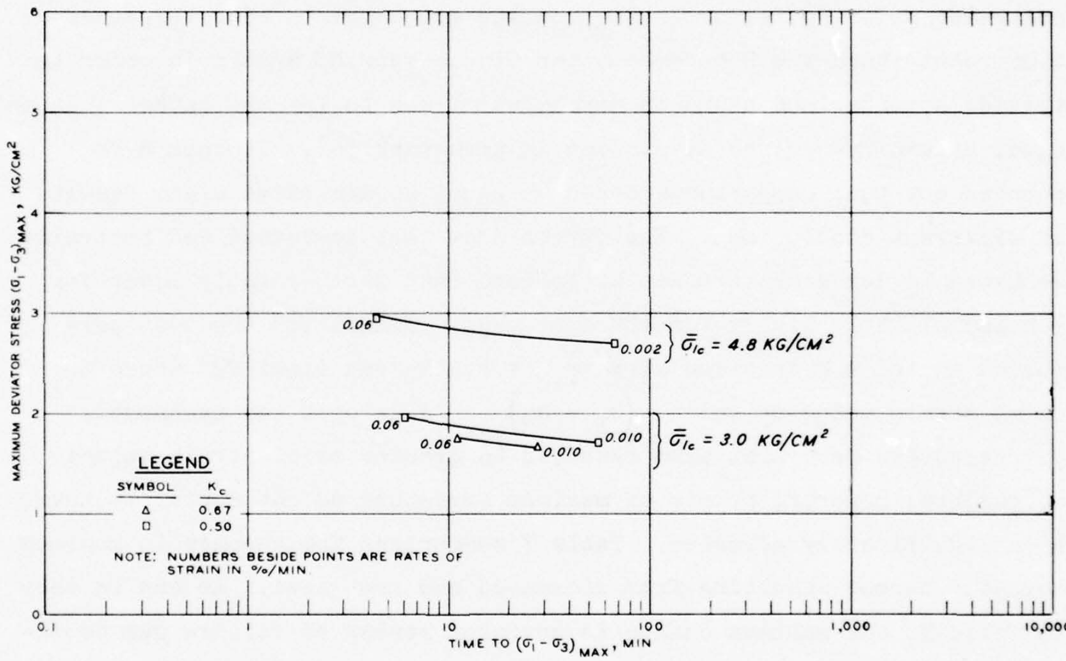

Figure 36. $(\sigma_1 - \sigma_3)_{max}$ versus time to $(\sigma_1 - \sigma_3)_{max}$ for isotropically and anisotropically consolidated specimens of EABPL clay sheared using three rates of strain

* The tests having rates of strain of 0.010 and 0.002 percent per minute were performed on 3.5-in.-high specimens. Due to equipment limitations, rates of strain for the 3.5-in.-high specimens could not be made equal to those of the standard 3.0-in.-high specimens.

Effects of decreased end restraint

47. Figure 37 shows stress-strain curves for specimens of Buckshot clay tested using low-friction caps and bases compared with those tested using standard caps and bases. Curves for specimens tested using standard caps and bases were developed using the standard 0.06 percent per minute rate of strain; those for specimens tested using low-friction caps and bases were developed using a rate of strain of 0.6 percent per minute. The 0.6 percent per minute strain rate for tests performed using low-friction caps and bases was chosen to decrease the time of shear so that sufficient time would not be allowed for the deviator stress to squeeze enough silicone grease from between the ends of the specimen and the cap and base to cause a significant increase in end restraint prior to failure. The results are compared with the standard 0.06 rather than the 0.6 percent per minute rate of strain in order to provide a comparison based on more equal times to failure rather than on equal strain rates (see discussion in paragraph 54). It should be pointed out that comparisons based on equal strain rates might result in different conclusions. The curves show that decreased end restraint resulted in deviator stresses at failure that were slightly lower for ICU and slightly higher for ACU specimens. Except for the test performed on the ACU specimen with $\bar{\sigma}_{1c} = 6.0\ kg/cm^2$ (test 22) where the axial strain value at which $\left(\sigma_1 - \sigma_3\right)_{max}$ developed was unchanged, decreased end restraint also resulted in greater axial strain values at failure; however, points of maximum curvature do not appear to have been significantly affected. Table 7 summarizes the changes in maximum deviator stress resulting from decreased end restraint. As can be seen in Table 7, the maximum change in deviator stress at failure due to decreased end restraint was less than 15 percent, thus suggesting that decreased end restraint has no significant effect on the strength of either ICU or ACU specimens. The finding that stress-strain characteristics of ICU specimens are relatively unaffected by decreased end restraint is consistent with previous work by Rowe and Barden[21] and Duncan, Seed, and Dunlop.[22]

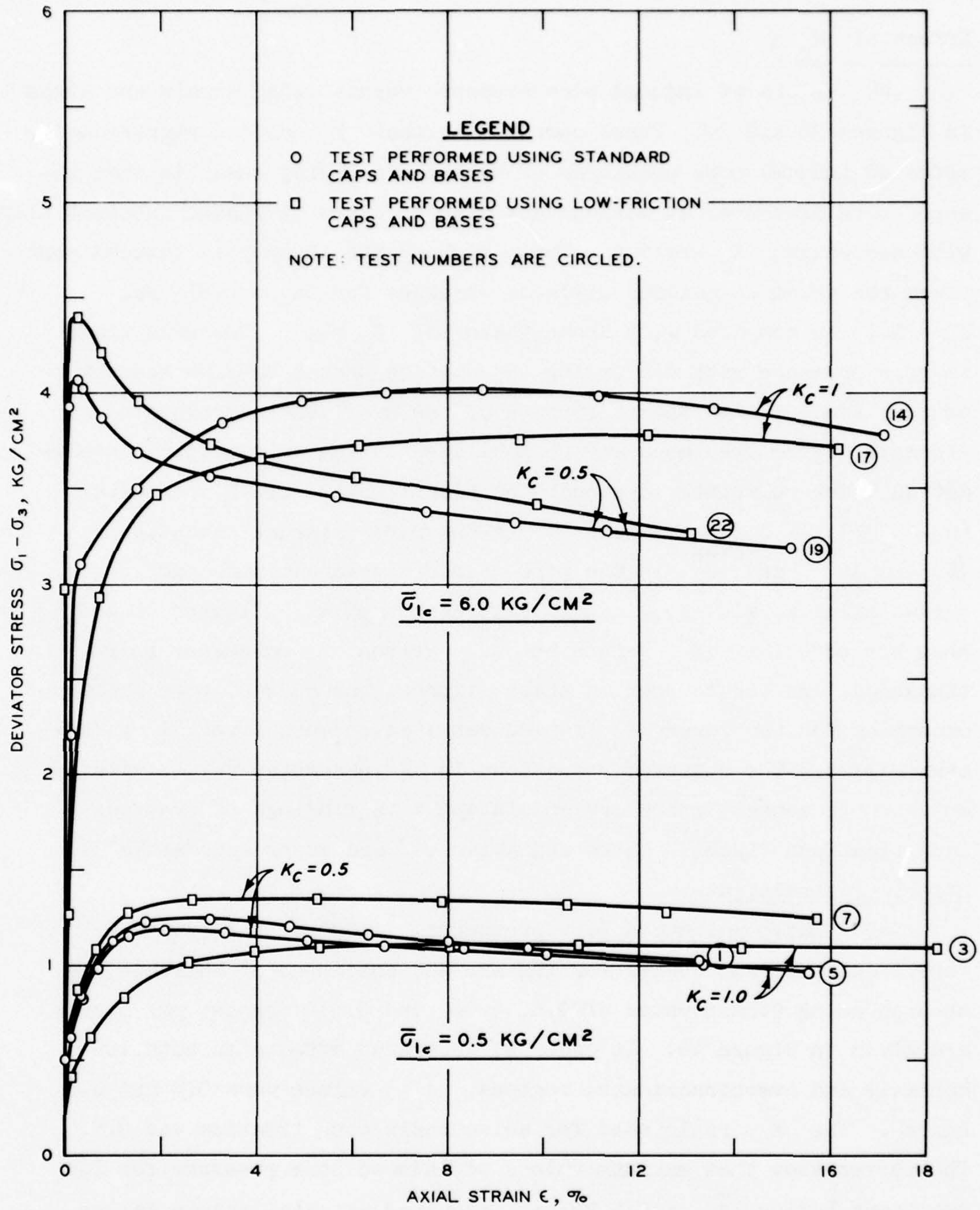

Figure 37. Deviator stress versus axial strain for isotropically and anisotropically consolidated specimens of Buckshot clay tested using standard and low-friction caps and bases

Induced Pore Pressures

Effect of K_c

48. Plots of induced pore pressure versus axial strain are given in Figures 38 and 39. These curves show that K_c ratios significantly affected induced pore pressures of both clays during shear in that induced pore pressures at maximum deviator stresses decreased substantially with decreasing K_c ratios. Table 8 shows the changes in induced pore pressures taken at maximum deviator stresses for $K_c = 0.67$ and $K_c = 0.5$ as compared with those taken for $K_c = 1$. The reductions in pore pressure with decreasing K_c ratios should be expected, of course, since a significant portion of the available undrained shear strength of the specimens may be mobilized during anisotropic consolidation under relatively drained conditions. Plots of A parameter $(u - u_o)/\left(\sigma_1 - \sigma_3\right)_{max}$, where u is the pore pressure taken at $\left(\sigma_1 - \sigma_3\right)_{max}$ and u_o is the pore pressure prior to undrained shear, versus axial strain are given in Figures 40 and 41. Figures 42 and 43 show the effect of K_c ratios on $\bar{\sigma}_{1c}$ versus A parameter relationships. As can be seen in these figures, the reduced pore pressures occurring for the lower K_c ratios resulted in much lower A parameter values. The observed reductions in A parameter values with anisotropic consolidation are consistent with findings of previous investigations (Ladd,[12] Khera and Krizek,[14] and Broms and Ratnam[8]).

Effect of strain rate

49. Maximum induced pore pressures. Induced pore pressure versus axial strain curves for ICU and ACU specimens of Buckshot clay sheared using strain rates of 0.6, 0.06, and 0.012 percent per minute are given in Figure 44. In order to determine effects in both the normally and overconsolidated regions, $\bar{\sigma}_{1c}$ values were 0.5 and 6.0 kg/cm^2. The K_c ratio used for anisotropic consolidation was 0.5. The curves show that maximum values of induced pore pressure for ICU specimens having $\bar{\sigma}_{1c} = 0.5\ kg/cm^2$ occurred at axial strain values of 0.7 and 0.4 percent and were 0.34 and 0.29 kg/cm^2, respectively. Maximum values of induced pore pressure for ACU specimens

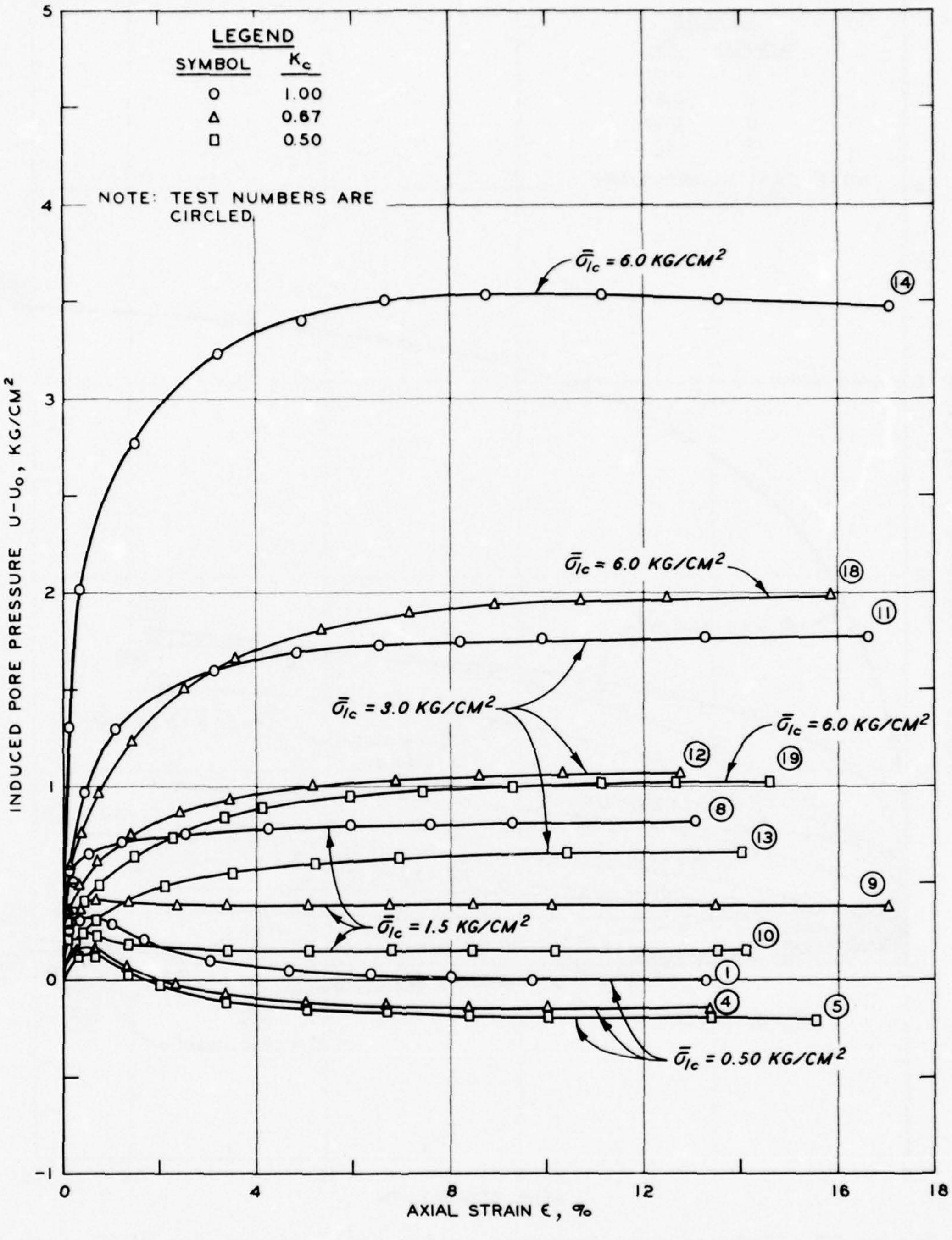

Figure 38. Induced pore pressure versus axial strain for Buckshot clay

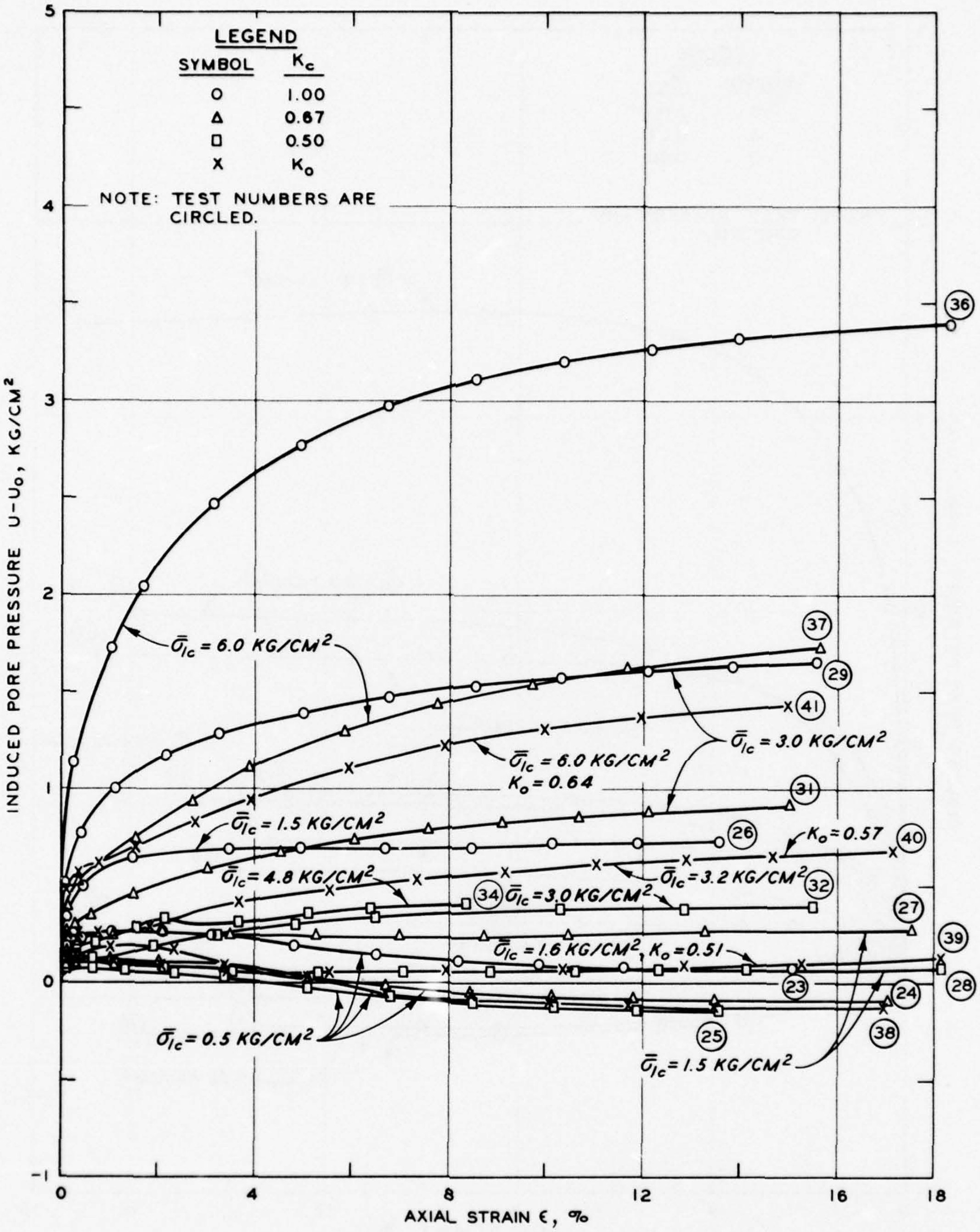

Figure 39. Induced pore pressure versus axial strain for EABPL clay

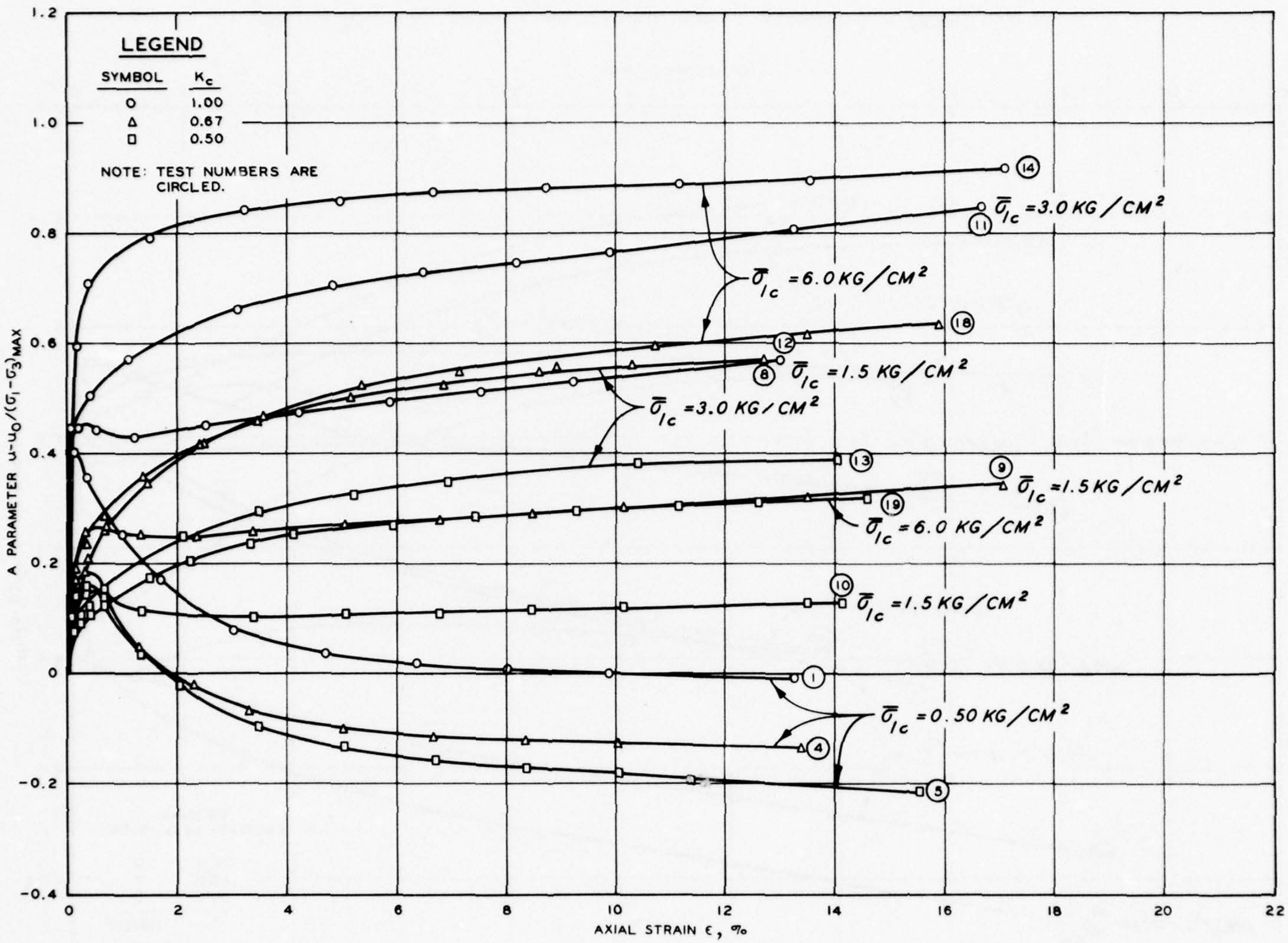

Figure 40. A parameter versus axial strain for Buckshot clay

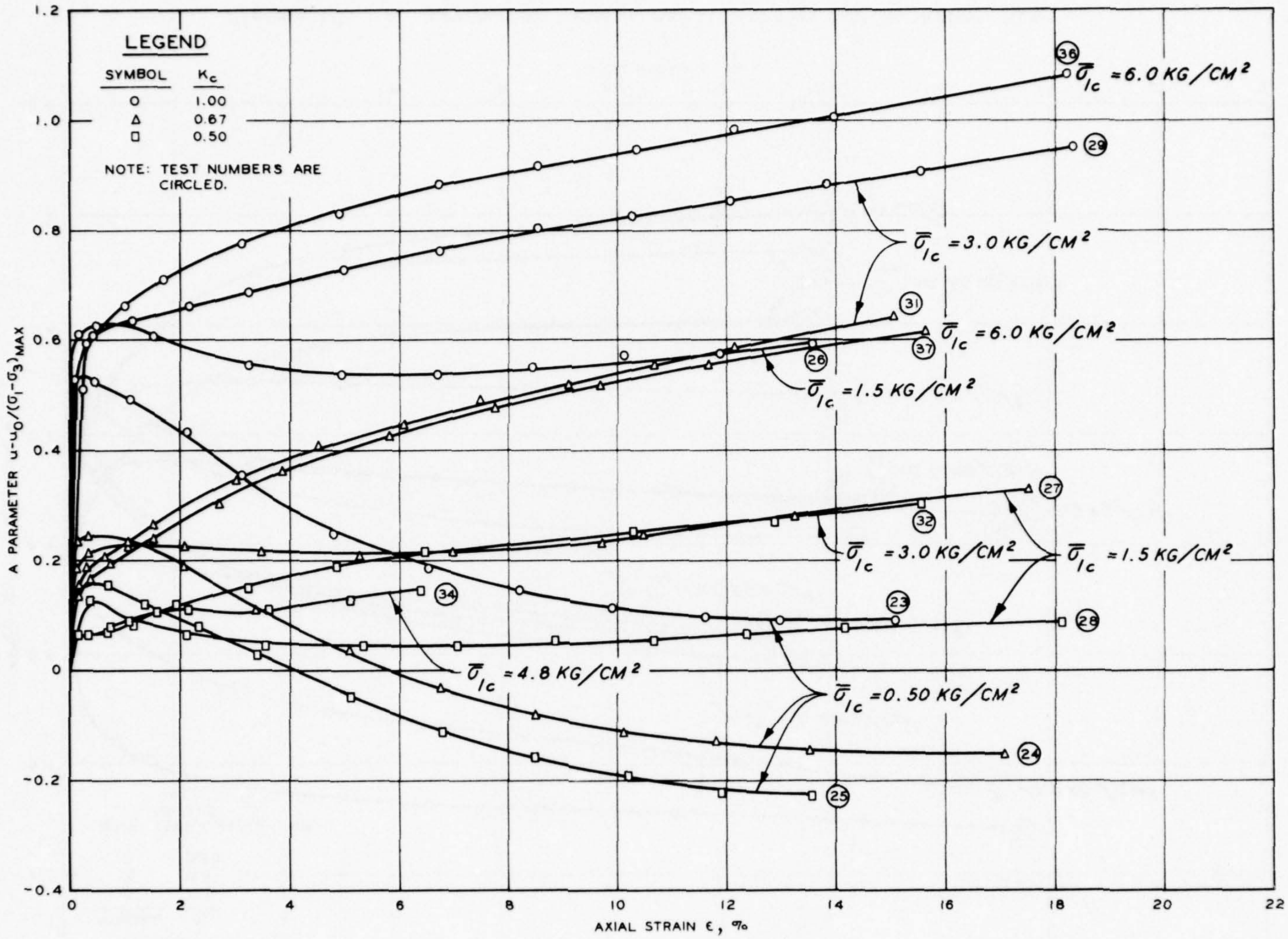

Figure 41. A parameter versus axial strain for EABPL clay

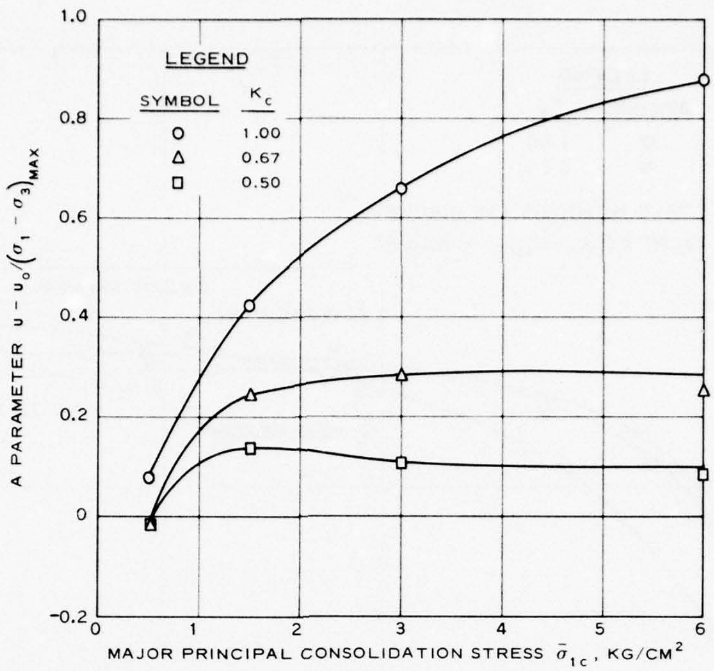

Figure 42. A parameter versus major principal consolidation stress for Buckshot clay

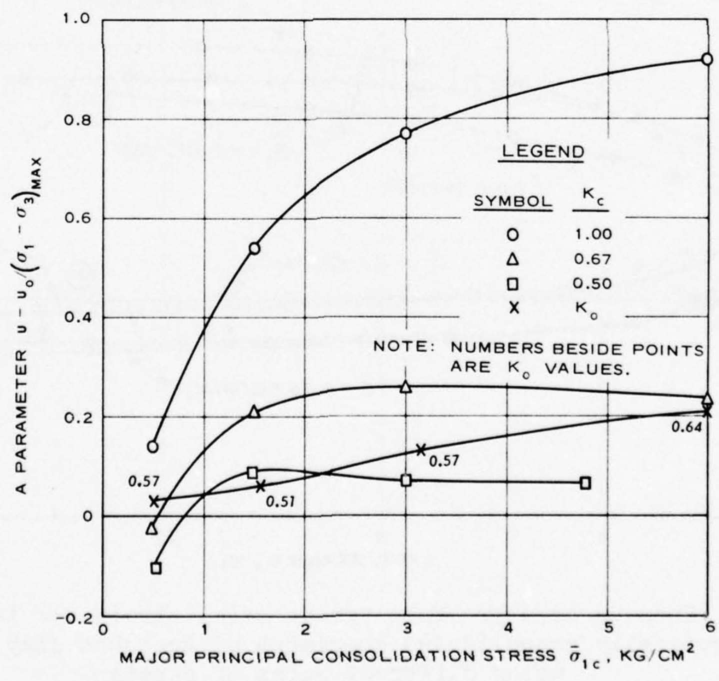

Figure 43. A parameter versus major principal consolidation stress for EABPL clay

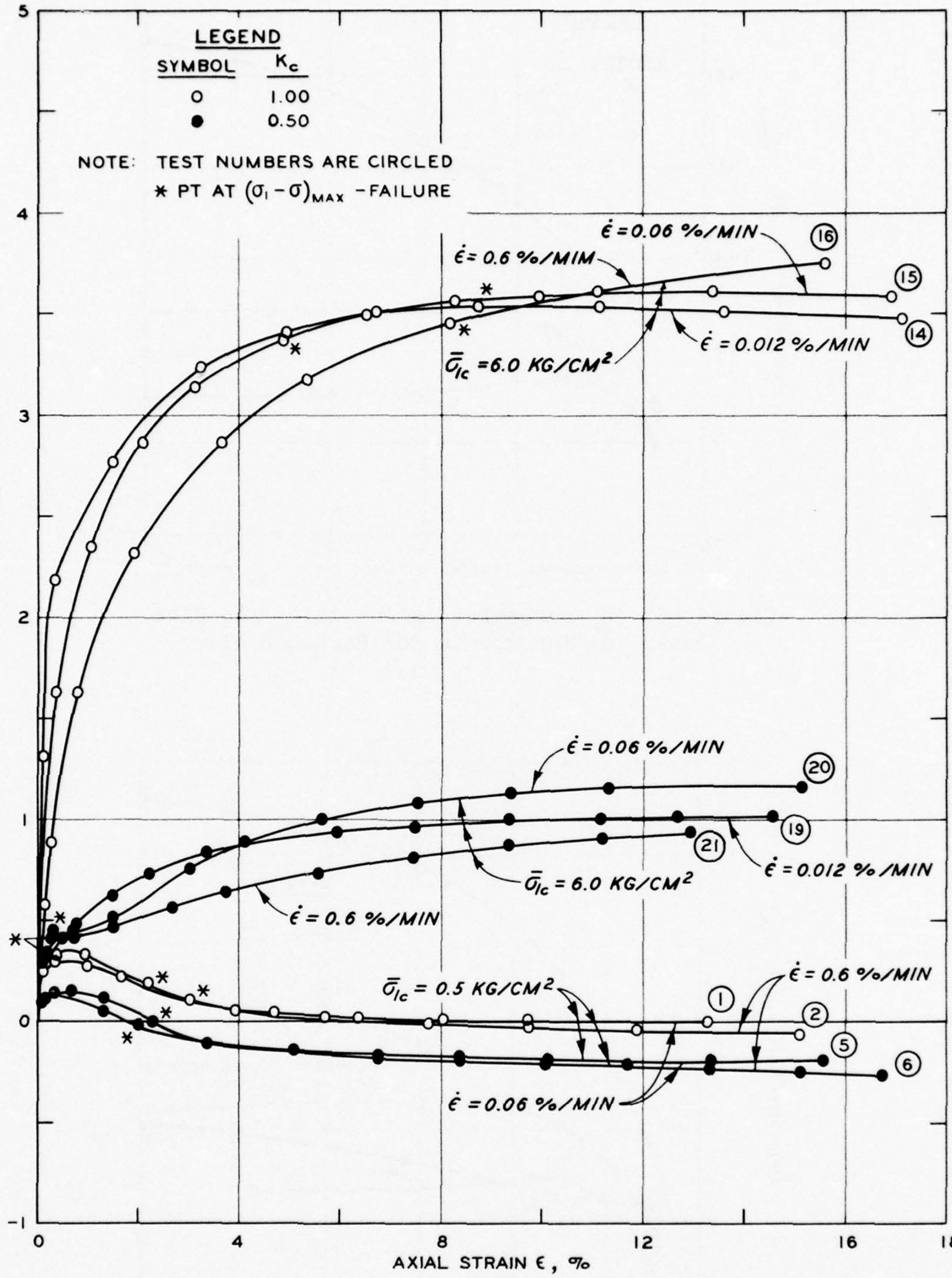

Figure 44. Induced pore pressure versus axial strain for isotropically and anisotropically consolidated specimens of Buckshot clay sheared using different rates of strain

with $\bar{\sigma}_{1c} = 0.5\ kg/cm^2$ were developed at 0.8 and 0.3 percent and were 0.19 and 0.18 kg/cm^2, respectively. In both cases the lower pore pressure and axial strain values occurred using the 0.06 percent per minute strain rate. Induced pore pressures for the ICU specimens having $\bar{\sigma}_{1c} = 6.0$ reached maximum values at axial strains ranging from 9 to 16 percent and ranged from 3.54 to 3.75 kg/cm^2. Both the maximum pore pressures and the strains at which they developed decreased with decreasing rates of strain. Induced pore pressures for the ACU specimens having $\bar{\sigma}_{1c} = 6.0\ kg/cm^2$ reached maximum values at axial strains ranging from 13 to 15 percent and varied from 0.93 to 1.16 kg/cm^2. The strains at which they developed decreased with decreasing rates of strain. The maximum pore pressure was developed for the 0.06 percent per minute strain rate, and the lowest pressure occurred for the 0.012 percent per minute strain rate. Pore pressures for the ACU specimens having $\bar{\sigma}_{1c} = 6.0\ kg/cm^2$ and tested using strain rates of 0.6 and 0.06 percent per minute peaked at low axial strains (0.3 and 0.4 percent) and then, after decreasing, began increasing at strains of 0.5-1 percent to the end of the tests. These results suggest that strain rate effects on maximum induced pore pressure values and the axial strain values at which they develop are similar for ICU and ACU overconsolidated specimens. In the case of normally consolidated specimens, neither the strain rate effects on maximum induced pore pressure nor the corresponding axial strain values appear to be altered by the method of consolidation if the low maximum induced pore pressure obtained for the test performed on the ACU specimen sheared at the fastest strain rate is neglected. There was no satisfactory explanation for the apparently low value.

50. Induced pore pressures at $\left(\sigma_1 - \sigma_3\right)_{max}$. Table 9 shows the difference between induced pore pressures at $\left(\sigma_1 - \sigma_3\right)_{max}$ for the 0.6 percent per minute strain rate and for each of the slower strain rates used. The table shows that at failure, values of induced pore pressure for both ICU and ACU specimens were not significantly affected by strain rate in either the normally consolidated $\left(\bar{\sigma}_{1c} = 6.0\ kg/cm^2\right)$ or overconsolidated $\left(\bar{\sigma}_{1c} = 0.5\ kg/cm^2\right)$ range.

51. Prior to $(\sigma_1 - \sigma_3)_{max}$. Plots of induced pore pressure versus elapsed time of shear at axial strain values of 1.0 percent for the tests having $\bar{\sigma}_{1c}$ = 0.5 kg/cm^2 and 0.2 percent for the tests having $\bar{\sigma}_{1c}$ = 6.0 kg/cm^2 are given in Figure 45. The axial strain values were

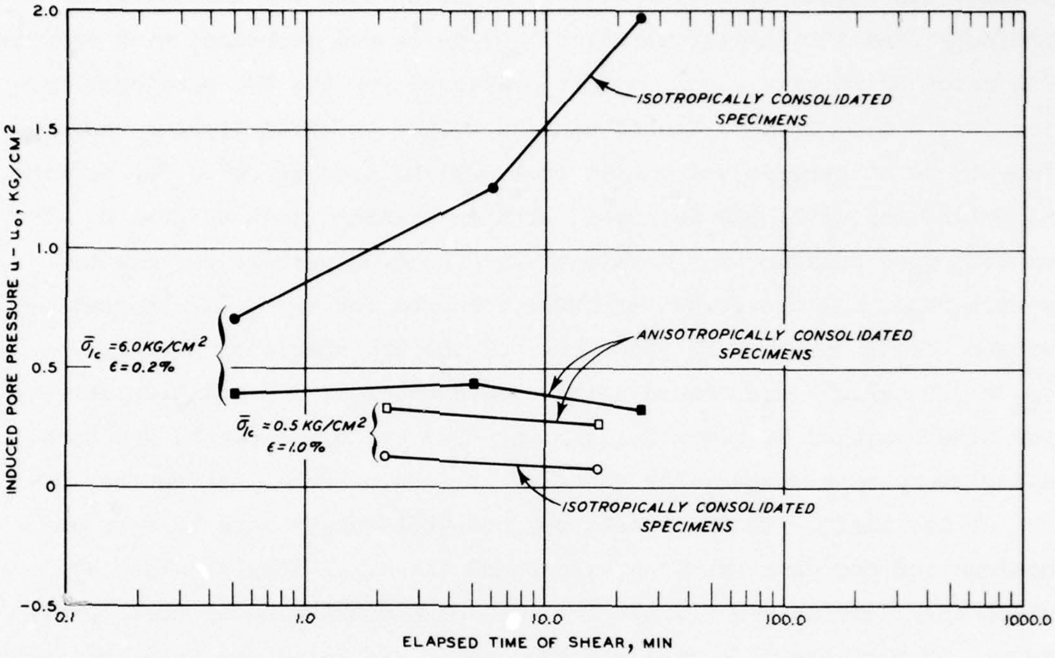

Figure 45. Induced pore pressure versus elapsed time of shear for isotropically and anisotropically consolidated specimens of Buckshot clay taken at axial strain values prior to the development of the maximum deviator stress

chosen so that conditions prior to the development of the maximum deviator stress would be represented. The plots for the overconsolidated specimens (i.e. those having $\bar{\sigma}_{1c}$ = 0.5 kg/cm^2) show that during the initial part of shear, induced pore pressures for both ICU and ACU specimens decreased similarly with slower strain rates, thus suggesting that the method of consolidation does not alter effects due to strain rate prior to the development of $(\sigma_1 - \sigma_3)_{max}$ in tests of overconsolidated specimens. For normally consolidated specimens (i.e. those having $\bar{\sigma}_{1c}$ = 6.0 kg/cm^2), however, the appropriate plot in Figure 45 shows that effects due to strain rate prior to failure were significantly altered by anisotropic consolidation. Shearing action of these specimens during anisotropic consolidation apparently erased effects due to stress history since the induced pore pressure values changed very little with slower strain rates instead of increasing as did the ICU specimens and as would be expected for normally consolidated specimens. A previous investigation at WES[23] has indicated that end restraint causes greater shear strains in the central portion of CU triaxial specimens during shear, resulting in a tendency for this portion of overconsolidated specimens to dilate and of normally consolidated specimens to consolidate. Pore pressure gradients within the specimen due to these conditions tend to dissipate with decreasing strain rates, and pore pressure measurements become more representative of those occurring in the middle portion. Thus slower strain rates should produce lower induced pore pressure measurements for overconsolidated specimens and higher induced pore pressures for normally consolidated specimens prior to the development of $\left(\sigma_1 - \sigma_3\right)_{max}$.

Effects of decreased end restraint

52. The relationships between pore pressure and axial strain for tests performed using standard and low-friction caps and bases are given in Figure 46. Specimens were consolidated using K_c ratios of 1.0 and 0.5 with $\bar{\sigma}_{1c}$ values of 0.5 and 6.0 kg/cm^2. The curves show that during the initial part of shear, induced pore pressures developed in tests using low-friction caps and bases were much less than those occurring with standard end platens, thus indicating that the response of the pore pressure measurement system used with the low-friction caps and bases may have been delayed. This possibility is further enhanced by the observation that the B value check at the end of consolidation indicated a slight delay in pore pressure responses (approximately 5 sec) for tests performed with low-friction caps and bases even though in one case the back pressure was increased from 60 to 120 psi. The delay may have been due to silicone grease permeating the filter strips, since significant amounts of grease were found on the outer edges of the Teflon disks at the end of the tests; however, it is felt that the curves shown for tests performed with low-friction caps and bases are

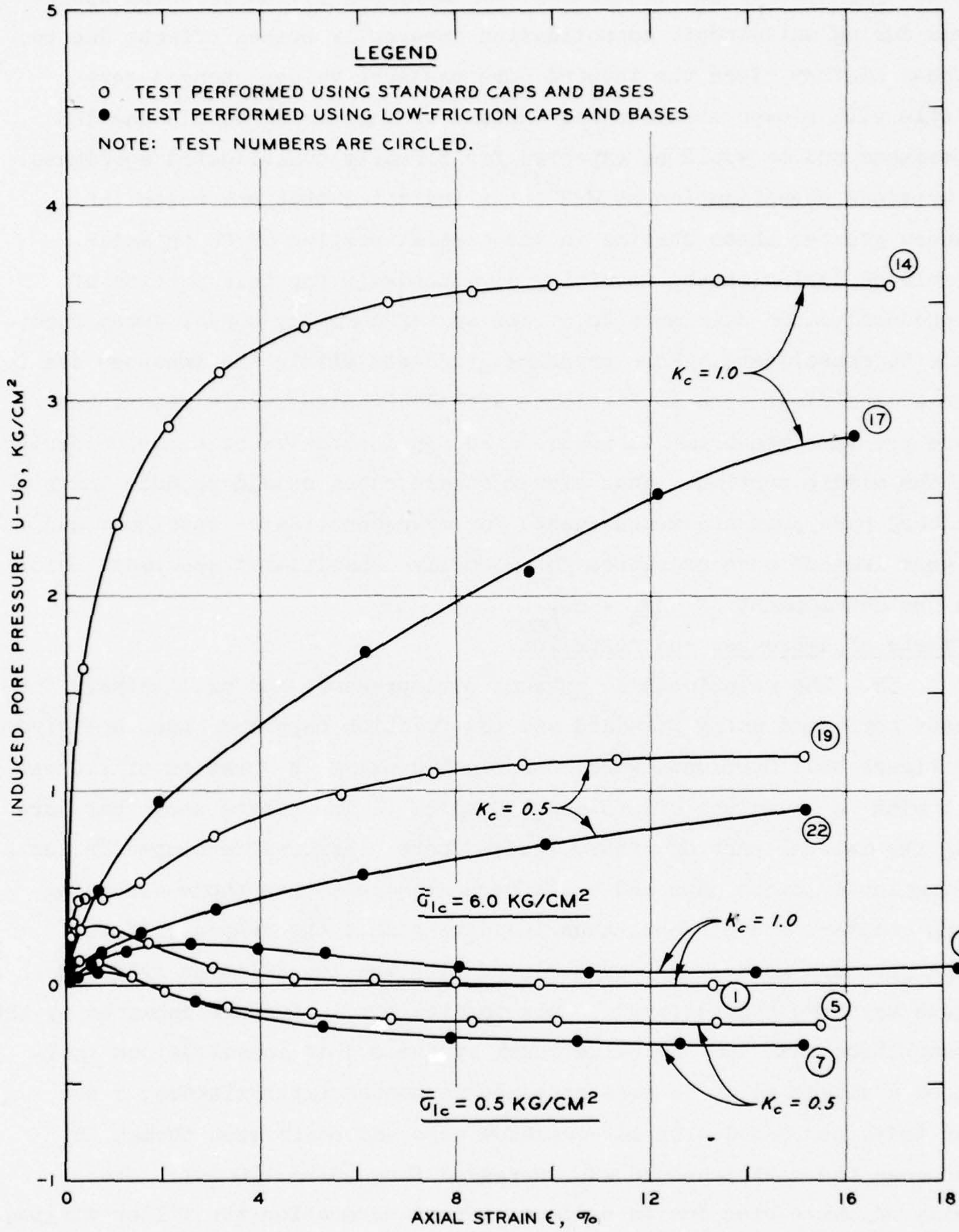

Figure 46. Induced pore pressure versus axial strain for isotropically and anisotropically consolidated specimens of Buckshot clay tested using standard and low-friction caps and bases

not representative of actual specimen conditions and that a comparison with those developed using standard caps and bases would be inappropriate.

Effective Stresses

53. Effective major principal stress ratio $\bar{\sigma}_1/\bar{\sigma}_3$ versus axial strain curves are given in Figures 47 and 48. Table 10 gives the maximum $\bar{\sigma}_1/\bar{\sigma}_3$ values for the K_c ratios and stresses used. This table shows that $(\bar{\sigma}_1/\bar{\sigma}_3)_{max}$ values for overconsolidated specimens $(\bar{\sigma}_{1c} < 6.0 \text{ kg/cm}^2)$ of Buckshot clay were much more sensitive to K_c ratios than were those of overconsolidated specimens of the EABPL clay. The maximum variation in $(\bar{\sigma}_1/\bar{\sigma}_3)_{max}$ values with K_c for the Buckshot clay was 2.46 and occurred at $\bar{\sigma}_{1c} = 0.5 \text{ kg/cm}^2$. The maximum variation in $(\bar{\sigma}_1/\bar{\sigma}_3)_{max}$ values with K_c for the EABPL clay was 0.28 and occurred at $\bar{\sigma}_{1c} = 1.5 \text{ kg/cm}^2$. Figure 49 shows curves representing the relationships between $(\bar{\sigma}_1/\bar{\sigma}_3)_{max}$ and $\bar{\sigma}_{1c}$ for both clays. These curves indicate that $(\bar{\sigma}_1/\bar{\sigma}_3)_{max}$ values for specimens of both clays approach the same curve as $\bar{\sigma}_{1c}$ values are increased. The curves become quite flat for the higher $\bar{\sigma}_{1c}$ values (normally consolidated specimens). The lowest $(\bar{\sigma}_1/\bar{\sigma}_3)_{max}$ value for the Buckshot clay was 2.63 and the lowest for the EABPL clay was 2.23. The lowest $(\bar{\sigma}_1/\bar{\sigma}_3)_{max}$ value for the K_o tests performed on the EABPL clay was 2.21. Vector curves for effective stresses are given in Figures 50 and 51.

Strength Envelopes

Criteria for comparing ACU and ICU strength envelopes

54. The problem of comparing ACU and ICU strengths is apparent

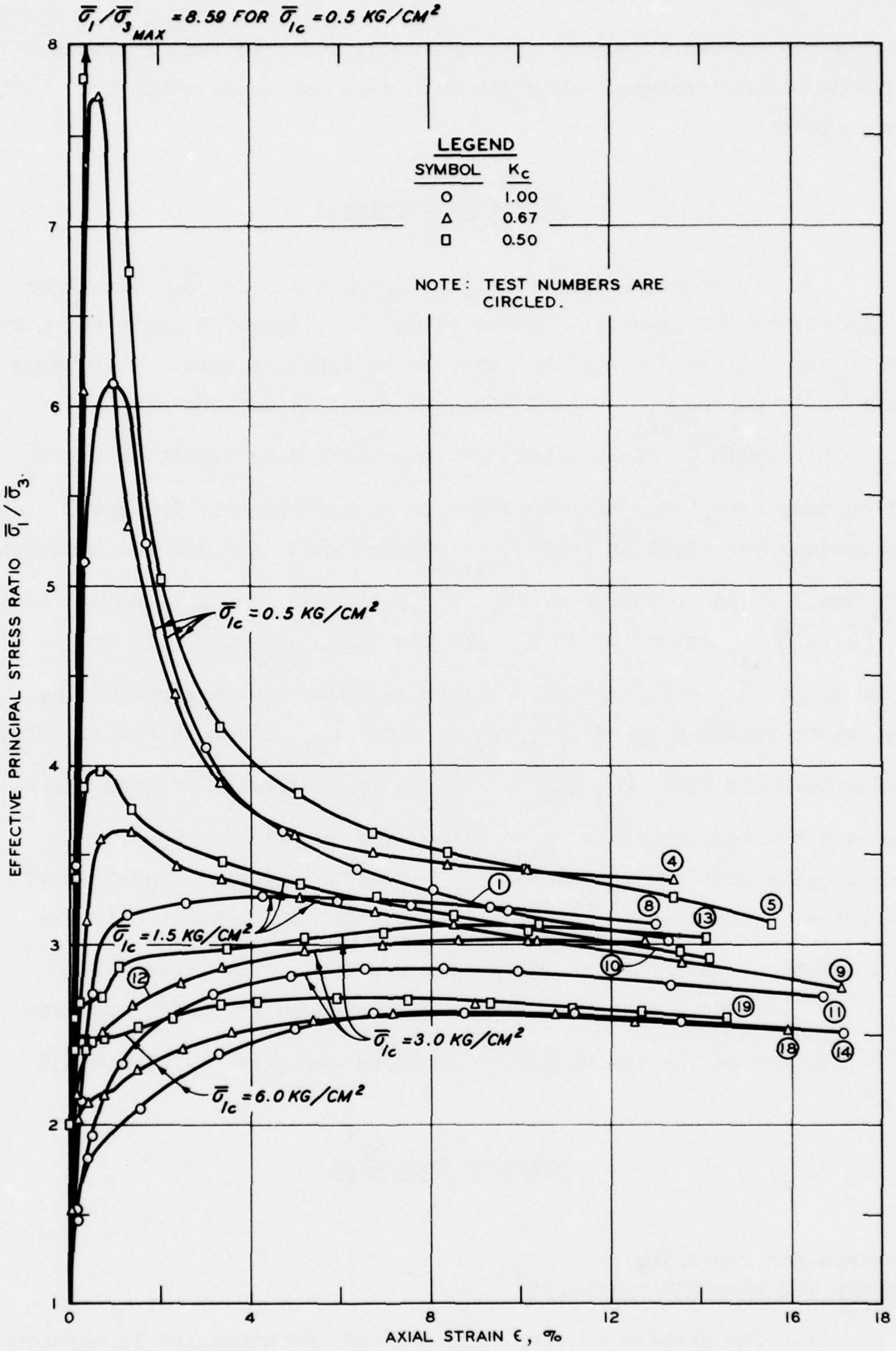

Figure 47. Effective principal stress ratio versus axial strain for Buckshot clay

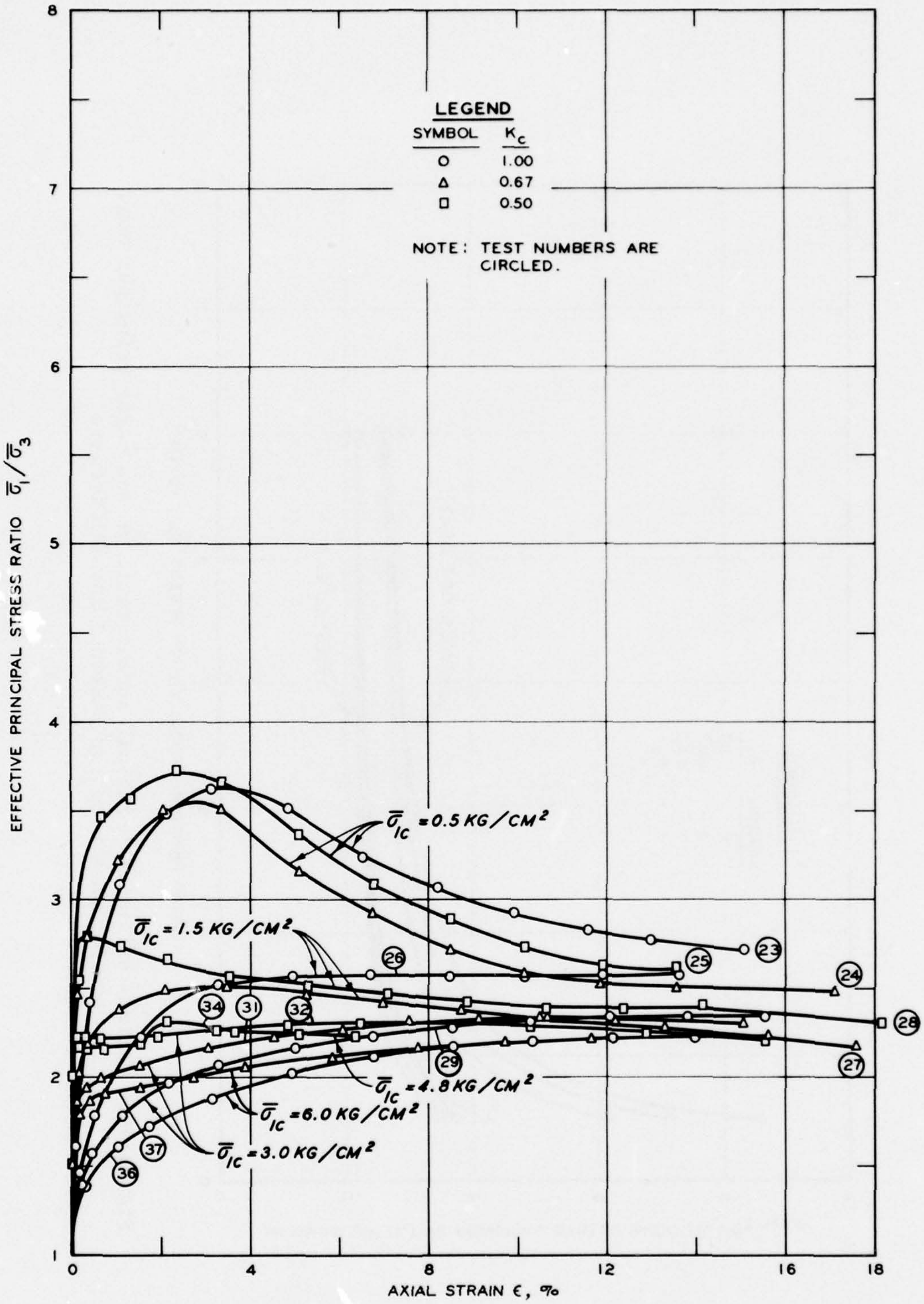

Figure 48. Effective principal stress ratio versus axial strain for EABPL clay

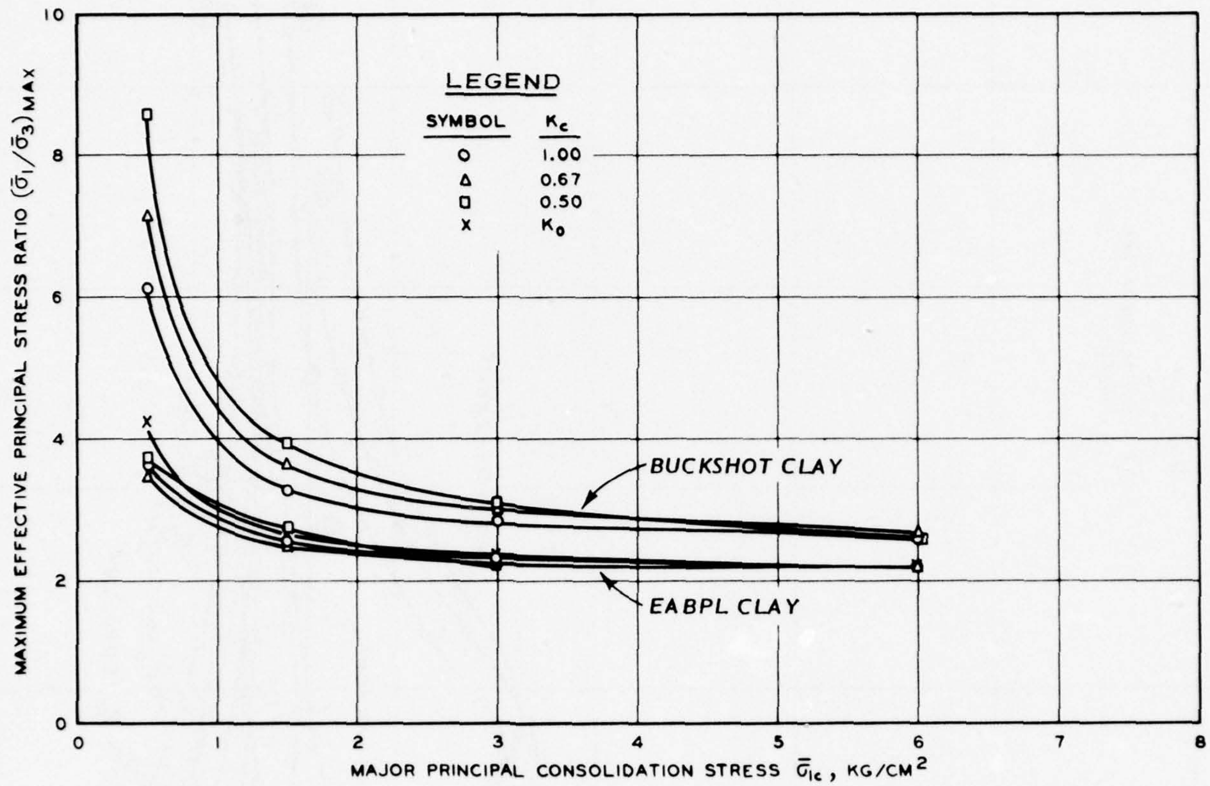

Figure 49. Maximum effective principal stress ratio versus major principal consolidation stress for Buckshot and EABPL clays

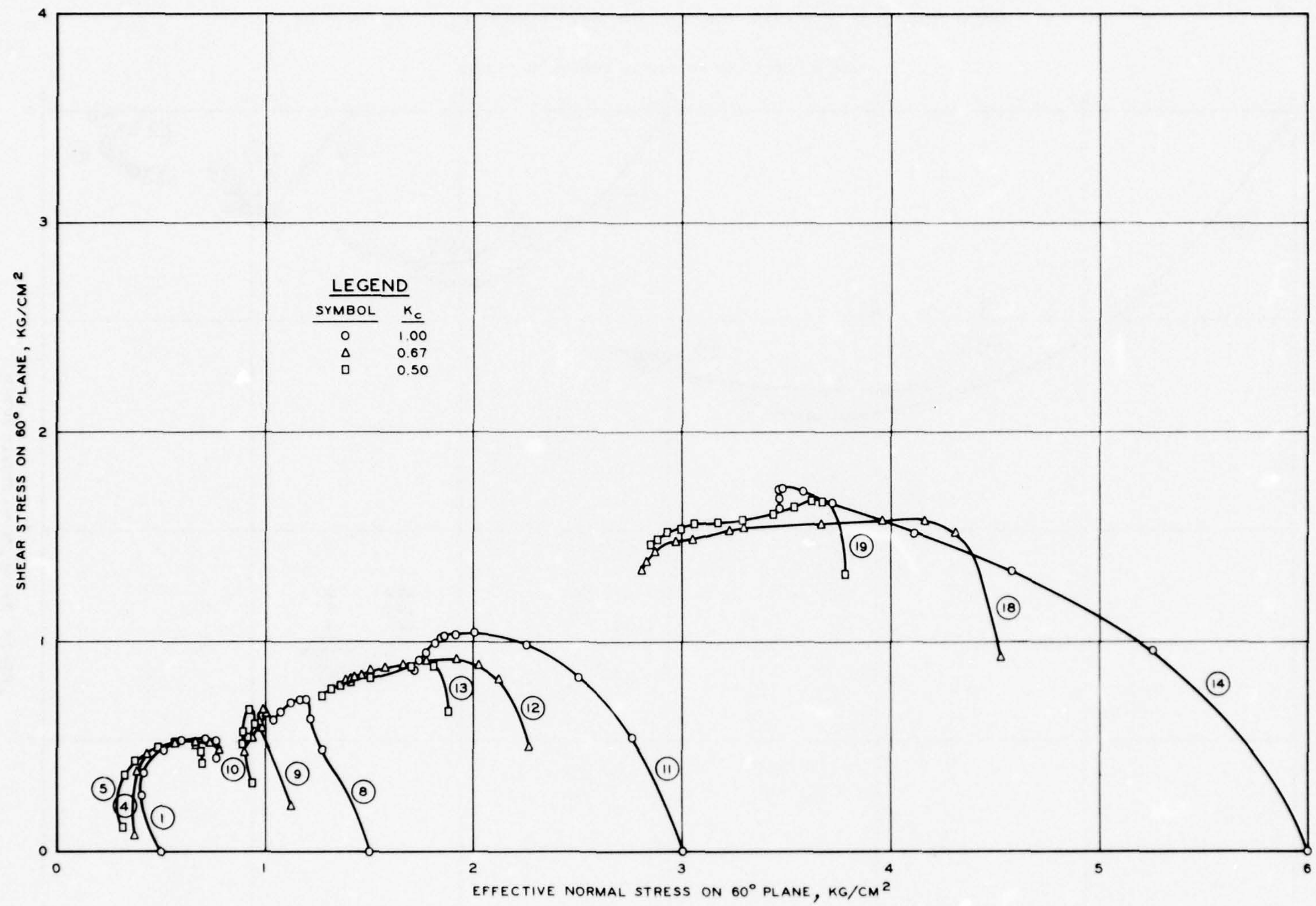

Figure 50. Stress paths on 60-deg plane for Buckshot clay

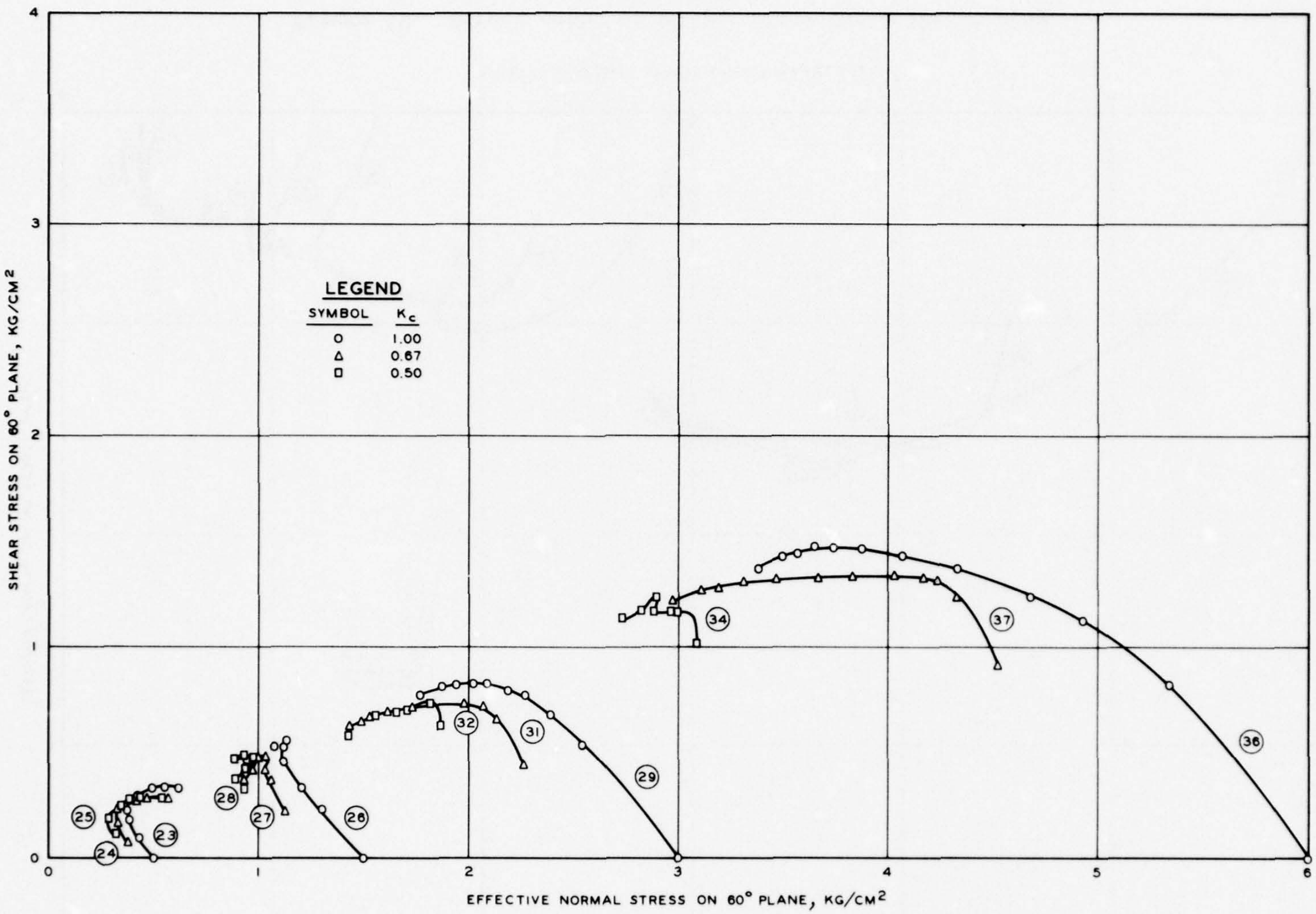

Figure 51. Stress paths on 60-deg plane for EABPL clay

in Figure 35, in which $(\sigma_1 - \sigma_3)_{max}$ versus elapsed time to failure relationships are presented. These results show that if strength comparisons are based upon equal strain rates, the ACU specimens always experience shorter times to failure (due to the small axial strain values at which $(\sigma_1 - \sigma_3)_{max}$ values develop), and as the strain rate is decreased, they may exhibit strengths higher or lower than or equal to those of the comparable ICU specimens. At strain rates ranging from 0.6 to 0.06 percent per minute, normally consolidated ACU specimens $(\bar{\sigma}_{1c} = 6.0 \text{ kg/cm}^2)$ failed in less than 5 min, thus placing the corresponding $(\sigma_1 - \sigma_3)_{max}$ values in question since they are in the range in which strain rate effects are very pronounced. For the same range of strain rates, the spread of times to failure for normally consolidated ICU specimens is from 13 to 80 min, and strain rate effects are not nearly as pronounced, as evidenced by the more horizontal slope of the $(\sigma_1 - \sigma_3)_{max}$ versus time to $(\sigma_1 - \sigma_3)_{max}$ curve. Obviously, for valid strength measurements, slower strain rates are required for ACU than for ICU specimens. If the slower strain rates required for ACU specimens are applied to ICU specimens, excessive times to failure result, thus requiring considerable testing time and the introduction of possible secondary effects (creep) on the measured strengths. Therefore, it appears reasonable to use equivalent times to failure instead of strain rates to compare ACU and ICU strengths. The strength envelopes presented in this section were derived using results from ACU and ICU tests having approximately equal times to failure.

Based on total stresses

55. Tangent to Mohr's circles. Mohr's diagrams and strength envelopes based on total stresses taken at $(\sigma_1 - \sigma_3)_{max}$ are given in Figures 52 and 53. The strength envelopes are drawn tangent to the circles. Apparent angles of internal friction based on normally consolidated specimens (i.e. those having $\bar{\sigma}_{1c} = 6.0 \text{ kg/cm}^2$) are given in the tabulation on page 75.

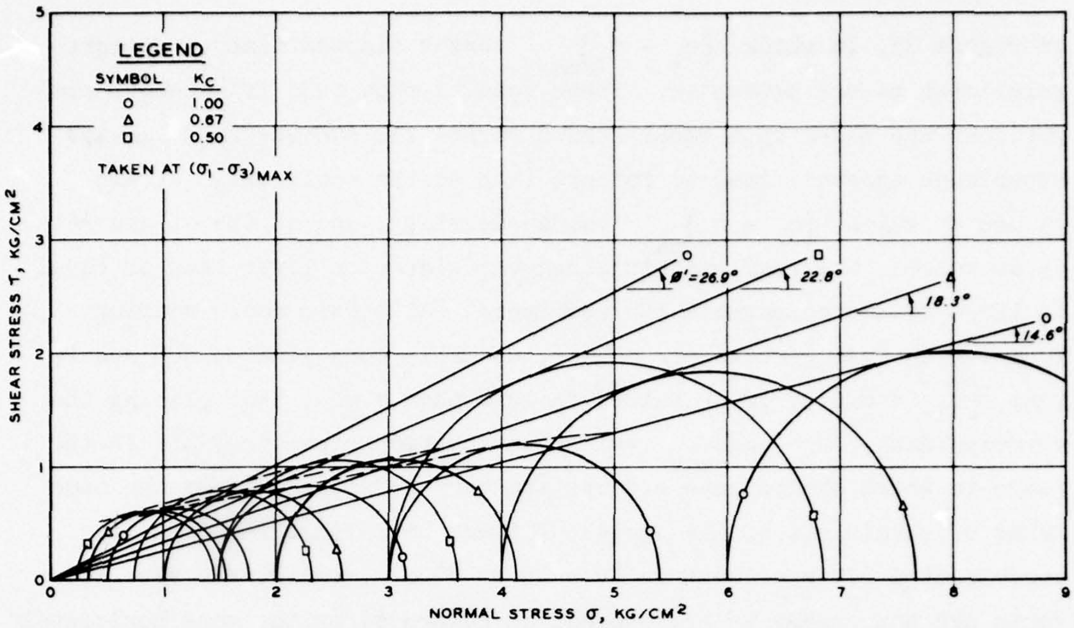

Figure 52. Mohr's diagrams and strength envelopes based on total stresses taken at $(\sigma_1 - \sigma_3)_{max}$ for Buckshot clay

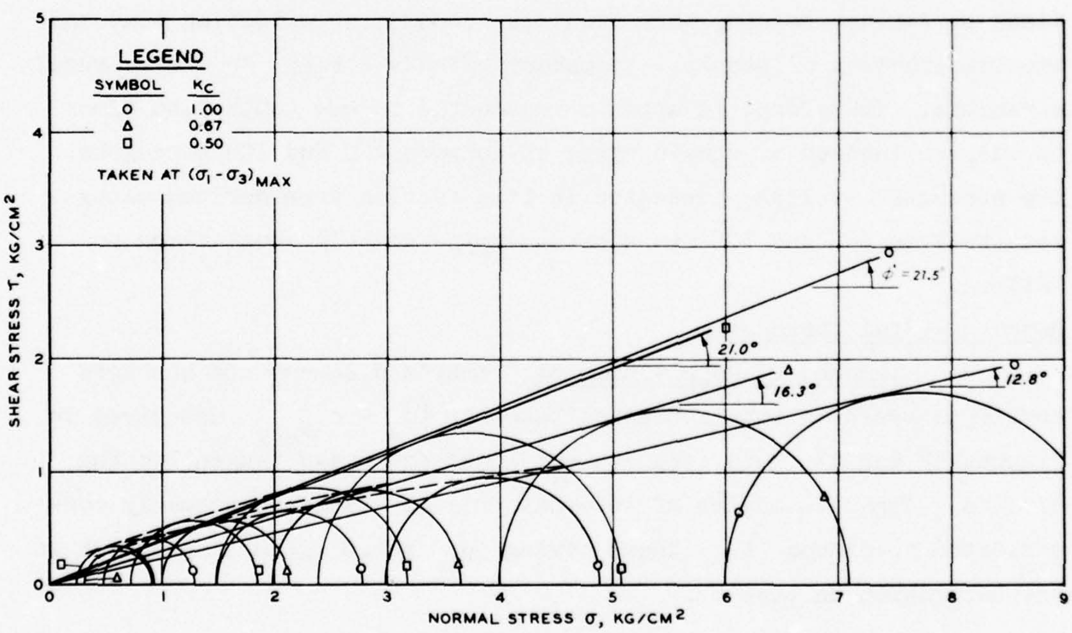

Figure 53. Mohr's diagrams and strength envelopes based on total stresses taken at $(\sigma_1 - \sigma_3)_{max}$ for EABPL clay

K_c Value	Angle of Internal Friction, ϕ, deg	
	Buckshot Clay	EABPL Clay
1	14.6	12.8
0.67	18.3	16.3
0.5	22.8	21.0

The strength envelopes are curved in the overconsolidated region $\left(\bar{\sigma}_{1c} = 0.5\text{-}3.0 \text{ kg/cm}^2\right)$. It should be remembered that since a $\bar{\sigma}_{1c}$ value greater than 3.0 kg/cm^2 would be required to again produce virgin compression characteristics, specimens having $\bar{\sigma}_{1c} = 3.0$ kg/cm^2 are slightly overconsolidated. Also shown in Figures 52 and 53 are effective stress envelopes for $K_c = 1.0$. As can be seen in these figures, a K_c ratio of 0.5 is very close to a failure condition for normally consolidated specimens of EABPL clay.

56. Envelopes based upon stresses on failure plane. Strength envelopes based on plots of shear stresses on the failure plane* at $\left(\sigma_1 - \sigma_3\right)_{max}$ versus effective normal stresses on the failure plane prior to undrained shear are given in Figures 54 and 55. Envelopes based on such plots are thought to better represent strength versus normal stress relationships since they are based on stresses within the specimens prior to shear instead of at failure, which is the case for envelopes based on Mohr's circles. The apparent angles of internal friction based on normally consolidated specimens are given in the following tabulation:

K_c Value	Apparent Angle of Internal Friction, ϕ, deg	
	Buckshot Clay	EABPL Clay
1	16.2	13.7
0.67	19.3	16.4
0.5	23.9	20.8

57. Taylor's method.[2] Figures 56 and 57 show a comparison of strength values derived using Taylor's method[2] for determining the

---

* A 60-deg failure plane was assumed.

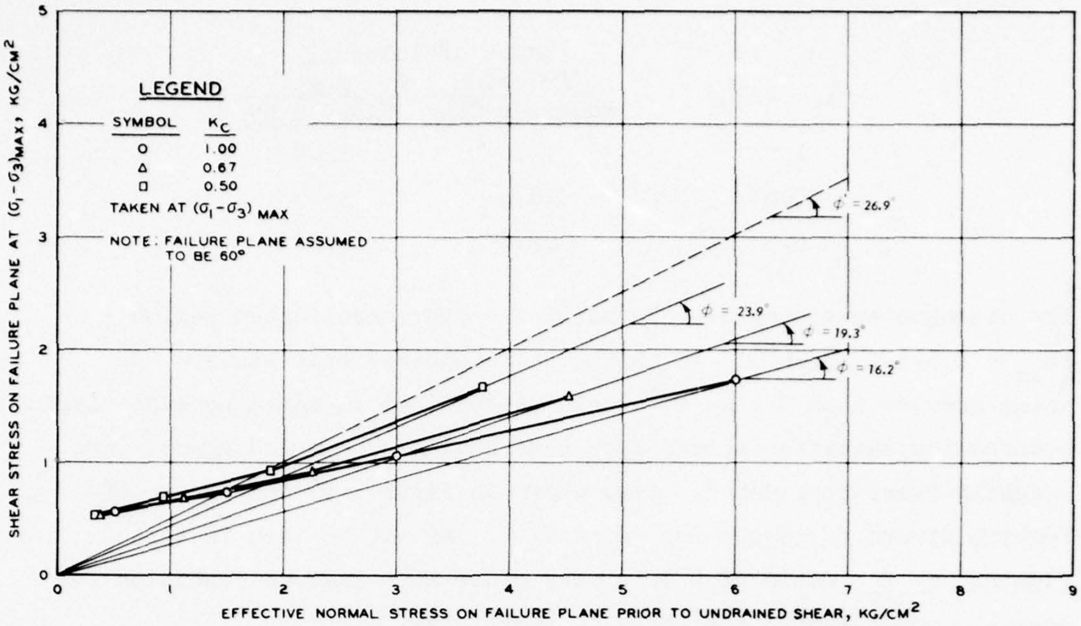

Figure 54. Strength envelopes based on plots of shear stress on the failure plane at $\left(\sigma_1 - \sigma_3\right)_{max}$ versus effective normal stress on the failure plane prior to undrained shear for Buckshot clay

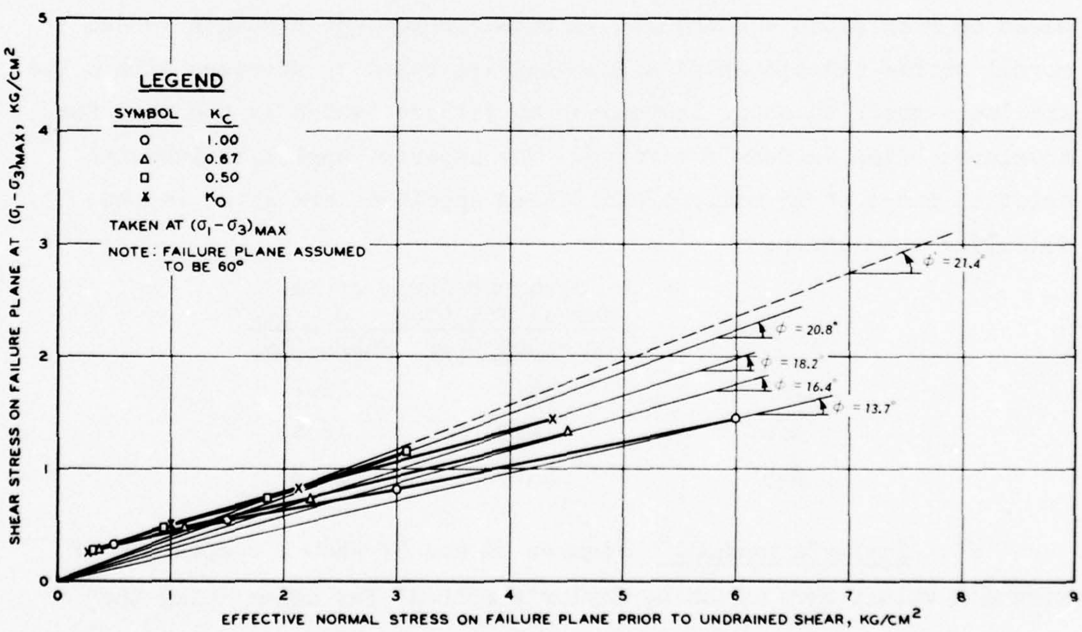

Figure 55. Strength envelopes based on plots of shear stress on the failure plane at $\left(\sigma_1 - \sigma_3\right)_{max}$ versus effective normal stress on the failure plane prior to undrained shear for EABPL clay

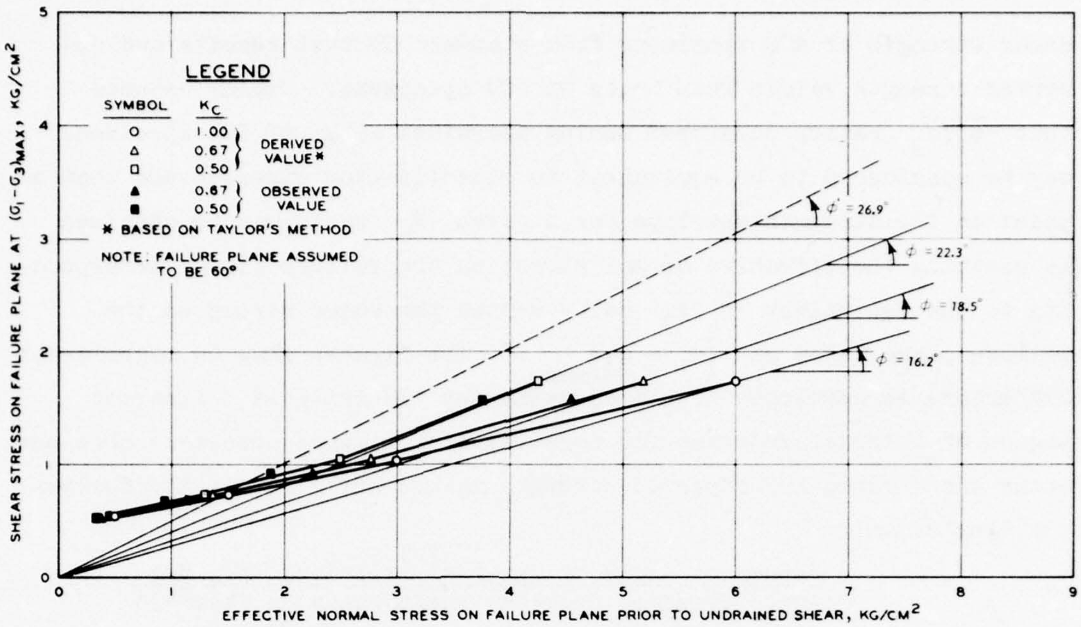

Figure 56. Comparison of observed and derived strength values for Buckshot clay

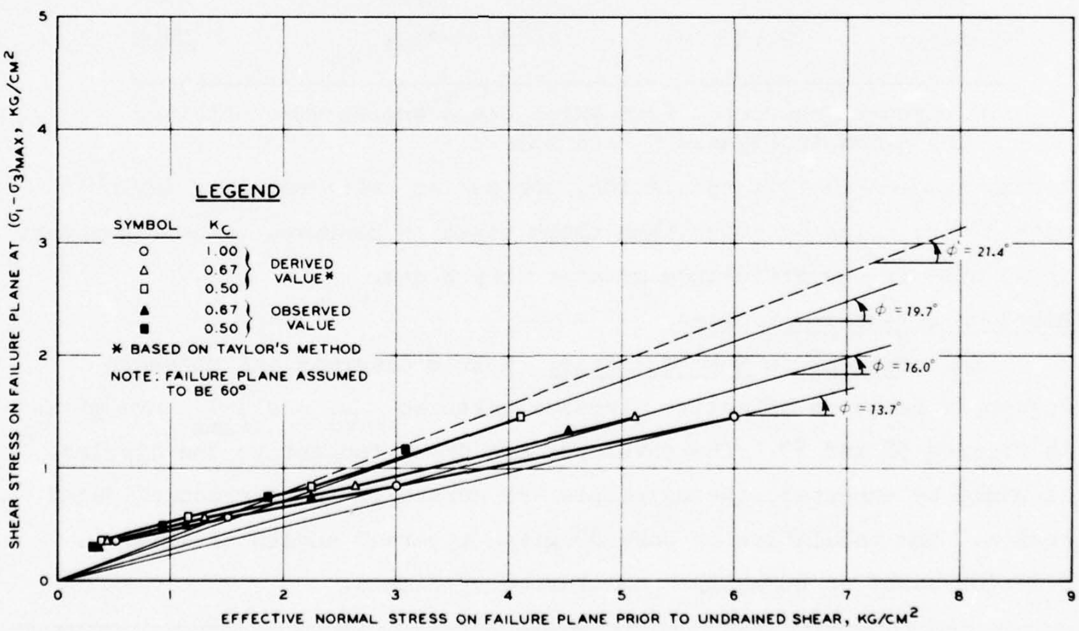

Figure 57. Comparison of observed and derived strength values for EABPL clay

shear strength of ACU specimens from standard CU test results and observed strength values from tests on ACU specimens. Taylor assumed that $\bar{\sigma}_1/\bar{\sigma}_3$ ratios developed during undrained shear of ICU specimens may be considered to be equivalent to consolidation stresses and that a point on the strength envelope for a given K_c ratio may be obtained by plotting the effective normal stress on the failure plane corresponding to the equivalent $\bar{\sigma}_1/\bar{\sigma}_3$ value versus the shear stress on the failure plane taken at $\left(\sigma_1 - \sigma_3\right)_{max}$.* The figures show no significant difference in envelopes developed using the two criteria. Apparent angles of internal friction for normally consolidated specimens obtained using the derived and observed strength values are given in the following tabulation:

K_c Value	Apparent Angle of Internal Friction, Ø, deg: Angle Based on Derived Strength Values: Buckshot Clay	EABPL Clay	Angle Based on Observed Strength Values†: Buckshot Clay	EABPL Clay
1	--	--	16.2	13.7
0.67	18.5	16.0	19.3	16.4
0.5	22.3	19.7	23.9	20.8

† Strength envelopes from which these angles were obtained are given in Figures 54 and 55.

As can be seen in this tabulation, the angles obtained using Taylor's method[2] are slightly lower than those based on observed values; however, in no case is the difference greater than 2 deg.

Based on effective stresses

58. Tangent to Mohr's circle. Mohr's diagrams and strength envelopes based on effective stresses taken at $\left(\sigma_1 - \sigma_3\right)_{max}$ are given in Figures 58 and 59. The envelopes are drawn tangent to the circles. As would be expected, the envelopes are curved in the overconsolidated region. The tabulation on page 80 gives apparent angles of internal friction based on normally consolidated specimens.

* An illustration of Taylor's method and plots of effective normal stresses on 60-deg planes versus $\bar{\sigma}_1/\bar{\sigma}_3$ values for ICU specimens are given in Appendix B.

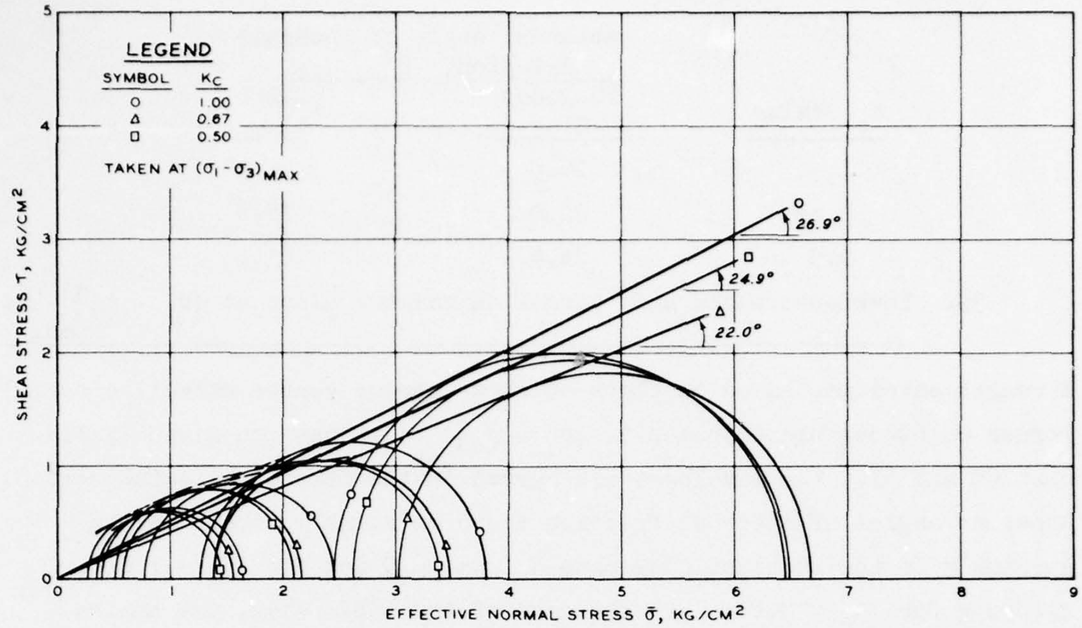

Figure 58. Mohr's diagrams and strength envelopes based on effective stresses taken at $\left(\sigma_1 - \sigma_3\right)_{max}$ for Buckshot clay

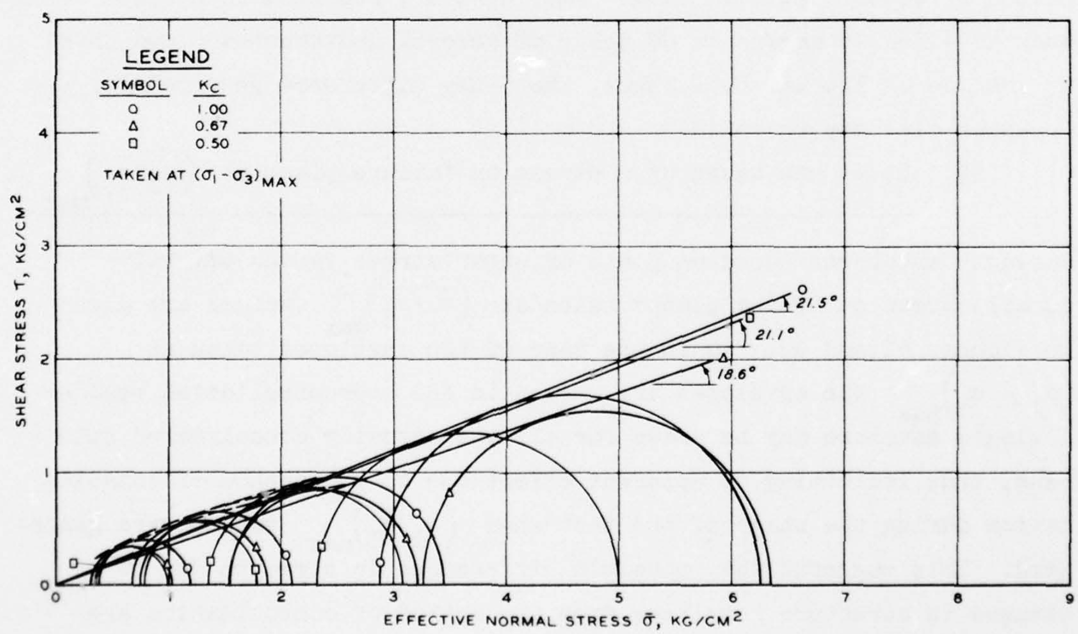

Figure 59. Mohr's diagrams and strength envelopes based on effective stresses taken at $\left(\sigma_1 - \sigma_3\right)_{max}$ for EABPL clay

K_c Value	Apparent Angle of Internal Friction, ϕ', deg: Buckshot Clay	Apparent Angle of Internal Friction, ϕ', deg: EABPL Clay
1	26.9	21.5
0.67	22.0	18.6
0.5	24.9	21.1

59. Envelopes based upon stress on failure plane at $(\sigma_1 - \sigma_3)_{max}$.

Strength envelopes based on plots of shear stress versus effective normal stress on 60-deg planes taken at $(\sigma_1 - \sigma_3)_{max}$ values are given in Figures 60 and 61. The envelopes are curved in the overconsolidated region. Apparent angles of internal friction based on normally consolidated specimens of the Buckshot clay ranged from 26.9 deg for $K_c = 1.0$ to 21.8 deg for $K_c = 0.67$. In the case of the EABPL clay, the angles ranged from 21.4 deg for $K_c = 1.0$ to 18.4 deg for $K_c = 0.67$. These results differ from those reported by Henkel and Sowa,[11] who reported no effect on envelopes based on effective stresses due to the method of consolidation. Ladd[12] has, however, reported differences of as much as 4 deg in angles in CU tests of several undisturbed clays using K_c ratios of 1.0 and 0.5. Thus, the 5-deg difference reported for the Buckshot clay may be valid.

60. Envelopes based upon stress on failure plane at $(\bar{\sigma}_1/\bar{\sigma}_3)_{max}$.

Strength envelopes based on plots of shear stress versus effective normal stress on 60-deg planes taken at $(\bar{\sigma}_1/\bar{\sigma}_3)_{max}$ values are given in Figures 62 and 63. As in the case of the envelopes taken at $(\sigma_1 - \sigma_3)_{max}$ the envelopes are curved in the overconsolidated region. A single envelope may be drawn for all the normally consolidated specimens, thus indicating no apparent effect due to the method of consolidation during the stage of the test when $(\bar{\sigma}_1/\bar{\sigma}_3)_{max}$ values were generated. This suggests that possible differences in strength due to changes in structure resulting from the method of consolidation are obliterated by the additional shearing action required to develop maximum $(\bar{\sigma}_1/\bar{\sigma}_3)$ values. The apparent angles of internal friction based on

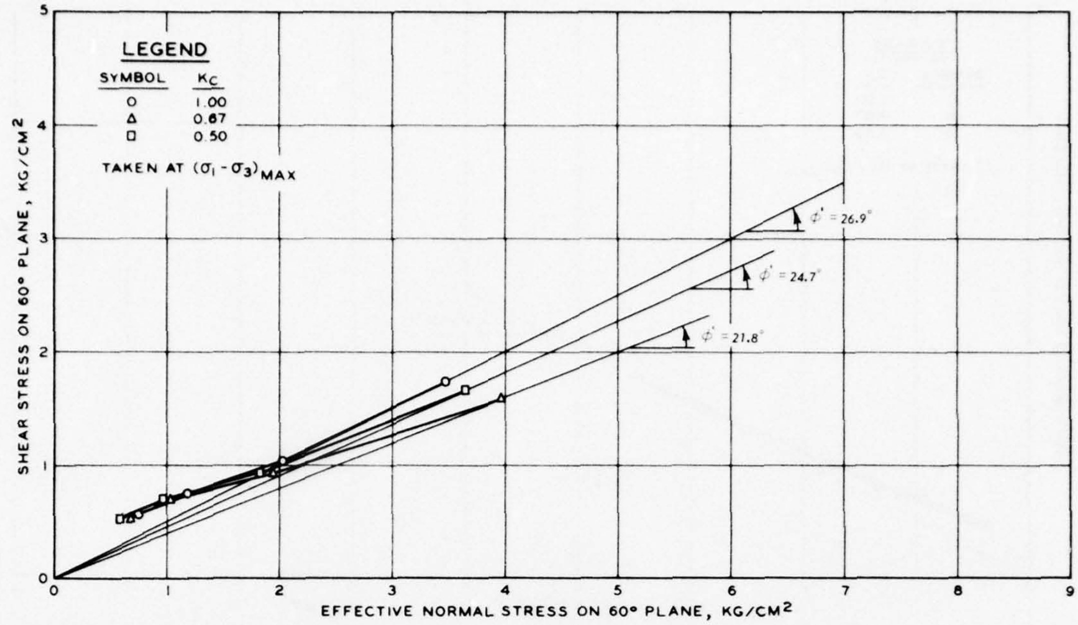

Figure 60. Strength envelopes based on effective stresses on 60-deg plane taken at $\left(\sigma_1 - \sigma_3\right)_{max}$ for Buckshot clay

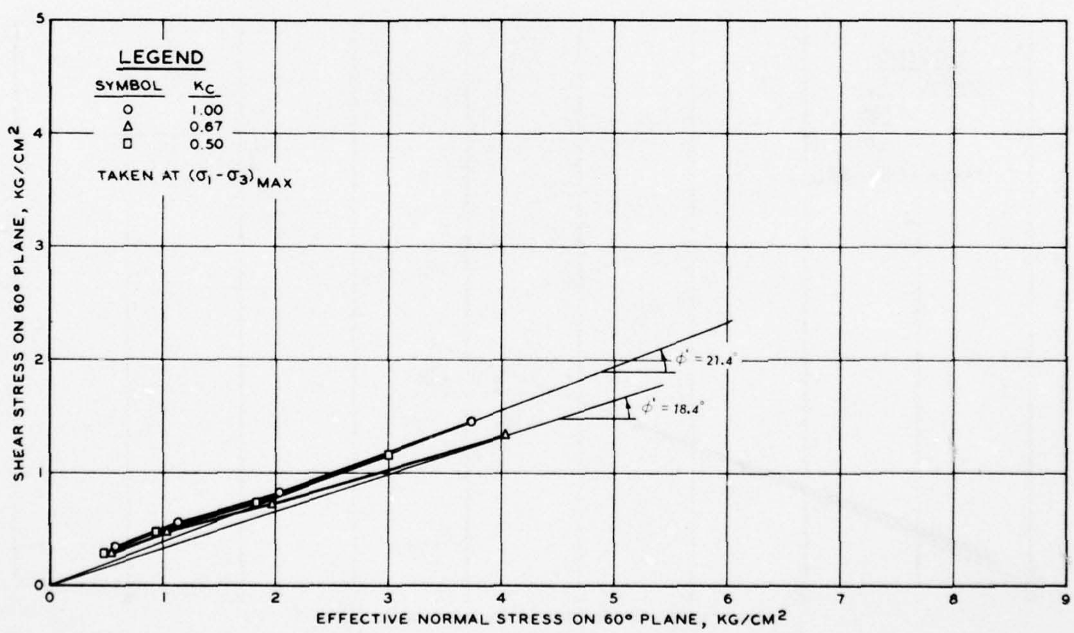

Figure 61. Strength envelopes based on effective stresses on 60-deg plane taken at $\left(\sigma_1 - \sigma_3\right)_{max}$ for EABPL clay

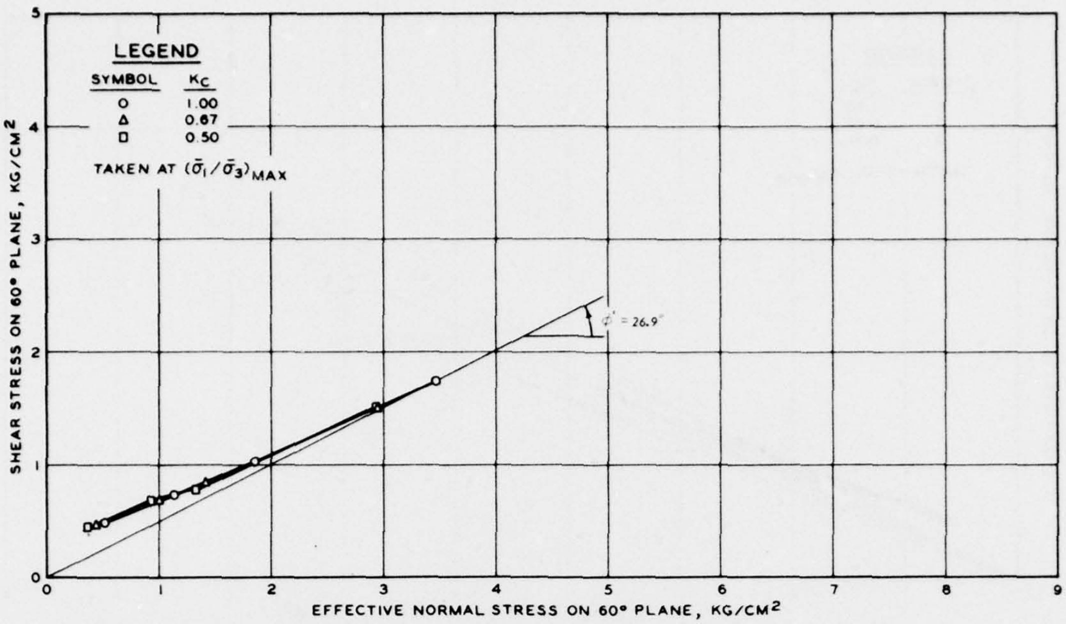

Figure 62. Strength envelopes based on effective stresses on 60-deg plane taken at $\left(\bar{\sigma}_1/\bar{\sigma}_3\right)_{max}$ for Buckshot clay

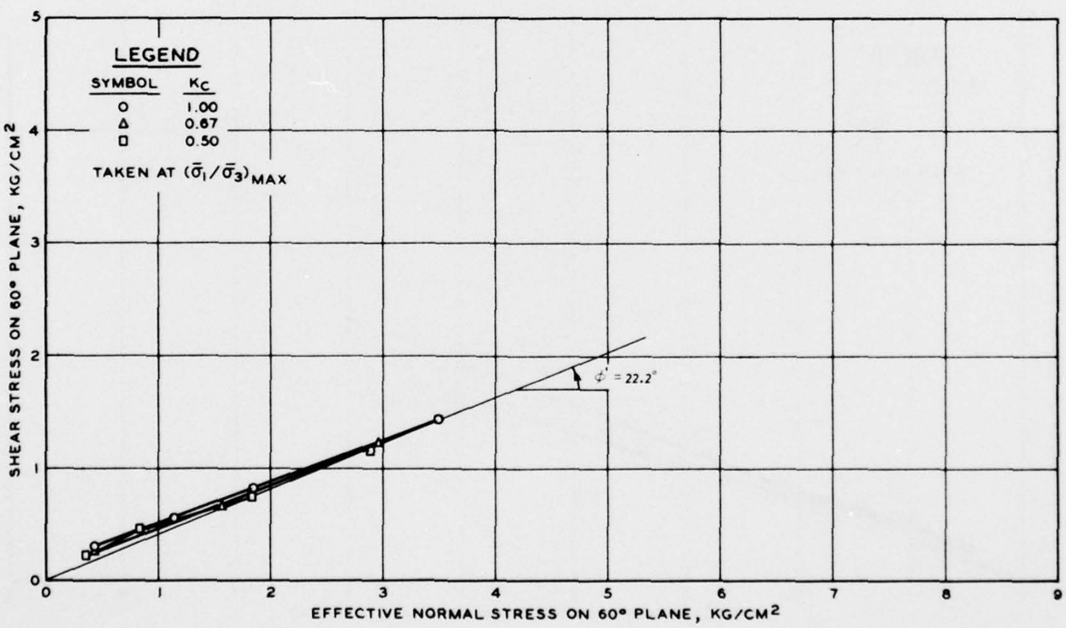

Figure 63. Strength envelopes based on effective stresses on 60-deg plane taken at $\left(\bar{\sigma}_1/\bar{\sigma}_3\right)_{max}$ for EABPL clay

the normally consolidated specimens were 26.9 deg for the Buckshot and 22.2 deg for the EABPL clay.

61. Tables 11 and 12 summarize angles of internal friction based on total and effective stresses, respectively, for normally consolidated specimens of both soils obtained as K_c ratios were varied.

Hyperbolic Stress-Strain Behavior

62. Various mathematical models have been used to represent the nonlinear stress-strain behavior of soils. The most commonly used expression is the hyperbolic model proposed by Kondner,[24] which is

$$\sigma_d = \frac{\varepsilon}{a + b\varepsilon} \tag{3}$$

where σ_d is the deviator stress, ε is the axial strain , and a and b are material parameters. However, in the case of anisotropic consolidation, the deviator stress acting on the specimen prior to undrained shear must be considered. Since the consolidation stress-strain path in the laboratory does not duplicate the consolidation history in the field, the consolidation deviator stress σ_{dc} and consolidation strains ε_c can be subtracted from the stresses and strains occurring during shear, and the hyperbolic model becomes

$$\sigma_d - \sigma_{dc} = \frac{\varepsilon}{a + b\varepsilon} \tag{4a}$$

where σ_{dc} is the consolidation deviator stress due to anisotropic consolidation, and ε is the axial strain in undrained shear. By transforming the equation to the following linear form, the constants a and b can be evaluated as the intercept and slope of a straight line, respectively.

$$\frac{\varepsilon}{\sigma_d - \sigma_{dc}} = a + b\varepsilon \tag{4b}$$

Figures 64-70 present the transformed hyperbolic stress-strain relationships for the Buckshot and EABPL clays for the various $\bar{\sigma}_{1c}$ and K_c

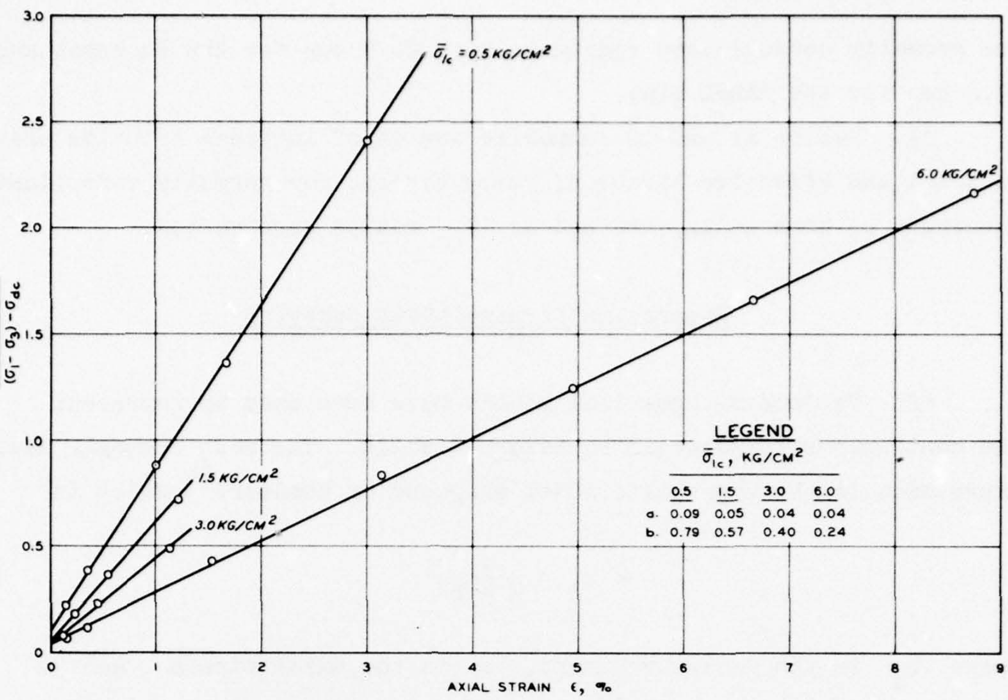

Figure 64. $\frac{\varepsilon}{(\sigma_1 - \sigma_3) - \sigma_{dc}}$ versus axial strain ε for $K_c = 1.0$ for Buckshot clay

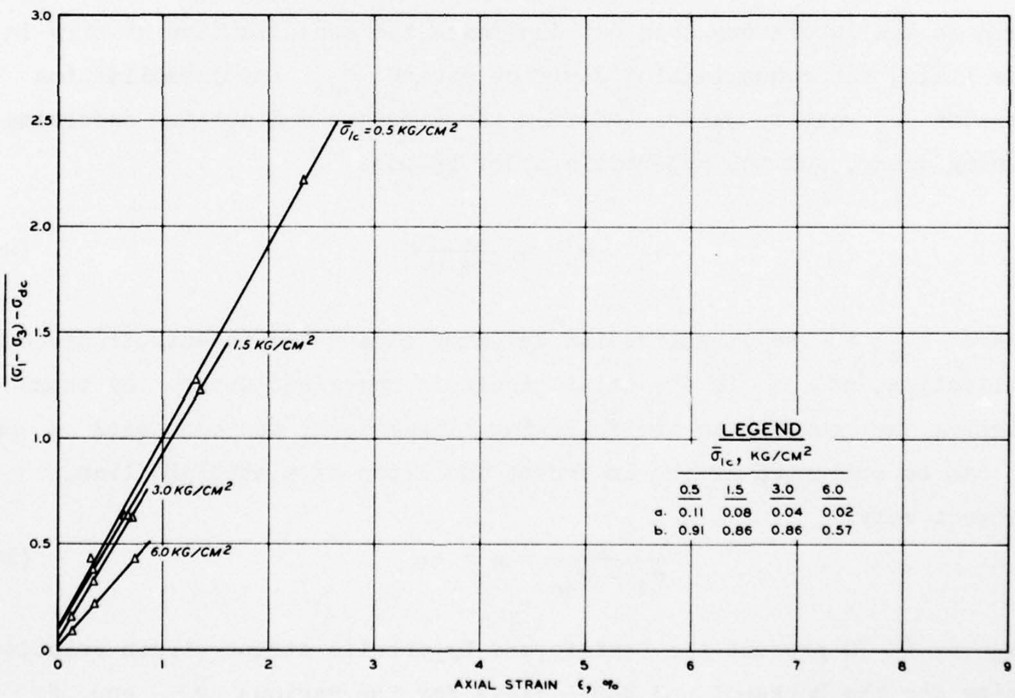

Figure 65. $\frac{\varepsilon}{(\sigma_1 - \sigma_3) - \sigma_{dc}}$ versus axial strain ε for $K_c = 0.67$ for Buckshot clay

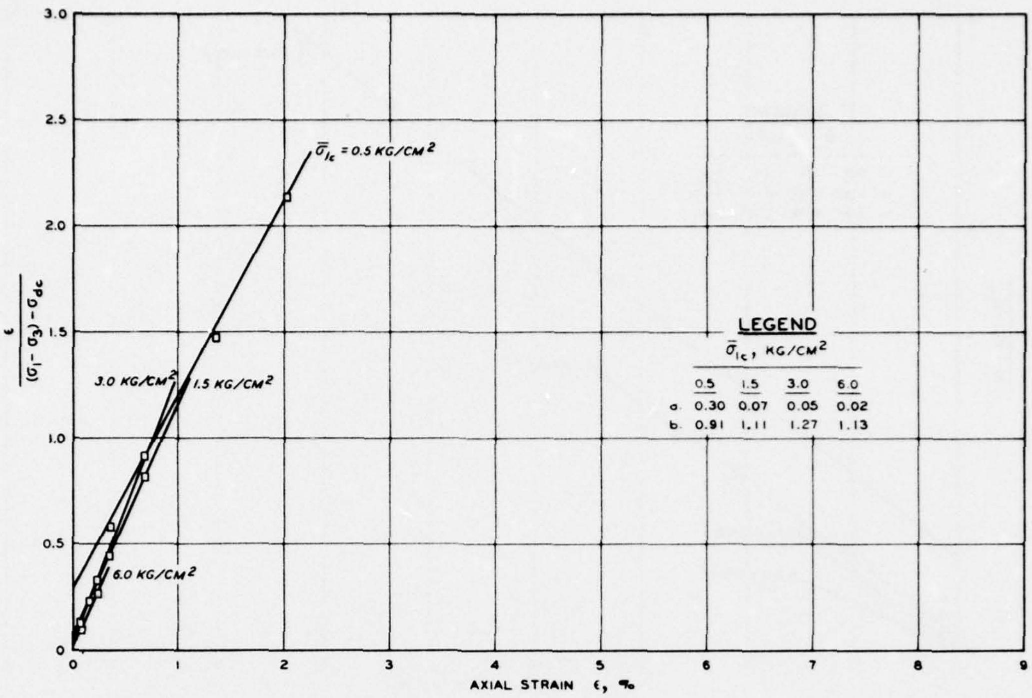

Figure 66. $\frac{\varepsilon}{(\sigma_1 - \sigma_3) - \sigma_{dc}}$ versus axial strain ε for $K_c = 0.5$ for Buckshot clay

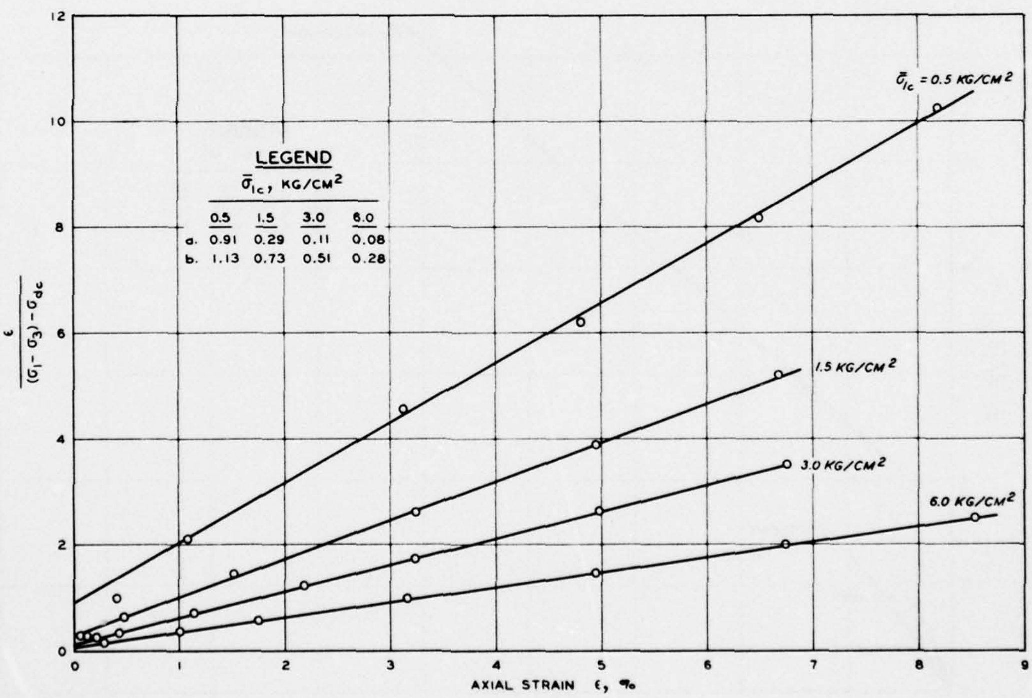

Figure 67. $\frac{\varepsilon}{(\sigma_1 - \sigma_3) - \sigma_{dc}}$ versus axial strain ε for $K_c = 1.0$ for EABPL clay

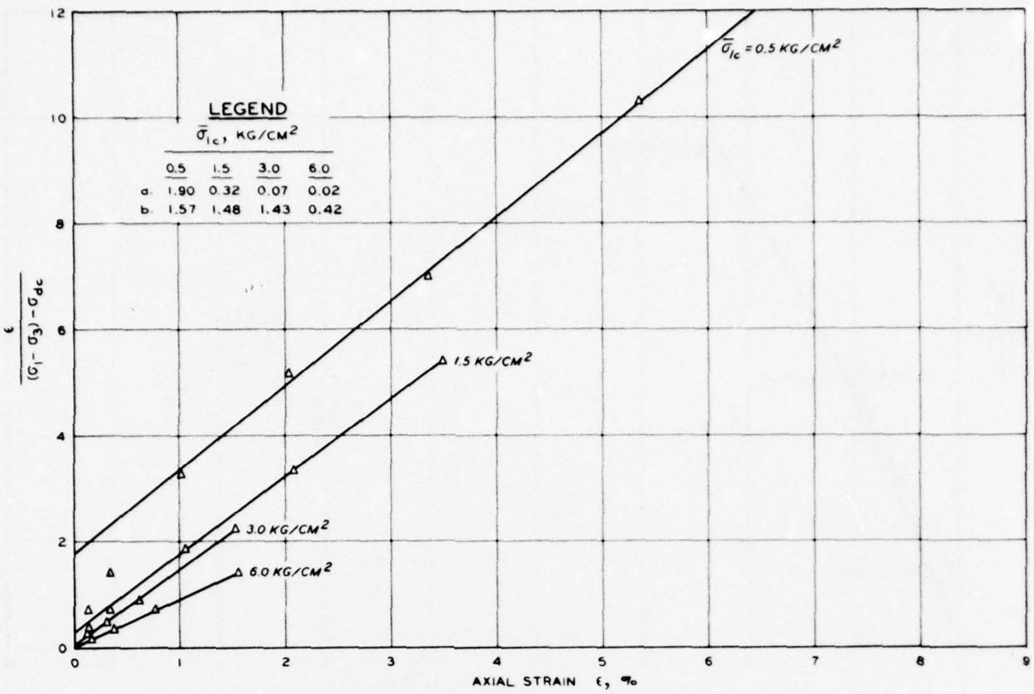

Figure 68. $\frac{\varepsilon}{(\sigma_1 - \sigma_3) - \sigma_{dc}}$ versus axial strain ε for $K_c = 0.67$ for EABPL clay

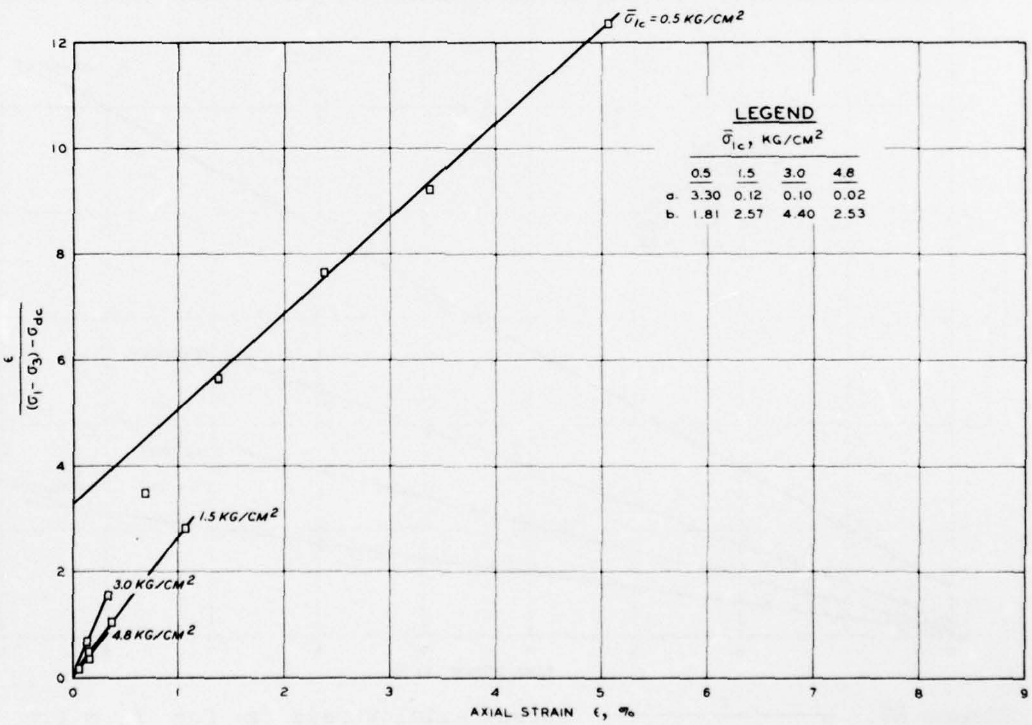

Figure 69. $\frac{\varepsilon}{(\sigma_1 - \sigma_3) - \sigma_{dc}}$ versus axial strain ε for $K_c = 0.5$ for EABPL clay

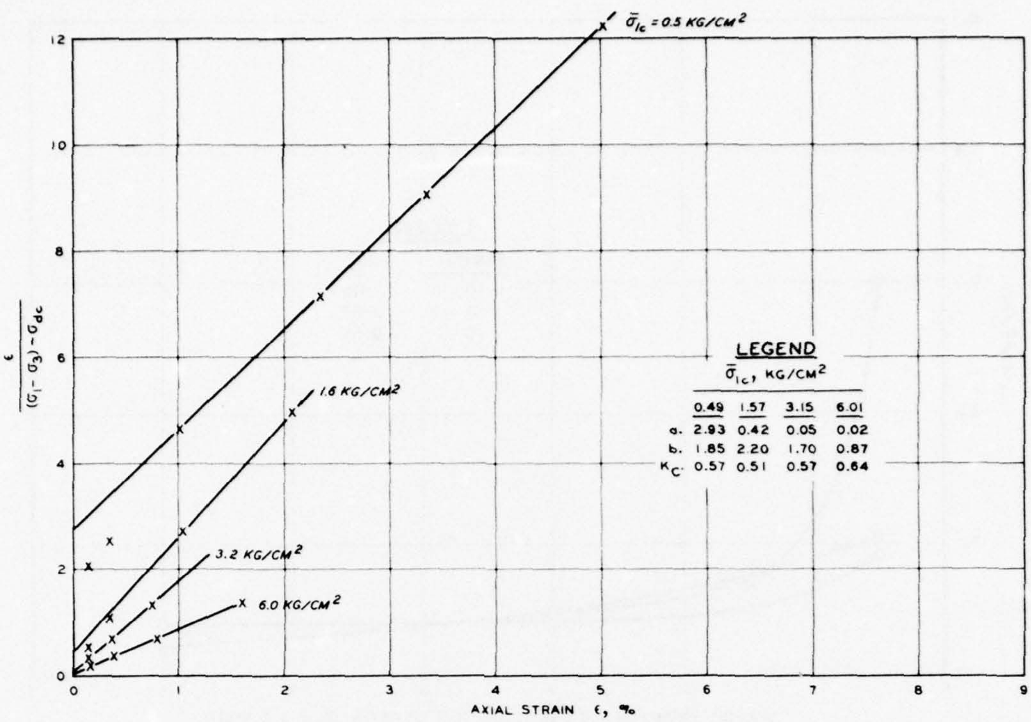

Figure 70. $\dfrac{\varepsilon}{(\sigma_1 - \sigma_3) - \sigma_{dc}}$ versus axial strain ε for K_c tests for EABPL clay

ratios. Except for some curvature of the initial portions of the EABPL transformed relationships, these results show that a hyperbolic representation of the stress-strain properties is a good approximation for both ACU and ICU specimens. Figures 71 and 72 present the variation of the material parameter a with $\bar{\sigma}_{1c}$ and K_c, respectively, for the Buckshot clay, while Figures 73 and 74 present the variation of a with $\bar{\sigma}_{1c}$ and K_c, respectively, for the EABPL clay. These results show that for the normally consolidated range, a (the reciprocal of the initial tangent modulus E_{1o}) is essentially independent of K_c. Conversely, for lower $\bar{\sigma}_{1c}$ values, i.e., in the overconsolidated range, a increases substantially with increased overconsolidation ratios (decreasing $\bar{\sigma}_{1c}$ values) and increases with decreasing values of K_c.

63. Figures 75 and 76 present the variation of the material parameter b with $\bar{\sigma}_{1c}$ and K_c, respectively, for the Buckshot clay, while Figures 77 and 78 present the variation of b with $\bar{\sigma}_{1c}$ and

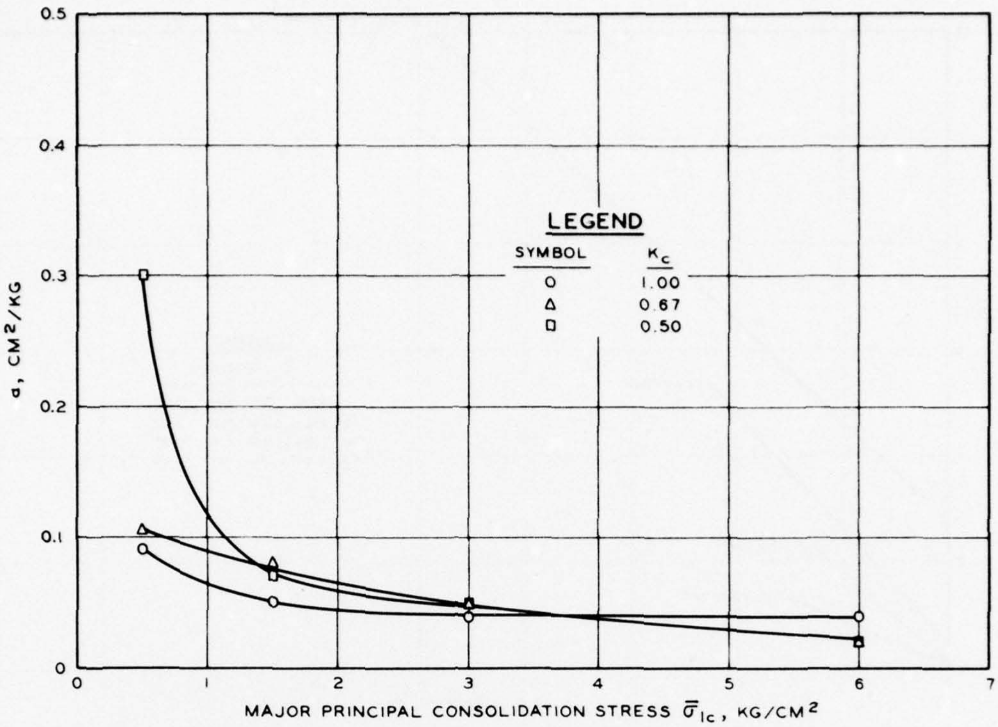

Figure 71. a parameter versus $\overline{\sigma}_{1c}$ for Buckshot clay

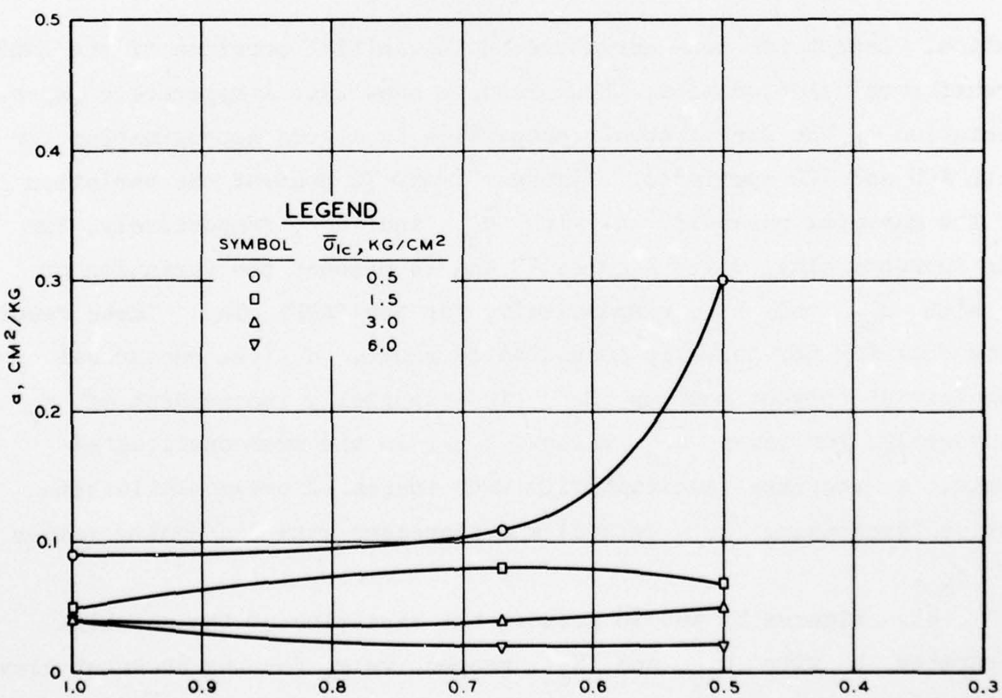

Figure 72. a parameter versus K_c for Buckshot clay

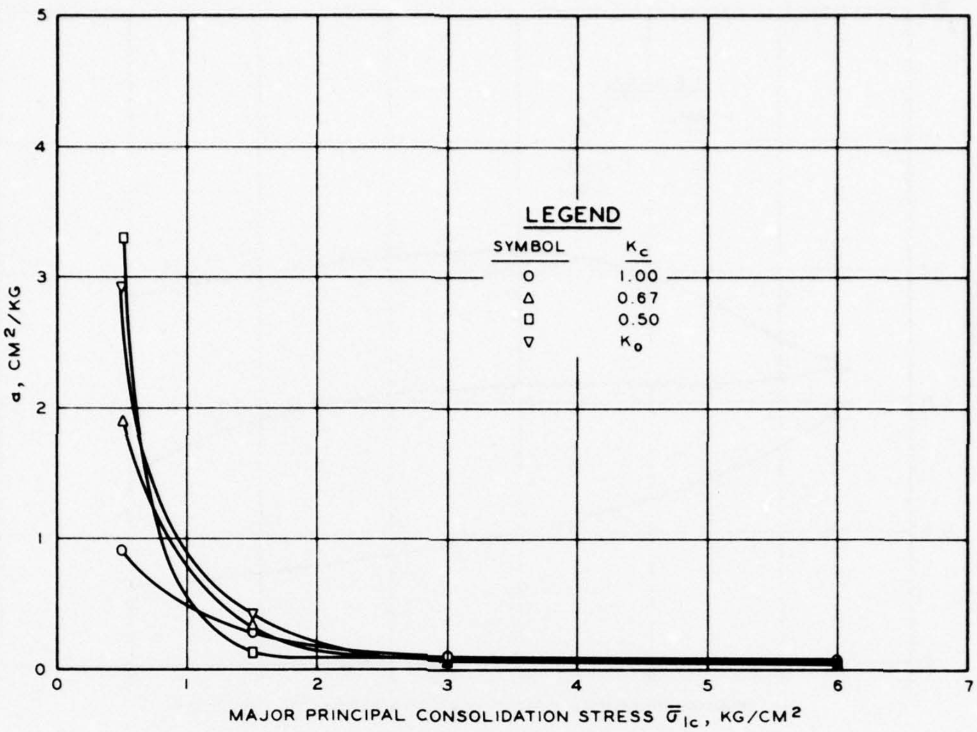

Figure 73. a parameter versus $\overline{\sigma}_{1c}$ for EABPL clay

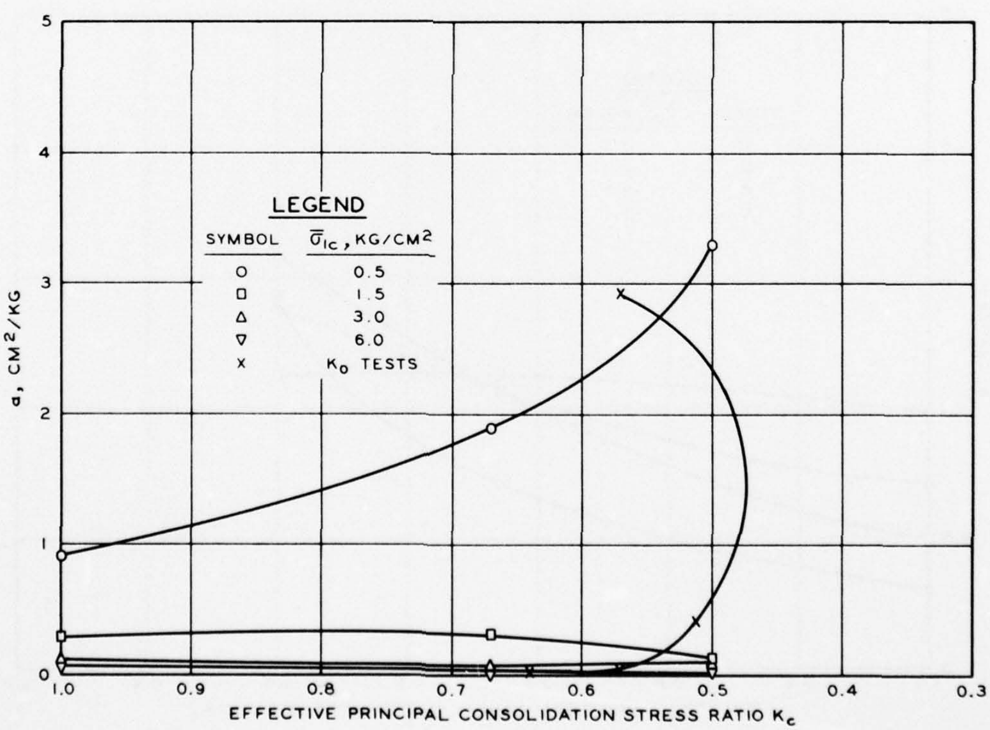

Figure 74. a parameter versus K_c for EABPL clay

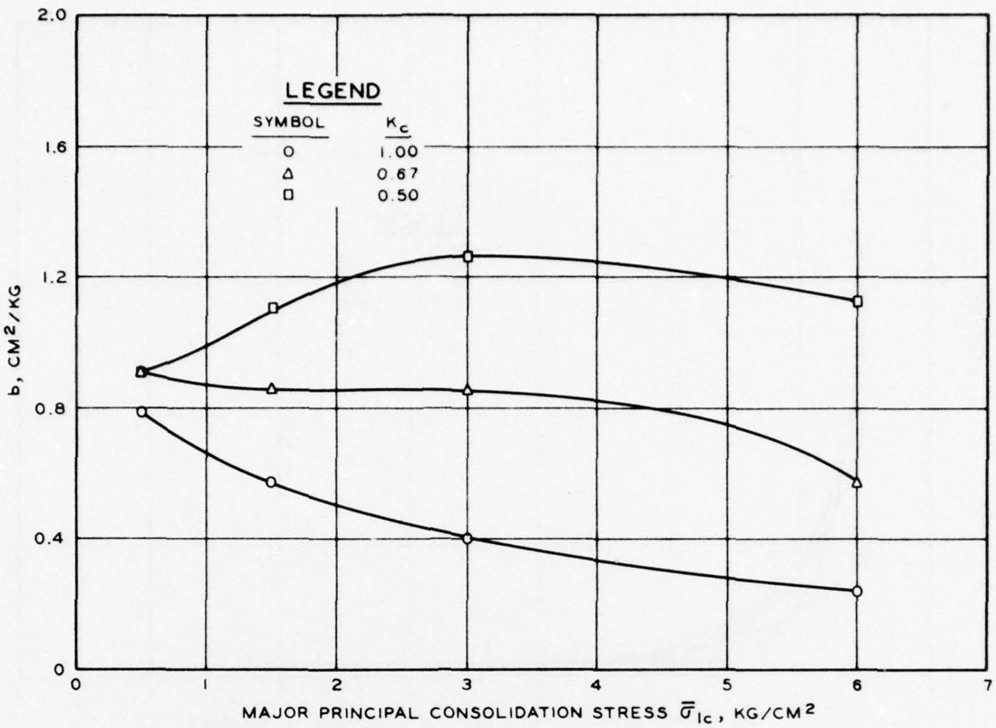

Figure 75. b parameter versus $\bar{\sigma}_{1c}$ for Buckshot clay

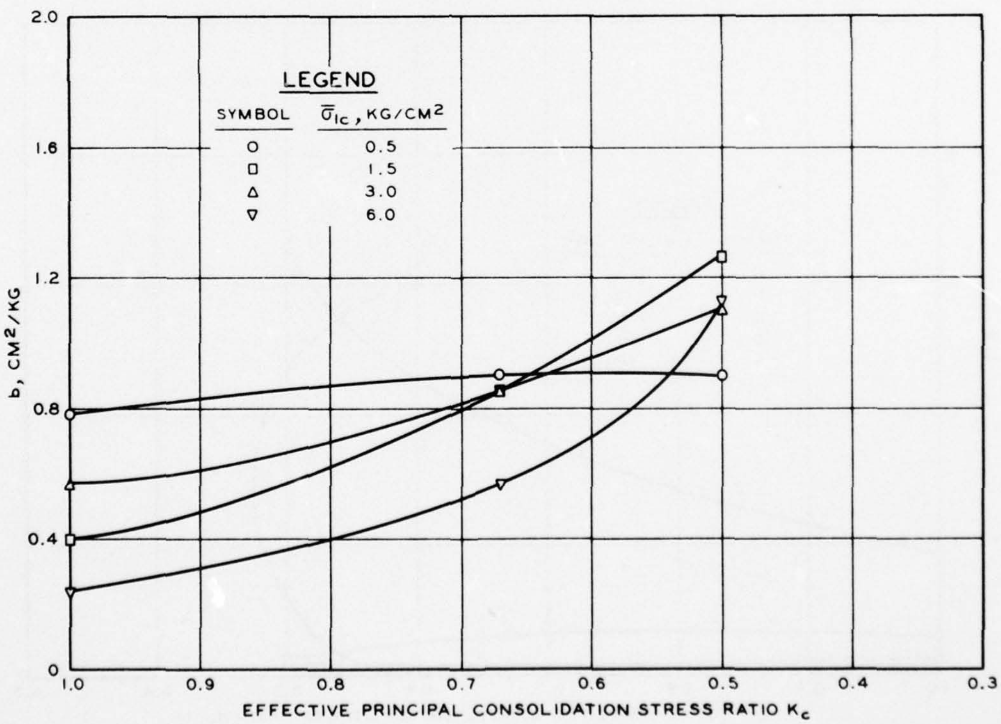

Figure 76. b parameter versus K_c for Buckshot clay

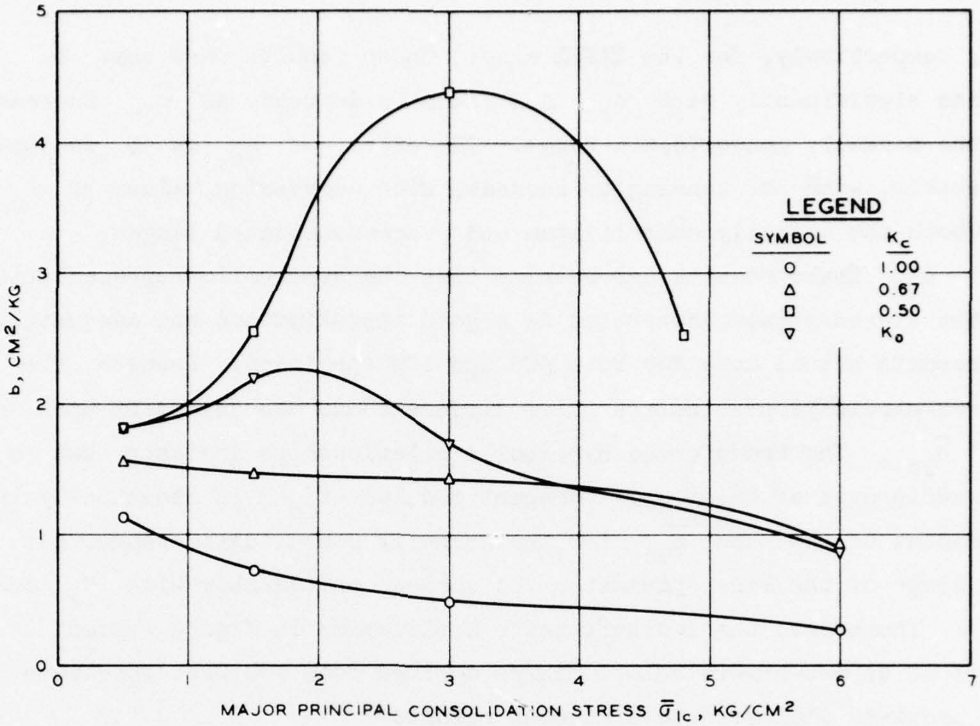

Figure 77. b parameter versus $\bar{\sigma}_{1c}$ for EABPL clay

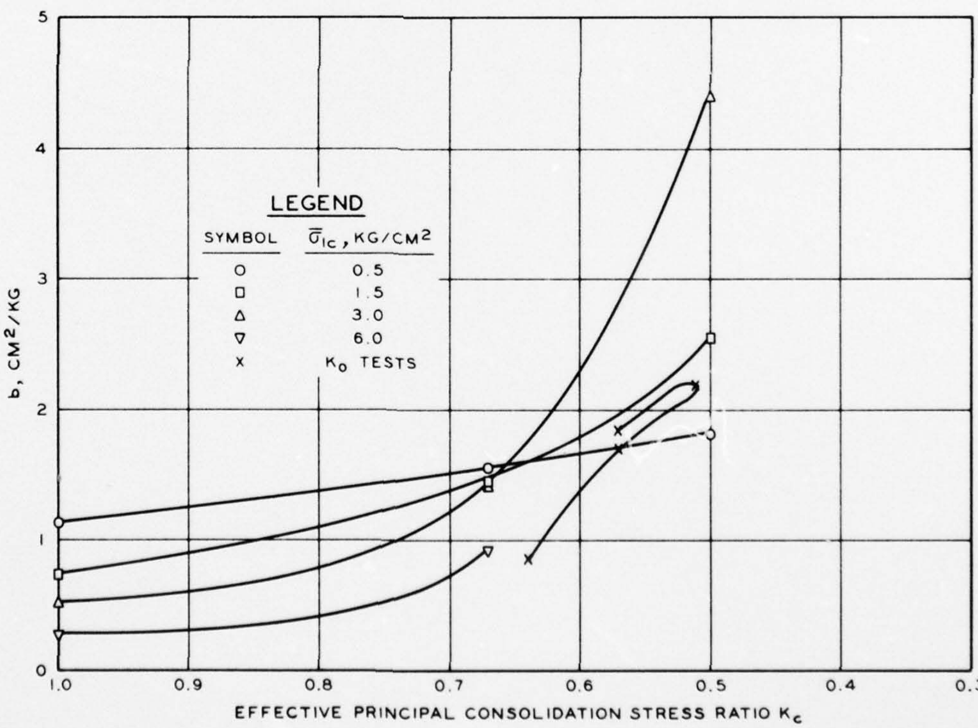

Figure 78. b parameter versus K_c for EABPL clay

K_c , respectively, for the EABPL clay. These results show that b varies significantly with $\bar{\sigma}_{1c}$ and tends to decrease as $\bar{\sigma}_{1c}$ increases in the normally consolidated range. The effect of K_c on b is considerable, with b tending to increase with decreasing values of K_c for both the normally consolidated and overconsolidated ranges.

64. These results demonstrate that the hyperbolic representation of the stress-strain properties is a good approximation and adequately represents actual data for both ACU and ICU specimens. However, the stress-strain properties are quite different and are dependent upon K_c and $\bar{\sigma}_{1c}$. The transformed hyperbolic relationships indicate that a , the reciprocal of the initial tangent modulus E_{1o} , is essentially independent of K_c and $\bar{\sigma}_{1c}$ for the normally consolidated range, but the slope of the line (parameter b) varies considerably with K_c and $\bar{\sigma}_{1c}$. Therefore, the indiscriminate application in finite element codes of stress-strain relationships derived from ICU test specimens to ACU problems will lead to erroneous results.

AD-A049 481 ARMY ENGINEER WATERWAYS EXPERIMENT STATION VICKSBURG MISS F/G 8/13
EFFECTS OF ANISOTROPIC VERSUS ISOTROPIC CONSOLIDATION IN CONSOL--ETC(U)
OCT 75 R T DONAGHE, F C TOWNSEND

UNCLASSIFIED WES-TR-S-75-13 NL

2 OF 2
AD
A049481

END
DATE
FILMED
3-78
DDC

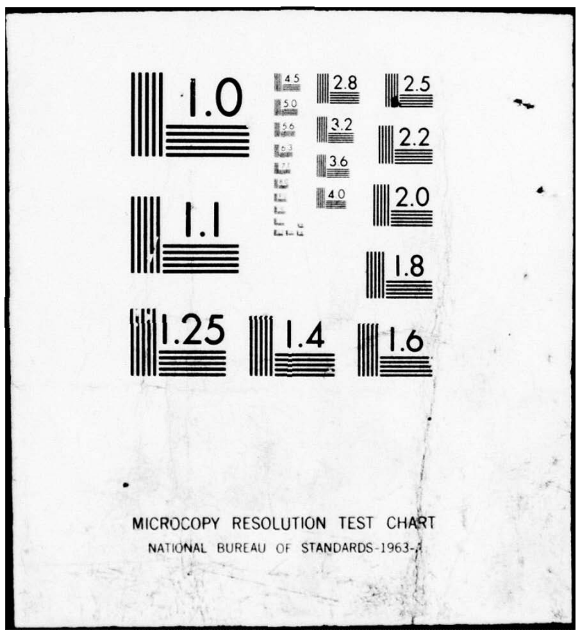
1.0
1.1
1.25
1.4
1.6
1.8
2.0
2.2
2.5
2.8
3.2
3.6
4.0
4.5
5.0
5.6
MICROCOPY RESOLUTION TEST CHART
NATIONAL BUREAU OF STANDARDS-1963-A

PART IV: CONCLUSIONS AND RECOMMENDATIONS

65. Based on the equipment, procedures, and materials used in this investigation, the following conclusions have been drawn.

Testing Methods

66. Slurry consolidometers provide an alternative method to compaction for sample preparation. The homogeneity of the slurry-consolidated samples is reflected in the uniform water contents and density distribution in the specimens. The deviation in water contents was less than ±0.9 and ±1.0 percentage points for the Buckshot and EABPL clays, respectively, while the deviation in densities was less than ±1.2 and ±1.1 pcf for the respective clays.

67. The effect of strain rate on the stress-strain characteristics was similar for both ICU and ACU specimens in that the maximum deviator stress decreased slightly with slower strain rates. The slight reduction in strength due to decreased strain rates was less in the overconsolidated range for ACU than for ICU specimens. Conversely, in the normally consolidated range, the ACU specimens exhibited a greater strength reduction with decreasing strain rate than did the ICU specimens. Because the decrease in strength due to strain rate was small (less than 10 percent per log cycle of time to failure), the recommended guideline in Reference 16 for time to maximum deviator stress of at least 30 min appears appropriate.

68. The values of induced pore pressure at maximum deviator stress for both ACU and ICU specimens were not significantly affected by strain rate in either the normally consolidated or overconsolidated range. This observation suggests that the recommended time to maximum deviator stress of at least 120 min for tests in which pore pressures are measured is excessive for these materials.

69. The use of low-friction end platens to reduce end restraint results in more uniform strains in the specimen. All specimens tested using conventional end platens failed by bulging, whereas specimens

tested with low-friction caps and bases deformed cylindrically or expanded slightly at one end.

70. Decreased end restraint resulted in slightly lower (less than 15 percent) maximum deviator stresses for ICU specimens and slightly higher values of $(\sigma_1 - \sigma_3)_{max}$ for ACU specimens for both the normally consolidated and overconsolidated ranges. Decreased end restraint also resulted in greater axial strain values at $(\sigma_1 - \sigma_3)_{max}$ for both consolidation paths (i.e. anisotropic or isotropic) and stress histories (i.e. overconsolidated and normally consolidated) except for ACU specimens in the normally consolidated range, in which no change was observed.

71. Development of induced pore pressure values was considerably slower and values were much lower for tests performed using low-friction caps and bases than for tests performed with standard caps and bases. These results and the observation that silicone grease was present on the outer edges of the caps and bases suggest that the grease may have permeated the filter strips connected to the pore pressure ports and invalidated the pore pressure measurements.

Engineering Characteristics

72. The change in volume during consolidation and water content at the end of consolidation are not a unique function of the major principal consolidation stress $\bar{\sigma}_{1c}$ but are related to the mean effective consolidation stress $(\bar{\sigma}_{oct})_c$ and to the deviator stress during consolidation. ACU specimens had higher water contents (lower volume changes) than did ICU specimens for the same $\bar{\sigma}_{1c}$. The effect of K_c ratio on volume change was more pronounced in the overconsolidated than in the normally consolidated ranges.

73. For any given $\bar{\sigma}_{1c}$ value, the maximum deviator stress $(\sigma_1 - \sigma_3)_{max}$ generally decreased with decreasing K_c ratio. Conversely, for any given water content, $(\sigma_1 - \sigma_3)_{max}$ is greater for ACU than for ICU specimens.

74. The increased strength for ACU specimens for a given water

content may be a function of K_c ratio, with K_o consolidation representing the upper limiting value. For a given water content, specimens consolidated under K_o conditions exhibited the greatest strengths, and lower strength values were obtained for specimens consolidated at K_c ratios less than or greater than K_o.

75. The strength ratio $s_u/\bar{\sigma}_{1c}$ was greater for ICU than for ACU specimens for a given $\bar{\sigma}_{1c}$. The ratio $s_u/\bar{\sigma}_{1c}$ was more dependent upon the K_c ratio in the overconsolidated range than in the normally consolidated range, in which it was only slightly affected by K_c ratios.

76. Stress-strain characteristics were significantly affected by K_c ratios. The axial strain values at $(\sigma_1 - \sigma_3)_{max}$ generally decreased with decreasing K_c ratio values. The reduction in axial strain values at $(\sigma_1 - \sigma_3)_{max}$ as K_c varied ranged from 33 to 98 percent for Buckshot and from 17 to 95 percent for EABPL clay, with the greatest reductions occurring in the normally consolidated range.

77. Induced pore pressures at the maximum deviator stress decreased substantially with decreasing K_c ratios for a given $\bar{\sigma}_{1c}$ value. Likewise, the A parameter values were considerably lower for ACU specimens.

78. Strength envelopes based upon total stresses taken at $(\sigma_1 - \sigma_3)_{max}$ for normally consolidated specimens show an increase in angles of internal friction with decreasing K_c ratios.

79. Total stress envelopes based on Taylor's method[2] of deriving strengths of ACU specimens from test results obtained from ICU specimens slightly underestimate observed values. In this context, Taylor's method[2] is an appropriate means of predicting strengths for various K_c ratios from conventional ICU tests.

80. Strength envelopes based upon effective stresses taken at $(\sigma_1 - \sigma_3)_{max}$ show a decrease in angles of internal friction with decreasing K_c ratios.

81. Strength envelopes based upon effective strength envelopes taken at $(\bar{\sigma}_1/\bar{\sigma}_3)_{max}$ exhibit no effect due to consolidation stress ratio K_c.

82. Excellent agreement was obtained between experimental K_o values in the normally consolidated range and Jaky's[20] empirical correlation $K_o = 1 - \sin \phi'$.

83. The stress-strain curves for both ACU and ICU specimens can be accurately represented by a hyperbolic expression $\sigma_d - \sigma_{dc} = \varepsilon/(a + b\varepsilon)$. The material parameter a (the reciprocal of the initial tangent modulus E_{1o}) is independent of K_c ratio in the normally consolidated range. However, a decreases with decreasing K_c values in the overconsolidated range. The hyperbolic parameter b varies significantly with K_c ratio and $\bar{\sigma}_{1c}$. These results demonstrate that the use of finite element codes of hyperbolic stress-strain relationships derived from ICU tests for ACU conditions will lead to erroneous results.

Recommendations for Future Research

84. Since the stress system imposed on soil specimens during CU triaxial compression tests is not comparable to most field conditions, further testing of anisotropically consolidated soils under stress systems that better simulate in situ conditions is needed. Stress systems applied by simple shear, plane strain, and triaxial extension devices are suggested. The tests should be performed on specimens of the EABPL and Buckshot clays trimmed from samples prepared in slurry consolidometers so that effects due to the various stress systems may be correlated with effects reported in this investigation.

85. It is also recommended that a similar investigation be conducted on compacted specimens of Buckshot clay in order to study effects due to soil structure prior to anisotropic consolidation.

REFERENCES

1. Rendulic, L., Discussion, "Relation Between Void Ratio and Effective Principal Stresses for a Remoulded, Silty Clay," Proceedings, International Conference on Soil Mechanics and Foundation Engineering, Vol 3, Jun 1936, pp 48-51.

2. Taylor, D. W., Fundamentals of Soil Mechanics, Wiley, New York, 1948.

3. Henkel, D. J., "The Relationships Between the Effective Stresses and Water Content in Saturated Clays," Geotechnique, Vol 10, No. 2, 1960, pp 41-54.

4. Skempton, A. W. and Bishop, A. W., Soils in Building Material--Their Elasticity and Inelasticity, North Holland Publication Co., Amsterdam, 1954, pp 417-482.

5. Lowe, J., III and Karafaith, L., "Effect of Anisotropic Consolidation on the Undrained Strength of Cohesive Soils," Research Conference on Shear Strength of Cohesive Soils, American Society of Civil Engineers, Boulder, Colo., 1960, pp 837-858.

6. Bjerrum, L. and Lo, K. Y., "An Analysis of the Undrained Shear Tests on Normally Consolidated Clays," Norwegian Geotechnical Institute, F3-1, Oslo, 1961.

7. Rutledge, P. D., "Cooperative Triaxial Shear Research Program," Progress Report on Soil Mechanics Fact Finding Survey, 1947, U. S. Army Engineer Waterways Experiment Station, CE, Vicksburg, Miss.

8. Broms, B. and Ratnam, M. V., "Shear Strength of Anisotropically Consolidated Clay," Journal, Soil Mechanics and Foundations Division, American Society of Civil Engineers, Vol 89, No. SM6, Nov 1963, pp 1-26.

9. Henkel, D. J., "The Shear Strength of Saturated Remolded Clays," Research Conference on the Shear Strength of Cohesive Soils, American Society of Civil Engineers, Boulder, Colo., 1960, pp 533-554.

10. Lee, K. L., "Strength of Anisotropically Consolidated Compacted Clay," Journal, Soil Mechanics and Foundations Division, American Society of Civil Engineers, Vol 96, No. SM6, Nov 1970, pp 2025-2043.

11. Henkel, D. J. and Sowa, V. A., "The Influence of Stress History on Stress Paths in the Undrained Triaxial Tests on Clays," Laboratory Shear Testing of Soils, Special Technical Publication No. 361, pp 280-291, 1963, American Society for Testing and Materials, Philadelphia, Pa.

12. Ladd, C. C., "Stress-Strain Behavior of Anisotropically Consolidated Clays During Undrained Shear," Proceedings, Sixth International Conference of Soil Mechanics and Foundation Engineering, Vol 1, 1965, pp 282-286.

13. Whitman, R. V., Ladd, C. C., and DaCruz, P., "Discussion of Session 3," Research Conference on Shear Strength of Cohesive Soils, American Society of Civil Engineers, Boulder, Colo., 1960, pp 1049-1056.

14. Khera, R. P. and Krizek, R. J., "Strength Behavior of an Anisotropically Consolidated Remolded Clay," Highway Research Record No. 190, 1967, pp 8-18, Highway Research Board--National Research Council, Washington, D. C.

15. Krizek, R. J. and Sheeran, D. E., "Operational Procedure for Slurry Consolidometer," Contract Report S-70-6, Report 1, Jun 1970, U. S. Army Engineer Waterways Experiment Station, CE, Vicksburg, Miss.; prepared by Northwestern University Technological Institute, Evanston, Ill., under Contract No. DACW 39-70-C-0053.

16. Department of the Army, Office, Chief of Engineers, "Engineering and Design: Laboratory Soils Testing," Engineer Manual EM 1110-2-1906, 30 Nov 1970, Washington, D. C.

17. Krizek, R. J. and Sheeran, D. E., "Slurry Preparation and Characteristics of Samples Consolidated in the Slurry Consolidometer," Contract Report S-70-6, Report 2, Jun 1970, U. S. Army Engineer Waterways Experiment Station, CE, Vicksburg, Miss.; prepared by Northwestern University Technological Institute, Evanston, Ill., under Contract No. DACW 39-70-C-0053.

18. Bhaskaran, R., Discussion, "Strength of Anisotropically Consolidated Compacted Clay," Journal, Soil Mechanics and Foundations Division, American Society of Civil Engineers, Vol 97, No. SM8, Aug 1971, pp 1128-1131.

19. Olson, J. P. and Wahls, H. E., "Predicting Effective Stress Paths," Journal, Soil Mechanics and Foundations Division, American Society of Civil Engineers, Vol 97, No. SM8, Aug 1971, pp 1139-1143.

20. Jaky, J., "Pressure in Silos," Proceedings, Second International Conference on Soil Mechanics and Foundation Engineering, Vol 1, Jun 1948, pp 103-107.

21. Rowe, W. D. and Barden, L., "Importance of Free Ends in Triaxial Testing," Journal, Soil Mechanics and Foundations Division, American Society of Civil Engineers, Vol 94, No. SM1, Jan 1968, pp 271-290.

22. Duncan, J. M., Seed, H. B., and Dunlop, P., "The Significance of Cap and Base Restraint," Journal, Soil Mechanics and Foundations Division, American Society of Civil Engineers, Vol 94, No. SM1, Jan 1968, pp 271-290.

23. Donaghe, R. T., "Effects of Strain Rate in Consolidated-Undrained Triaxial Compression Tests of Cohesive Soils; Vicksburg Buckshot Clay (CH)," Miscellaneous Paper S-70-8, Report 2, May 1971, U. S. Army Engineer Waterways Experiment Station, CE, Vicksburg, Miss.

24. Kondner, R. L., "Hyperbolic Stress-Strain Response: Cohesive Soils," Journal, Soil Mechanics and Foundations Division, American Society of Civil Engineers, Vol 89, No. SM1, Feb 1963, pp 115-143.

Table 1

Testing Program

Strength and Deformation Properties of Isotropically and Anisotropically Consolidated Clays		
$K_c = \bar{\sigma}_{3c}/\bar{\sigma}_{1c}$	$\bar{\sigma}_{1c}$, kg/cm^2	$\bar{\sigma}_{3c}$, kg/cm^2
Testing to Determine Effect of Varying Effective Principal Consolidation Stress Ratio $\bar{\sigma}_{3c}/\bar{\sigma}_{1c}$ (Using Standard Caps and Bases and Axial Strain Rate of 0.06 Percent/Min)*		
1	0.5	0.5
0.67	0.5	0.33
0.5	0.5	0.25
1	1.5	1.5
0.67	1.5	1.0
0.5	1.5	0.75
1	3.0	3.0
0.67	3.0	2.0
0.5	3.0	1.5
1	6.0	6.0
0.67	6.0	4.0
0.5	6.0	3.0
Testing Series to Determine Effect of Tenfold Increase in Rate of Strain (Using Standard Caps and Bases and Axial Strain Rate of 0.6 Percent/Min)**		
1	0.5	0.5
0.5	0.5	0.25
1	6.0	6.0
0.5	6.0	3.0
Testing Series to Determine Effect of End Restraint (Using Enlarged Low-friction Caps and Bases and Axial Strain Rate of 0.06 Percent/Min)**		
1	0.5	0.5
0.5	0.5	0.25
1	6.0	6.0
0.5	6.0	3.0
Testing Series to Determine Effect of K_o Consolidation (Using Standard Caps and Bases and Axial Strain Rate of 0.06 Percent/Min)†		
K_o	0.5	††
K_o	1.5	††
K_o	3.0	††
K_o	6.0	††

* Tests to be performed on Buckshot and EABPL clay.
** Tests to be performed on Buckshot clay only.
† Tests to be performed on EABPL clay only.
†† $\bar{\sigma}_{3c}$ value will be that necessary to obtain K_o condition (no lateral strain).

Results of

$\bar{\sigma}_{1c}$ kg/cm^2	$K_c = \bar{\sigma}_{3c}/\bar{\sigma}_{1c}$	Test No.	Initial Specimen Conditions: Water Content %	Void Ratio	Saturation %	Dry Density pcf	Consolidation Data: Water Out cm^3	Time of Consolidation days
0.5	1	1	32.5	0.864	100+	90.4	0.40	7
	1	2	32.6	0.861	100+	90.2	0.38	5
	1	3**	33.5	0.899	100	88.4	0.50	2
	0.67	4	32.4	0.862	100+	90.2	0.22	2
	0.5	5	32.3	0.870	100+	90.1	0.12	2
	0.5	6	32.5	0.861	100+	90.2	0.03	2
	0.5	7**	32.0	0.852	100+	90.6	0.02	3
1.5	1	8	32.4	0.865	100+	90.3	2.30	3
	0.67	9	32.6	0.862	100+	90.2	1.48	4
	0.5	10	32.7	0.862	100+	90.4	1.17	7
3.0	1	11	32.7	0.874	100+	89.9	5.85	2
	0.67	12	32.7	0.866	100+	89.9	4.09	7
	0.5	13	32.7	0.871	100+	90.0	3.73	9
6.0	1	14	32.0	0.869	99.0	89.8	9.81	2
	1	15	32.6	0.863	100+	90.1	4.64	2
	1	16	32.8	0.869	100+	89.8	9.63	4
	1	17**	32.4	0.849	100+	90.7	4.92	3
	0.67	18	32.3	0.858	100+	90.3	8.44	9
	0.5	19	31.8	0.867	98.7	89.9	8.41	11
	0.5	20	32.8	0.873	100+	89.9	8.15	9
	0.5	21	32.7	0.868	100+	89.9	8.47	13
	0.5	22**	32.2	0.858	100+	90.3	3.88	10

Note: Symbols used in the headings are defined in EM 1110-2-1906 (Reference 16).

* Based on middle 80 percent of specimen after shear.

** Test performed using low-friction cap and base.

2

Table 2

Results of CU Triaxial Tests Performed on Vicksburg Buckshot Clay

Consolidation Data				Axial Loading Data						
				at Max $\bar{\sigma}_1/\bar{\sigma}_3$						
Water Out cm^3	Time of Consolidation days	Final Water Content* %	Rate of Axial Strain %/min	$\sigma_1 - \sigma_3$ kg/cm^2	$u - u_o$ kg/cm^2	$\bar{\sigma}_3$ kg/cm^2	$\bar{\sigma}_1/\bar{\sigma}_3$	$A = \frac{u - u_o}{\sigma_1 - \sigma_3}$	Strain %	σ_1 - kg/cm
0.40	7	32.9	0.06	1.13	0.28	0.22	6.13	0.25	1.00	1.2
0.38	5	32.9	0.6	1.29	0.33	0.17	8.54	0.33	0.97	1.3
0.50	2	33.9	0.6	1.01	0.21	0.29	4.52	0.21	2.58	1.1
0.22	2	33.0	0.06	1.06	0.16	0.17	7.17	0.15	0.64	1.2
0.12	2	33.0	0.06	0.99	0.12	0.13	8.59	0.12	0.67	1.1
0.03	2	33.2	0.6	1.09	0.15	0.10	11.89	0.14	0.67	1.2
0.02	3	32.8	0.6	1.28	0.04	0.21	7.10	0.03	1.31	1.3
2.30	3	31.2	0.06	1.64	0.78	0.72	3.28	0.48	4.22	1.6
1.48	4	32.0	0.06	1.59	0.40	0.60	3.64	0.25	1.35	1.5
1.17	7	32.2	0.06	1.57	0.22	0.53	3.96	0.14	0.68	1.5
5.85	2	28.1	0.06	2.37	1.73	1.27	2.87	0.73	6.52	2.4
4.09	7	29.9	0.06	1.90	1.07	0.93	3.04	0.56	10.31	2.1
3.73	9	30.0	0.06	1.80	0.63	0.87	3.06	0.35	6.93	2.1
9.81	2	24.2	0.012	4.02	3.54	2.46	2.63	0.88	8.73	4.0
4.64	2	24.8	0.06	4.05	3.59	2.41	2.68	0.89	9.96	4.1
9.63	4	25.0	0.6	4.05	3.79	2.21	2.83	0.94	18.97	4.2
4.92	3	25.0	0.6	3.59	3.10	2.90	2.24	0.86	20.73	3.7
8.44	9	25.6	0.06	3.46	1.94	2.06	2.68	0.56	8.92	3.6
8.41	11	25.5	0.012	3.50	0.95	2.05	2.70	0.27	5.94	3.8
8.15	9	26.3	0.06	4.07	0.45	2.55	2.60	0.11	0.23	4.0
8.47	13	26.2	0.6	4.38	0.41	2.59	2.69	0.09	0.30	4.3
3.88	10	26.2	0.6	3.16	0.98	2.02	2.56	0.31	18.89	4.3

(Reference 16).

Clay

Axial Loading Data

$\bar{\sigma}_1/\bar{\sigma}_3$			at Max $\sigma_1 - \sigma_3$						
$\bar{\sigma}_3$	$A = \frac{u - u_o}{\sigma_1 - \sigma_3}$	Strain %	$\sigma_1 - \sigma_3$ kg/cm^2	$u - u_o$ kg/cm^2	$\bar{\sigma}_3$ kg/cm^2	$\bar{\sigma}_1/\bar{\sigma}_3$	$A = \frac{u - u_o}{\sigma_1 - \sigma_3}$	Strain %	Elapsed Time min
13	0.25	1.00	1.25	0.10	0.40	4.10	0.08	3.00	50
54	0.33	0.97	1.39	0.18	0.32	5.37	0.13	2.14	4
52	0.21	2.58	1.11	0.07	0.43	3.58	0.06	10.74	26
17	0.15	0.64	1.21	-0.03	0.36	4.40	-0.02	2.31	38
59	0.12	0.67	1.19	-0.03	0.28	5.31	-0.02	2.01	33
89	0.14	0.67	1.29	-0.01	0.26	6.02	-0.01	2.34	4
10	0.03	1.31	1.35	-0.22	0.47	3.89	-0.16	5.24	13
.28	0.48	4.22	1.68	0.72	0.78	3.17	0.43	1.21	20
.64	0.25	1.35	1.59	0.40	0.60	3.64	0.25	1.35	22
.96	0.14	0.68	1.57	0.22	0.53	3.96	0.14	0.68	11
.87	0.73	6.52	2.41	1.60	1.40	2.72	0.66	3.14	79
.04	0.56	10.31	2.10	0.61	1.40	2.50	0.29	0.69	11
.06	0.35	6.93	2.12	0.23	1.28	2.67	0.11	0.21	3
.63	0.88	8.73	4.02	3.54	2.46	2.63	0.88	8.73	706
.68	0.89	9.96	4.12	3.39	2.61	2.58	0.82	4.83	162
.83	0.94	18.97	4.21	3.45	2.55	2.65	0.82	8.18	13
.24	0.86	20.73	3.79	2.54	3.46	2.09	0.67	12.14	30
.68	0.56	8.92	3.66	0.96	3.04	2.21	0.26	0.71	11
.70	0.27	5.94	3.85	0.35	2.65	2.45	0.09	0.22	100
.60	0.11	0.23	4.07	0.45	2.55	2.60	0.11	0.23	3
.69	0.09	0.30	4.38	0.41	2.59	2.69	0.09	0.30	>1
.56	0.31	18.89	4.35	0.09	2.91	2.50	0.02	0.23	>1

/

$\bar{\sigma}_{1c}$ kg/cm^2	$K_c = \bar{\sigma}_{3c}/\bar{\sigma}_{1c}$	Test No.	Initial Specimen Conditions: Water Content %	Void Ratio	Saturation %	Dry Density pcf	Consolidation Data: Water Out cm^3	Time of Consolidation days
0.5	1	23	48.2	1.326	98.7	73.0	1.16	8
	0.67	24	47.8	1.317	98.6	73.3	0.70	7
	0.5	25	48.2	1.328	98.8	72.9	0.47	3
1.5	1	26	47.7	1.313	98.9	73.4	4.45	5
	0.67	27	48.0	1.322	98.7	73.1	3.84	6
	0.5	28	47.8	1.321	98.4	73.1	3.44	11
3.0	1	29	47.5	1.315	98.3	73.3	8.46	7
	0.67	30**	46.5	1.269	99.6	74.8	7.09	8
	0.67	31	48.1	1.328	98.5	72.9	6.92	7
	0.5	32**	46.3	1.269	99.3	74.8	7.20	7
	0.5	33	48.0	1.322	98.8	73.1	7.21	12
4.8	0.5	34**	46.2	1.267	99.2	74.9	10.91	9
	0.5	35	46.1	1.261	99.4	75.1	12.54	8
6.0††	1	36	47.9	1.323	98.6	73.1	13.38	5
	0.67	37	47.8	1.310	99.2	73.5	12.06	11
K_o Tests								
0.49	0.57	38	46.5	1.279	98.9	74.5	0.30	3
1.57	0.51	39	46.6	1.273	99.5	74.7	2.84	3
3.15	0.57	40	46.5	1.276	99.1	74.6	6.56	6
6.01	0.64	41	46.1	1.271	98.7	74.8	12.10	9

Note: Symbols used in the headings are defined in EM 1110-2-1906 (Reference 16).

* Based on middle 80 percent of specimen after shear.

** Test performed on 3.5-in.-high specimen after previous test on standard 3.0-in.-high

† $(\bar{\sigma}_1/\bar{\sigma}_3)_{max}$ not developed using 0.002 percent/min strain rate.

†† Test at $\bar{\sigma}_{1c} = 6.0$ kg/cm^2 with $K_c = 0.5$ not performed since axial deformation duri

2

Table 3

Results of CU Triaxial Compression Tests Performed on EABPL Clay

				Axial Loading Data							
				at Max $\bar{\sigma}_1/\bar{\sigma}_3$							
[cut]solidation Data		Final Water Content*	Rate of Axial Strain	$\sigma_1 - \sigma_3$	$u - u_o$	$\bar{\sigma}_3$		$A = \frac{u - u_o}{\sigma_1 - \sigma_3}$	Strain	$\sigma_1 - \sigma_3$	u [cut]
[cut]r [cut]t [cut]3	Time of Consolidation days	%	%/min	kg/cm^2	kg/cm^2	kg/cm^2	$\bar{\sigma}_1/\bar{\sigma}_3$		%	kg/cm^2	kg/[cut]
16	8	47.9	0.06	0.68	0.24	0.26	3.63	0.36	3.12	0.80	0.
70	7	47.8	0.06	0.65	0.07	0.26	3.51	0.11	3.38	0.68	-0.
47	3	48.5	0.06	0.56	0.04	0.21	3.73	0.08	2.37	0.68	-0.
45	5	43.6	0.06	1.29	0.69	0.81	2.58	0.54	6.69	1.29	0.
84	6	44.5	0.06	1.14	0.24	0.76	2.51	0.21	3.49	1.14	0.
44	11	44.8	0.06	1.09	0.14	0.61	2.79	0.13	0.35	1.13	0.
46	7	39.8	0.06	1.88	1.60	1.40	2.35	0.85	12.04	1.91	1.
09	8	41.9	0.010	1.57	0.82	1.18	2.33	0.52	9.11	1.67	0.
92	7	41.7	0.06	1.57	0.78	1.22	2.29	0.50	9.03	1.75	0.
20	7	41.5	0.010	1.70	0.11	1.39	2.23	0.07	0.32	1.70	0.
21	12	41.3	0.06	1.97	0.18	1.32	2.50	0.09	0.38	1.97	0.
91	9	37.0	0.002	†	†	†	†	†	†	2.70	0.
54	8	37.0	0.06	2.96	0.22	2.28	2.30	0.07	0.34	2.96	0.
38	5	34.5	0.06	3.29	3.33	2.67	2.23	1.01	13.91	3.38	3.
06	11	35.7	0.06	2.81	1.73	2.27	2.24	0.62	15.61	3.09	0.
30	3	47.7	0.06	0.54	0.12	0.16	4.27	0.22	2.35	0.62	0.
84	3	45.2	0.06	1.10	0.14	0.66	2.66	0.13	0.35	1.19	0.
56	6	41.3	0.06	1.60	0.66	1.14	2.40	0.41	14.68	1.91	0.
10	9	35.6	0.06	2.98	1.37	2.47	2.21	0.46	11.94	3.32	0.

[cut]ence 16).

[cut]andard 3.0-in.-high specimen indicated a height to diameter ratio after consolidation considerably less than 2[cut]

[cut]ial deformation during consolidation exceeded available piston travel (1.0 in.).

Axial Loading Data

$\frac{u_o}{\sigma_3}$	Strain %	at Max $\sigma_1 - \sigma_3$: $\sigma_1 - \sigma_3$ kg/cm^2	$u - u_o$ kg/cm^2	$\bar{\sigma}_3$ kg/cm^2	$\bar{\sigma}_1/\bar{\sigma}_3$	$A = \frac{u - u_o}{\sigma_1 - \sigma_3}$	Strain %	Elapsed Time min
	3.12	0.80	0.12	0.39	3.07	0.14	8.20	134
	3.38	0.68	-0.02	0.35	2.93	-0.03	6.75	111
	2.37	0.68	-0.07	0.32	3.09	-0.11	6.78	139
	6.69	1.29	0.69	0.81	2.58	0.54	6.69	107
	3.49	1.14	0.24	0.76	2.51	0.21	3.49	83
	0.35	1.13	0.10	0.65	2.73	0.09	1.06	17
	12.04	1.91	1.46	1.54	2.24	0.77	6.76	107
	9.11	1.67	0.44	1.56	2.07	0.26	1.52	28
	9.03	1.75	0.35	1.65	2.06	0.20	0.72	11
	0.32	1.70	0.11	1.39	2.23	0.07	0.32	56
	0.38	1.97	0.18	1.32	2.50	0.09	0.38	6
	†	2.70	0.17	2.33	2.16	0.07	0.15	67
	0.34	2.96	0.22	2.28	2.30	0.07	0.34	4
	13.91	3.38	3.11	2.89	2.17	0.92	8.54	132
	15.61	3.09	0.74	3.26	1.95	0.24	1.55	22
	2.35	0.62	0.02	0.26	3.37	0.03	5.04	107
	0.35	1.19	0.07	0.73	2.63	0.06	2.08	33
	14.68	1.91	0.24	1.56	2.23	0.13	0.73	11
	11.94	3.32	0.70	3.14	2.06	0.21	1.59	22

n considerably less than 2:1.

Table 4

Final Water Content Distribution for Buckshot Clay

$\bar{\sigma}_{1c}$ kg/cm^2	K_c	Test No.	Water Content at End of Test, %: Total Specimens 5 Slices	Middle 3 Slices	Middle Slice
0.5	1	1	32.86	32.92	33.21
	1	2	32.92	32.91	32.82
	1	3	33.86	33.86	33.92
	0.67	4	32.90	32.95	33.08
	0.5	5	33.02	33.02	33.07
	0.5	6	33.18	33.18	33.14
	0.5	7	32.82	32.82	32.99
1.5	1	8	31.23	31.18	31.14
	0.67	9	32.04	32.02	32.01
	0.5	10	32.19	32.15	32.13
3.0	1	11	28.35	28.12	28.06
	0.67	12	29.96	29.85	29.81
	0.5	13	30.13	30.01	29.95
6.0	1	14	24.33	24.18	24.28
	1	15	24.97	24.79	24.78
	1	16	25.12	24.95	24.88
	1	17	25.01	25.01	24.93
	0.67	18	25.83	25.63	25.65
	0.5	19	25.67	25.50	25.55
	0.5	20	26.45	26.29	26.30
	0.5	21	26.40	26.21	26.15
	0.5	22	26.17	26.17	26.20

Table 5

Final Water Content Distribution for EABPL Clay

$\bar{\sigma}_{1c}$ kg/cm^2	K_c	Test No.	Water Content at End of Test, %: Total Specimens 5 Slices	Middle 3 Slices	Middle Slice
0.5	1	23	47.88	47.86	48.15
	0.67	24	47.83	47.84	48.11
	0.5	25	48.45	48.46	48.79
1.5	1	26	43.87	43.59	43.44
	0.67	27	44.70	44.50	44.50
	0.5	28	44.97	44.84	44.83
3.0	1	29	40.06	39.76	39.70
	0.67	30	42.05	41.68	41.61
	0.67	31	42.11	41.89	41.90
	0.5	32	41.60	41.28	41.10
	0.5	33	41.82	41.53	41.53
4.8	0.5	34	37.39	36.95	36.77
	0.5	35	37.36	36.95	36.90
6.0	1	36	34.95	34.52	34.46
	0.67	37	36.23	35.74	35.63
K_o Tests					
0.49	0.57	38	47.77	47.74	47.81
1.57	0.51	39	45.26	45.12	45.15
3.15	1.8	40	41.59	41.27	41.24
6.01	3.84	41	36.09	35.64	35.57

Table 6

Reductions in Maximum Deviator Stress with Increasing Times to Failure for Buckshot Clay

Rate of Strain, $\dot{\varepsilon}$ %/min	Time to Failure min	Maximum Deviator Stress kg/cm^2	Reduction in Maximum Deviator Stress Relative to That at $\dot{\varepsilon}$ = 0.6 %/min, %
		ICU Specimens (K_c = 1) at $\bar{\sigma}_{1c} = 0.5\ kg/cm^2$ $(\bar{\sigma}_{1p}/\bar{\sigma}_{1c} = 6.0)$	
0.6	4	1.39	--
0.06	50	1.25	10
0.012	--	--	--
		ACU Specimens (K_c = 0.5) at $\bar{\sigma}_{1c} = 0.5\ kg/cm^2$ $(\bar{\sigma}_{1p}/\bar{\sigma}_{1c} = 6.0)$	
0.6	4	1.29	--
0.06	33	1.19	4
0.012	--	--	--
		ICU Specimens (K_c = 1) at $\bar{\sigma}_{1c} = 6.0\ kg/cm^2$ $(\bar{\sigma}_{1p}/\bar{\sigma}_{1c} = 1.0)$	
0.6	13	4.21	--
0.06	162	4.12	2
0.012	706	4.02	5
		ACU Specimens (K_c = 0.5) at $\bar{\sigma}_{1c} = 6.0\ kg/cm^2$ $(\bar{\sigma}_{1p}/\bar{\sigma}_{1c} = 1.0)$	
0.6	>1	4.38	--
0.06	3	4.07	7
0.012	100	3.85	12

Table 7

Changes in Maximum Deviator Stress Resulting from Decreased End Restraint for Buckshot Clay

Caps and Bases	Maximum Deviator Stress kg/cm^2	Change in Maximum Deviator Stress Relative to That Developed Using Standard Caps and Bases, %
	ICU Specimens ($K_c = 1$) at $\bar{\sigma}_{1c} = 0.5\ kg/cm^2$	
Low friction	1.11	-11
Standard	1.25	--
	ACU Specimens ($K_c = 0.5$) at $\bar{\sigma}_{1c} = 0.5\ kg/cm^2$	
Low friction	1.35	+12
Standard	1.19	--
	ICU Specimens ($K_c = 1$) at $\bar{\sigma}_{1c} = 6.0\ kg/cm^2$	
Low friction	3.79	-8
Standard	4.12	--
	ACU Specimens ($K_c = 0.5$) at $\bar{\sigma}_{1c} = 6.0\ kg/cm^2$	
Low friction	4.35	+6
Standard	4.07	--

Table 8

Differences in Induced Pore Pressures Taken at Maximum Deviator Stresses for $K_c = 0.67$ and $K_c = 0.5$ as Compared with Induced Pore Pressure at $K_c = 1$

$\bar{\sigma}_{1c}$, kg/cm^2	Induced Pore Pressure at $(\sigma_1 - \sigma_3)_{max}$ for $K_c = 1$, kg/cm^2	Percent Difference in Induced Pore Pressure at $(\sigma_1 - \sigma_3)_{max}$ for Indicated Values of K_c: Between $K_c = 1$ and $K_c = 0.67$	Between $K_c = 1$ and $K_c = 0.5$
Buckshot Clay			
0.5	0.10	-130	-130
1.5	0.72	-44	-69
3.0	1.60	-62	-86
6.0	3.54	-73	-87
EABPL Clay			
0.5	0.12	-117	-158
1.5	0.69	-65	-86
3.0	1.46	-70	-93
6.0	3.11	-76	*

* Test not performed.

Table 9

Comparisons Between Induced Pore Pressures and Strain Rates for Buckshot Clay

Rate of Strain, $\dot{\varepsilon}$ %/min	Induced Pore Pressure at $(\sigma_1 - \sigma_3)_{max}$, kg/cm^2	Change in Induced Pore Pressure at $(\sigma_1 - \sigma_3)_{max}$ Relative to That Developed at $\dot{\varepsilon}$ = 0.6 %/min, kg/cm^2
	ICU Specimens (K_c = 1) at $\bar{\sigma}_{1c}$ = 0.5 kg/cm^2	
0.6	0.18	--
0.06	0.10	-0.08
0.012	--	--
	ACU Specimens (K_c = 0.5) at $\bar{\sigma}_{1c}$ = 0.5 kg/cm^2	
0.6	-0.01	--
0.06	-0.03	-0.02
0.012	--	--
	ICU Specimens (K_c = 1) at $\bar{\sigma}_{1c}$ = 6.0 kg/cm^2	
0.6	3.45	--
0.06	3.39	-0.06
0.012	3.54	+0.09
	ACU Specimens (K_c = 0.5) at $\bar{\sigma}_{1c}$ = 6.0 kg/cm^2	
0.6	0.41	--
0.06	0.45	+0.04
0.012	0.35	-0.06

Table 10

Maximum $\bar{\sigma}_1/\bar{\sigma}_3$ Values for K_c Ratios Used

K_c	$(\bar{\sigma}_1/\bar{\sigma}_3)_{max}$ $\bar{\sigma}_{1c} = 0.5$ kg/cm^2	$\bar{\sigma}_{1c} = 1.5$ kg/cm^2	$\bar{\sigma}_{1c} = 3.0$ kg/cm^2	$\bar{\sigma}_{1c} = 6.0$ kg/cm^2
		Buckshot Clay		
1	6.13	3.28	2.87	2.63
0.67	7.17	3.64	3.04	2.68
0.5	8.59	3.96	3.06	2.70
		EABPL Clay		
1	3.63	2.58	2.35	2.23
0.67	3.51	2.51	2.33	2.24
0.5	3.73	2.79	2.23	*

* Test not performed.

Table 11

Angles of Internal Friction Based on Total Stresses

K_c	Angle, deg			
	Based on Mohr's Diagram Taken at $(\sigma_1 - \sigma_3)_{max}$; Envelope Drawn Tangent to Circle	Based on Shear Stress Versus Total Normal Stress on Failure Plane Taken at $(\sigma_1 - \sigma_3)_{max}$	Based on Taylor's Method Taken at $(\sigma_1 - \sigma_3)_{max}$	Based on Effective Normal Stress on Failure Plane Prior to Shear Versus Shear Stress on Failure Plane Taken at $(\sigma_1 - \sigma_3)_{max}$
		Normally Consolidated Buckshot Clay		
1	14.6	13.9	--	16.2
0.67	18.3	17.8	18.5	19.3
0.5	22.8	23.0	22.3	23.9
		Normally Consolidated EABPL Clay		
1	12.8	12.1	--	13.7
0.67	16.3	15.6	16.0	16.4
0.5	21.0	20.2	19.7	20.8

Table 12

Angles of Internal Friction Based on Effective Stresses

	Angle, deg		
K_c	Based on Mohr's Diagram Taken at $(\sigma_1 - \sigma_3)_{max}$; Envelope Drawn Tangent to Circle	Based on Stresses on 60-deg Plane Taken at $(\sigma_1 - \sigma_3)_{max}$	Based on Stresses on 60-deg Plane Taken at $(\bar{\sigma}_1/\bar{\sigma}_3)_{max}$
	Normally Consolidated Buckshot Clay		
1	26.9	26.9	26.9
0.67	22.0	21.8	26.9
0.5	24.9	24.7	26.9
	Normally Consolidated EABPL Clay		
1	21.5	21.4	22.2
0.67	18.6	18.4	22.2
0.5	21.1	21.4	22.2

APPENDIX A: DERIVATION OF EQUATION USED TO CORRECT SPECIMEN CROSS-SECTIONAL AREAS FOR BULGING

1. The derivation of the equation used to correct specimen cross-sectional areas for localized bulging and the effects of corrections on deviator stresses computed assuming that specimens remain cylindrical in shape during axial loading are given in Figure A1.

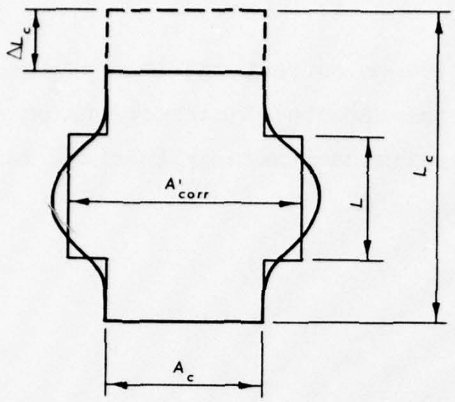

$$L = \frac{L_c}{2} - \Delta L_c$$

SINCE $\Delta L_c = \epsilon L_c$

$$L = \frac{L_c}{2} - \epsilon L_c$$

OR $L = \frac{L_c}{2}(1 - 2\epsilon)$

$$A'_{corr} = \frac{V}{2} \div L = \frac{A_c L_c}{2} \div L$$

$$A'_{corr} = \frac{A_c L_c}{2} \div \frac{L_c}{2}(1 - 2\epsilon)$$

$$A'_{corr} = \frac{A_c}{1 - 2\epsilon}$$

DETERMINATION OF A'_{corr} WHEN BULGING IS CONFINED TO CENTRAL HALF OF SPECIMEN

FOR THE CASE WHEN BULGING IS CONFINED TO THE CENTRAL TWO-THIRDS OF THE SPECIMEN:

$$A'_{corr} = \frac{A_c}{1 - 1.5\epsilon}$$

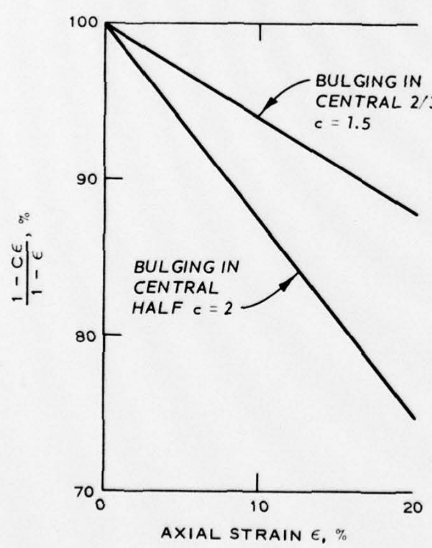

$\frac{1 - C\epsilon}{1 - \epsilon}$ = RATIO OF AREA CORRECTED USING THE USUAL ASSUMPTION OF A CYLINDRICAL CROSS-SECTION MAINTAINED DURING SHEAR TO THE AREA CORRECTED ASSUMING LOCALIZED CENTRAL BULGING. IT IS THEREFORE THE RATIO OF THE DEVIATOR STRESSES BASED ON LOCALIZED BULGING TO THOSE COMPUTED IN THE USUAL WAY.

Figure A1. Effects of localized bulging on computed deviator stresses

APPENDIX B: TAYLOR'S METHOD OF DETERMINING ACU STRENGTHS FROM ICU TESTS

1. Figure B1 illustrates Taylor's method[2*] applied to the isotropically consolidated Buckshot clay specimen having $\bar{\sigma}_{1c} = 6.0\ kg/cm^2$ (test 14). During undrained shear, $\bar{\sigma}_3/\bar{\sigma}_1$ values decreased until

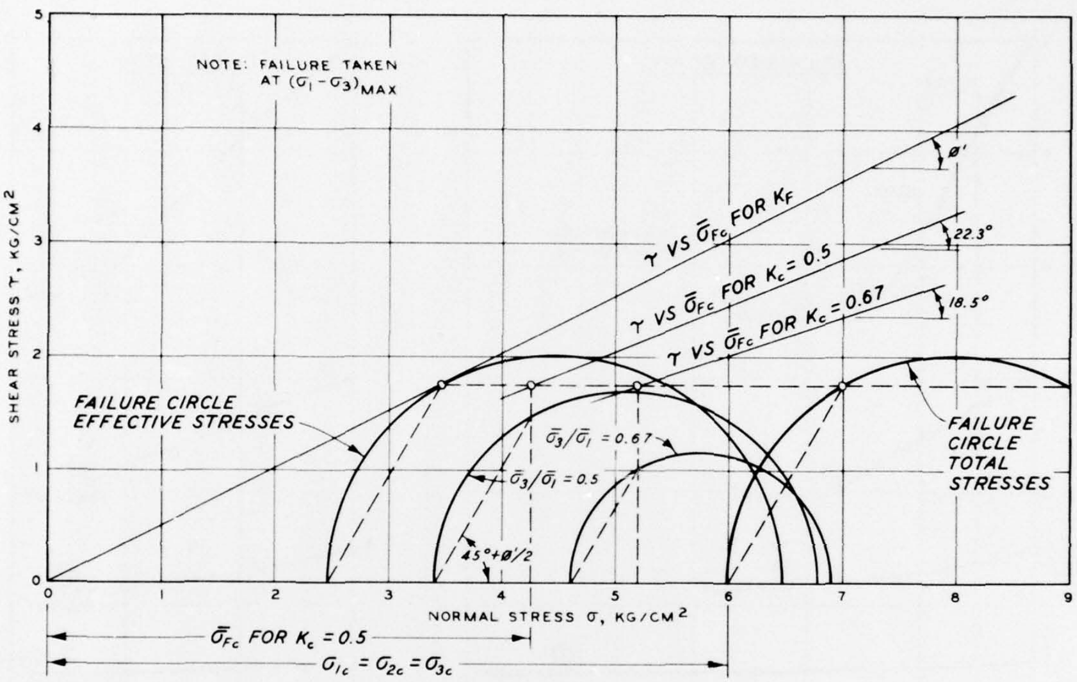

Figure B1. Taylor's method for determining τ versus σ_{fc} envelopes for $K_c = 0.5$ and $K_c = 0.67$ based on test on isotropically consolidated Buckshot clay specimen having $\bar{\sigma}_{1c} = 6.0\ kg/cm^2$ (test 14)

$(\sigma_1 - \sigma_3)_{max}$ was reached. Since Taylor assumes that $\bar{\sigma}_3/\bar{\sigma}_1$ at any point during undrained shear represents the starting conditions for a test consolidated to that ratio, Mohr's circles for $\bar{\sigma}_3/\bar{\sigma}_1 = 0.67$ and $\bar{\sigma}_3/\bar{\sigma}_1 = 0.5$ were drawn and the corresponding effective normal stress values on the failure plane $\bar{\sigma}_f$ plotted versus the shear stress on the

---

* Raised number refers to similarly numbered item in the References at the end of the main text.

failure plane at $\left(\sigma_1 - \sigma_3\right)_{max}$. These points locate a point on the appropriate shear stress on failure plane at failure τ_{ff} versus effective normal stress on failure plane prior to shear $\bar{\sigma}_{fc}$ envelope. In practice a plot of effective normal stress on the failure plane versus $\bar{\sigma}_3/\bar{\sigma}_1$ ratios can be made (Figure B2) and the τ_{ff} versus $\bar{\sigma}_{fc}$ points may be plotted directly.

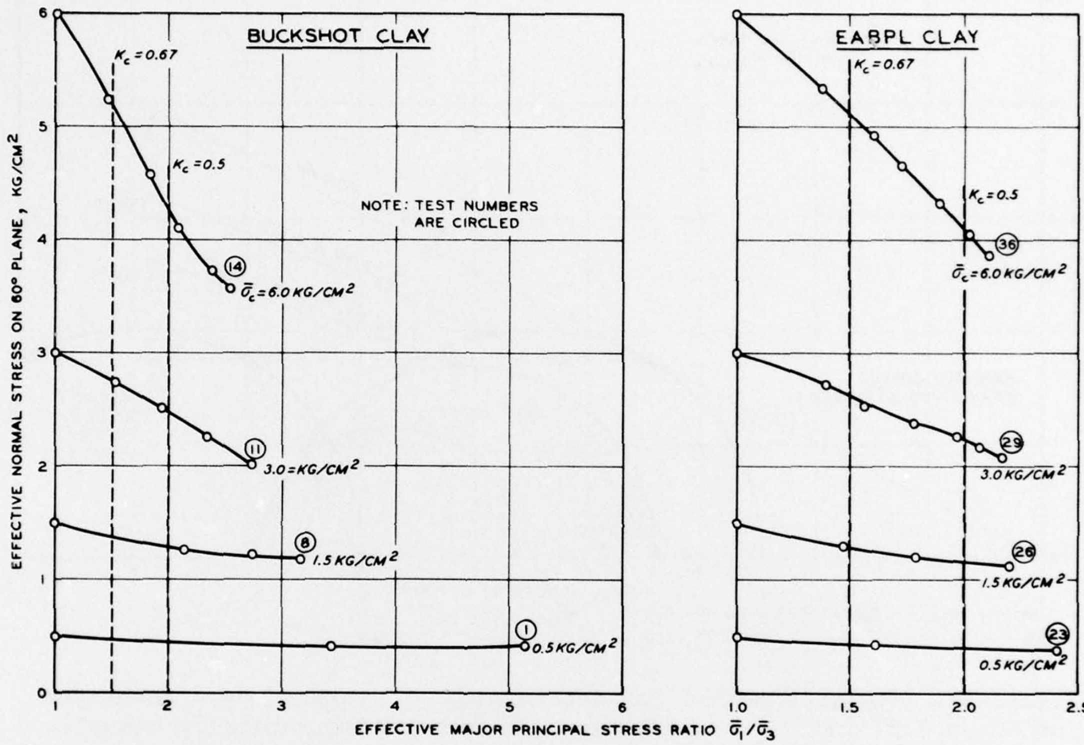

Figure B2. Effective normal stress on 60-deg plane versus effective major principal stress ratio during undrained shear of isotropically consolidated specimens of Buckshot and EABPL clays

APPENDIX C: NOTATION

a	Material parameter; intercept of a straight line; reciprocal of initial tangent modulus
A	Skempton's A pore pressure parameter; $A = (\Delta u - \Delta\sigma_3)/(\Delta\sigma_1 - \Delta\sigma_3)$
A_f	Skempton's A parameter at failure $\left(\text{i.e. at } (\sigma_1 - \sigma_3)_{max}\right)$ where $A = (\Delta u - \Delta\sigma_3)/(\Delta\sigma_1 - \Delta\sigma_3)$
A_o	Specimen cross-sectional area prior to consolidation
ACU	Anisotropically consolidated-undrained during shear
b	Material parameter; slope of a straight line
B	Skempton's B pore pressure parameter; $B = \Delta u/\Delta\sigma_3$
CU	Consolidated-undrained
E_{1o}	Initial tangent modulus
ICU	Isotropically consolidated-undrained during shear
K_c	Effective principal consolidation stress ratio; $K_c = \bar{\sigma}_{3c}/\bar{\sigma}_{1c}$
K_f	Effective principal stress ratio at $(\sigma_1 - \sigma_3)_{max}$
K_o	Effective principal consolidation stress ratio for no lateral strain
LL	Liquid limit
s_u	Undrained strength; $s_u = (\sigma_1 - \sigma_3)_{max}/2$
$s_u/\bar{\sigma}_{1c}$	Ratio of undrained strength to vertical consolidation stress
u	Pore pressure
u_o	Pore pressure prior to shear
V	Volume
α	Parameter of volumetric strain due to $(\bar{\sigma}_{oct})_c$.
β	Parameter of volumetric strain due to $(\bar{\tau}_{oct})_c$
ΔV	Change in volume
ΔV_{K_c}	Change in volume due to anisotropic consolidation
$\Delta V_{K_{c=1}}$	Change in volume due to isotropic consolidation
ε	Axial strain in undrained shear
$\dot{\varepsilon}$	Rate of strain

ε_c	Axial strain during consolidation
σ	Normal stress
σ_d	Deviator stress; $\sigma_d = \sigma_1 - \sigma_3$
σ_{dc}	Deviator stress due to anisotropic consolidation
σ_1	Major principal stress
σ_2	Intermediate principal stress
σ_3	Minor principal stress
$\sigma_1 - \sigma_3$	Deviator stress; $\sigma_1 - \sigma_3 = \sigma_d$
$(\sigma_1 - \sigma_3)_{max}$	Maximum deviator stress
$\bar{\sigma}_c$	Effective normal consolidation stress
$\bar{\sigma}_f$	Effective normal stress on failure plane
$\bar{\sigma}_{fc}$	Effective normal consolidation stress on failure plane
$(\bar{\sigma}_{oct})_c$	Mean effective consolidation stress; $(\bar{\sigma}_{oct})_c = (\bar{\sigma}_{1c} + \bar{\sigma}_{2c} + \bar{\sigma}_{3c})/3$
$\bar{\sigma}_1$	Effective major principal stress
$\bar{\sigma}_2$	Effective intermediate principal stress
$\bar{\sigma}_3$	Effective minor principal stress
$\bar{\sigma}_{1c}$	Effective major principal or vertical consolidation stress
$\bar{\sigma}_{2c}$	Effective intermediate consolidation stress
$\bar{\sigma}_{3c}$	Effective minor principal or lateral consolidation stress
$\bar{\sigma}_{1p}$	Maximum past vertical effective consolidation stress
$\bar{\sigma}_1/\bar{\sigma}_3$	Effective principal stress ratio
$(\bar{\sigma}_1/\bar{\sigma}_3)_{max}$	Maximum principal stress ratio
τ	Shear stress
τ_{ff}	Shear stress on failure plane at failure, i.e. at $(\sigma_1 - \sigma_3)_{max}$
$(\bar{\tau}_{oct})_c$	Octahedral shear stress during consolidation; $(\bar{\tau}_{oct})_c = \frac{1}{3}\left[(\bar{\sigma}_{1c} - \bar{\sigma}_{3c})^2 + (\bar{\sigma}_{1c} - \bar{\sigma}_{2c})^2 + (\bar{\sigma}_{2c} - \bar{\sigma}_{3c})^2\right]^{1/2}$
ϕ	Angle of internal friction
ϕ'	Effective angle of internal friction

In accordance with ER 70-2-3, paragraph 6c(1)(b), dated 15 February 1973, a facsimile catalog card in Library of Congress format is reproduced below.

Donaghe, Robert T
Effects of anisotropic versus isotropic consolidation in consolidated-undrained triaxial compression tests of cohesive soils, by Robert T. Donaghe and Frank C. Townsend. Vicksburg, U. S. Army Engineer Waterways Experiment Station, 1975.
1 v. (various pagings) illus. 27 cm. (U. S. Waterways Experiment Station. Technical report S-75-13)
Prepared for U. S. Army Engineer Division, Lower Mississippi Valley, Vicksburg, Miss.
Includes bibliography.

1. Cohesive soils. 2. Consolidation. 3. R tests (Soils). 4. Triaxial shear tests. I. Townsend, Frank C., joint author. II. U. S. Army Engineer Division, Lower Mississippi Valley. (Series: U. S. Waterways Experiment Station, Vicksburg, Miss. Technical report S-75-13)
TA7.W34 no.S-75-13